UNIVERSIDAD COMPLUTENSE DE MADRID

FACULTAD DE FARMACIA

TESIS DOCTORAL

Desarrollo de modelos predictivos para determinar la estabilidad de medicamentos de forma acelerada

In Silico modelling and prediction of pharmaceutical stability

MEMORIA PARA OPTAR AL GRADO DE DOCTOR

PRESENTADA POR

Peter Francis O'Connell

DIRECTORA

Dolores Remedios Serrano López

UNIVERSIDAD COMPLUTENSE DE MADRID

FACULTAD DE FARMACIA

TESIS DOCTORAL

Desarrollo de Modelos Predictivos para Determinar la Estabilidad de Medicamentos de Forma Acelerada // In Silico Modelling and Prediction of Pharmaceutical Stability

MEMORIA PARA OPTAR AL GRADO DE DOCTOR

PRESENTADA POR

Peter Francis O'Connell

DIRECTORA

Dolores Remedios Serrano López

UNIVERSIDAD COMPLUTENSE DE MADRID

FACULTAD DE FARMACIA

PROGRAMA DOCTORADO FARMACIA D9BI

TESIS DOCTORAL:

Desarrollo de modelos predictivos para determinar la estabilidad de medicamentos de forma acelerada

In-Silico modelling and prediction of pharmaceutical stability

Peter Francis O'Connell

DIRECTOR

Dra. Dolores Remedios Serrano López

MADRID, 2022

To acquire knowledge,
one must study;
but to acquire wisdom
one must observe.

Marylin vos Savant

Acknowledgements

"Don't bite off more than you can chew because nobody looks attractive spitting it back out."

Carroll Bryant

First and foremost, the completion of this PhD has possibly been the most arduous task I have undertaken in my career to date. I have had to juggle entrepreneurial endeavours with a full-time laboratory position while attempting to complete a PhD in another country. My PhD journey also coincided with difficulties aIt has necessitated a lot of sacrifice on my behalf and there are countless people who have, unknown to themselves provided inspiration and support to enable me to realise my ambitions.

I can only describe myself as an accidental academic who stumbled into this position from a technical role in industry and often felt myself coming down with a case of 'imposter syndrome' when dealing with my colleagues, collaborators and various supervisors and mentors. Therefore, I cannot adequately express how grateful I am to my supervisor Dra. Dolores Remedios Serrano López for her unending support and guidance. It was Loli who provided the inspiration for this research and my PhD journey coincided with the start of her own academic career at UCM and I am not the least bit surprised at the success she has made in developing an extensive research group in such a short space of time.

As a non-native speaker of Spanish and while having to perform a significant portion of my research abroad due to Covid restrictions and my industrial placement in Ireland I must also express my gratitude to the administrative and technical staff at the Faculty of Pharmacy of the Complutense University of Madrid who have had to deal with my many queries and requests.

This project could not have been completed without the academic and industrial support of those who offered to provide access to research facilities. Chief amongst those is Prof. Anne Marie Healy in the School of Pharmacy and Pharmaceutical Sciences in Trinity College Dublin. I must also acknowledge the contribution of Dr. Nigel McSweeney of Cuspor Limited and Prof. Helen

Sheridan of the NatPro Centre for Natural Products Research who were aware of the critical time demands of my PhD while I was under their employment.

A PhD can be a lonely endeavour so the value of colleagues to provide a respite from the rigours of day-to-day activities and also to provide an outlet for any frustrations encountered during the journey cannot be underestimated. My PhD traversed two institutions and multiple research groups so while it is impossible to list all those who provided support, I must offer my special thanks to Shipra, Maria, Junying, Ismael, Elizabeth, Cillian and Shilong from NatPro and also to my erstwhile colleagues from the Healy Research Group namely Jer, Karl, Zelalem, Dinesh, Stefano, Kate and May.

Finally, to my family, while I tried to shield you from my personal stresses of the last four years of semi-organised chaos, my absence from family life cannot have gone unnoticed during the period in question. I apologise for effectively abandoning you but as this chapter in my life ends, I hope to be able to make up for the lost time in the very near future.

Funding acknowledgements

This research was partially funded by Science Foundation Ireland (SFI) under Grant Numbers SFI/12/RC/2275 and SFI/12/RC/2278.

Abbreviations

A	Collision Frequency
ANOVA	Analysis of Variance
API	Active pharmaceutical ingredient
APS	Accelerated Predictive Stability
ASAP	Accelerated Stability Assessment Program
ASD	Amorphous Solid Dispersion
B	Moisture Sensitivity Factor
BET	Brunauer, Emmet, Teller
BM	Ball-milling
BUD	Budesonide
CCX	Celecoxib
Cp	Heat Capacity
DSC	Differential Scanning Calorimetry
DVS	Dynamic vapor sorption
E_a	Activation Energy
FTIR	Fourier Transform Infrared
GAB	Gugenheim, Anderson, de Boer
GRS	Griseofulvin
H_c	Heat of Crystallisation
HME	Hot Melt Extrusion
HPLC	High Performance Liquid Chromatography
HPMC AS	Hypromellose acetate succinate
ICH	International Council for Harmonisation
K	Degradation rate
MC	Monte Carlo (simulations)
NFD	Nifedipine
NIR	Near Infrared
PLSR	Partial Least Squares Regression

PVP-VA	Poly-vinylpyrrolidone vinyl acetate
PXRD	Powder X Ray Diffraction
QbD	Quality by Design
RBPS	Risk Based Predictive Stability
RH	Relative humidity
RIT	Ritonavir
SD	Spray Dried
SEM	Scanning Electron Microscopy
SOL	Soluplus™
T_g	Glass Transition Temperature
TGA	Thermogravimetric Analysis
T_m	Melt Temperature
WVTR	Water Vapour Transmission Rate
Xc	Weight Fraction of Excipient: API
ΔH_f	Enthalpy of fusion
ΔH_r	Relaxation Enthalpy

Table of Contents

Acknowledgements **5**

Funding acknowledgements **7**

Abbreviations **8**

Table of Contents **10**

Table of Figures **12**

Resumen **16**

Summary **19**

1. Introduction **23**

1.1 Role of Stability 23

1.2. Existing Stability Studies 24

1.2.1. Traditional Stability Studies **24**

1.2.2. Accelerated Stability Studies **26**

1.3. Chemical and Physical Stability 27

1.4. Influence of Formulation on Stability 28

1.5. Influence of Storage on Drug Product 29

1.6. Modelling and Prediction 30

1.6.1. Guide to Performing an APS Study **33**

2. Hypothesis & Aims **40**

2.1 Hypothesis 40

2.2 Aims 41

3.0. Accelerated Predictive Stability (APS) strategies applied to screening pharmaceutical formulations: A comparison of spray dried and hot melt extruded nifedipine amorphous solid dispersions **43**

3.1 Introduction 46

3.2 Materials and methods 48

3.2.1 Materials 48

3.2.2 Methods 48

3.3 Results 56

3.3.1 Preparation and characterisation of NFD amorphous solid dispersions 56

3.3.2 Dissolution studies 61

3.3.3 Accelerated Predictive Chemical and Physical Stability Studies 62

3.3.4 Spectroscopic NIR correlation with chemical and physical stability 66

3.4 Discussion 71
3.5 Conclusions 74
Acknowledgements 75
References 76
Supplementary Material 79
4.0. Physical Accelerated Predictive Stability of Amorphous Solid Dispersions 89
Abstract: 90
Graphical abstract: 91
4.1 Introduction 92
4.2 Materials and Methods 94
4.2.1 Materials 94
4.2.2 Methods 94
4.2.3 Solid-state characterisation 96
4.2.4 Quantification of amorphous content 98
4.2.5 Ageing of the samples 99
4.2.6 Modelling of physical stability 100
4.3 Results 101
4.3.1 Preparation and characterisation of the formulations 101
4.3.2 Modelling of physical stability 104
4.4 Discussion 116
4.5 Conclusions 121
Acknowledgements 121
Supplementary material 125
5.0. Discussion 145
5.1 Future Perspectives 147
6.0 Conclusions 149
6.1 Conclusiones 149

Table of Figures

Figure 1: Factors impacting pharmaceutical stability. 23
Figure 2:Stability Studies During Pharmaceutical Product Lifecycle. 24
Figure 3: Stability Parameters. 28
Figure 4: Factors affecting Pharmaceutical Stability. 29
Figure 5: Role of Packaging in Drug Product Stability. 30
Figure 6: Key Dates in Development of APS Approaches 31
Figure 7: Steps required to perform an APS Study 34
Figure 8: Typical Inputs and Outputs of an APS Study 35
Figure 9: Sample Ageing conditions for APS of NFD amorphous solid dispersions. 52
Figure 10: SEM micrographs of NFD amorphous solid dispersions. 56
Figure 11: PXRD patterns and DSC thermograms of NFD systems. 58
Figure 12: FTIR of NFD amorphous solid dispersions 59
Figure 13: Moisture absorption isotherms for NFD amorphous solid dispersions. 61
Figure 14:Dissolution profile of NFD ASDs and physical mixtures (PM). 62
Figure 15: Comparison of predicted and long-term chemical stability of NFD amorphous solid dispersions for materials stored at 25°C / 10% relative humidity 64
Figure 16: Comparison of predicted and long-term physical stability of NFD amorphous solid dispersions for materials stored at 25°C / 10% relative humidity. 65
Figure 17: Accelerated chemical stability studies. The potency (NFD remaining in the formulation expressed in %) is illustrated at different time points and different conditions for the two spray dried formulations. 67
Figure 18: Accelerated physical stability studies. The percentage of crystalline NFD is expressed at different time points and different conditions for the four formulations. 68
Figure 19:. PLSR correlation model between NIR spectra and drug content of the four NFD formulations. 69
Figure 20: PLSR correlation model between NIR spectra and crystalline NFD content of the four NFD formulations. 70
Figure 21: Graphical representation of diffusion and Avrami crystallisation models. 72
Figure 22: Graphical representation of relaxation enthalpy (ΔHr), heat capacity (Cp) and mild temperature glass transition (Tg) of NFD-PVPVA-SD system storage at 70°C /10 %rh 73

Figure 23: pXRD patterns budesonide, ritonavir, griseofulvin, celecoxib 102

Figure 24: DSC thermograms budesonide, ritonavir, griseofulvin, celecoxib 103

Figure 25: Zero-order modelling of the physical stability of the spray dried budesonide at different condition..... 106

Figure 26: Long-term physical stability prediction of spray dried budesonide formulation using 1st, 2nd, Avrami, and diffusion kinetic models 107

Figure 27: Avrami modelling of the physical stability of the co-spray dried budesonide-HPMC AS formulation at different conditions: 108

Figure 28: Long-term physical stability prediction of co-spray dried budesonide-HMPC AS formulation using Avrami kinetic model. 109

Figure 29: Diffusion modelling of the physical stability of the co-spray dried budesonide-PVP K90 formulation at different conditions: 110

Figure 30: Long term physical stability prediction of co-spray dried budesonide:PVP K90 (1:1 w/w) formulation at 25 °C/10% RH, 25 °C/50% RH and 40 °C/75% RH. 111

Figure 31: Diffusion modelling of the physical stability of the co-spray dried griseofulvin-HPMC AS formulation at different conditions: 111

Figure 32: Long term physical stability prediction of co-spray dried griseofulvin-HPMC AS (1:1 w/w) formulation at 25 °C/10% RH, 25 °C/50% RH and 40 °C/75% RH. 112

Figure 33: Different models of the physical stability of the co-spray dried ritonavir-HPMC AS formulation (2:1, w:w) at different conditions:..... 113

Figure 34: Long term physical stability prediction of co-spray dried ritonavir-HPMC AS (2:1 w/w) formulation at 25 °C/10% RH and 25 °C/50% RH. 114

Figure 35: Different models of the physical stability of the co-spray dried ritonavir-PVP K90 formulation (2:1, w:w) at :different conditions..... 115

Figure 36: Long term physical stability prediction of co-spray dried ritonavir-PVP K90 (2:1 w/w) formulation at 25 °C/10% RH and 25 °C/50% RH. 115

Figure 37: Hydrogen bonding acceptor and donor groups of the different drugs and excipients utilised in the preparation of the amorphous systems. 117

Figure 38: Proposed crystallisation models for amorphous systems. 118

Resumen
Summary

Resumen

Desarrollo de modelos predictivos para determinar la estabilidad de medicamentos de forma acelerada

Los estudios de estabilidad farmacéutica siguen siendo un parámetro clave en el desarrollo y la fabricación tanto de sustancias farmacológicas como de medicamentos y producto terminado. Los datos recopilados de los estudios de estabilidad a lo largo de todo el ciclo de vida del desarrollo de fármacos se pueden utilizar para identificar estrategias óptimas de formulación y fabricación, determinar los requisitos de acondicionamiento y almacenamiento, asignar fechas de vida útil o de testeo. Actualmente, esta información sirve tanto como una herramienta de aprendizaje clave para la industria como para cumplir con un requisito regulatorio para la aprobación de medicamentos.

Las herramientas de predicción como la Estabilidad Predictiva Acelerada (APS), la Estabilidad Predictiva Basada en el Riesgo (RBPS) y el Programa de Evaluación de Estabilidad Acelerada (ASAP) han ganado importancia en la industria farmacéutica como un medio para mejorar la comprensión de los mecanismos de degradación de fármacos y otras características clave de estabilidad de medicamentos.

Las dispersiones sólidas amorfas son actualmente uno de los enfoques más comunes utilizados por la industria farmacéutica para superar los problemas de solubilidad y disolución al abordar la formulación de un fármaco poco soluble en agua para su administración oral. Mejorar la solubilidad de los fármacos hidrofóbicos sigue siendo un desafío para su administración oral, ya que su baja solubilidad a menudo conlleva una biodisponibilidad muy baja siendo necesaria la administración de dosis más elevadas. La dispersión de un ingrediente farmacéutico activo (API) dentro de un vehículo amorfo, es decir, un polímero que controla la liberación del fármaco, es una de las estrategias más comunes para aumentar la velocidad de disolución de los fármacos hidrofóbicos. Existen varios métodos que se pueden usar para producir dispersiones sólidas amorfas, pero solo unos pocos, como el secado por atomización (SD) y la extrusión por fusión en caliente (HME), son fácilmente escalables.

Para diseñar con éxito dispersiones sólidas amorfas estables, hay varias consideraciones claves a tener en cuenta, como el tipo de proceso de fabricación a utilizar, la elección del polímero adecuado y la cinética de cristalización del fármaco, así como la alta tendencia de un fármaco amorfo a recristalizarse. Sigue siendo un desafío predecir qué tipo de proceso de fabricación y qué excipientes conducirán a la mejor dispersión sólida amorfa de un fármaco en términos de estabilidad química y física.

El objetivo general de este proyecto es investigar la idoneidad de los distintos estudios de estabilidad acelerada para determinar la estabilidad física y química de las dispersiones sólidas amorfas, y al mismo tiempo identificar la relación entre los ingredientes farmacéuticos activos y los excipientes que pueden afectar los atributos de calidad críticos de un fármaco potencial durante el almacenamiento. Este objetivos global se pueden desglosar en varios objetivos secundarios que se describen a continuación.

1. Desarrollar métodos analíticos y estadísticos que permitan el análisis y modelado de la estabilidad física y química de una serie de dispersiones sólidas amorfas.
2. Preparar dispersiones sólidas amorfas utilizando ingredientes farmacéuticos activos BCS Clase II seleccionados (budesonida, ritonavir, griseofulvina y celecoxib) y varios excipientes amorfos tales como la polivinilpirrolidona K 90 (PVP K90) y el succinato de acetato de hipromelosa (HMPCAS) con el fin de realizar estudios de estabilidad de tanto dispersiones sólidas amorfas en material pulverulento y compactado aplicando un enfoque de estabilidad predictiva acelerada (APS).
3. Diseñar estrategias de APS aplicadas a la selección de procesos de formulación farmacéutica aplicado a las dispersiones sólidas amorfas de nifedipino extruidas por fusión en caliente y secadas por atomización.
4. Validar todas las predicciones de estabilidad química y física frente a los datos de estabilidad en tiempo real recopilados en condiciones de almacenamiento de estabilidad a largo plazo según ICH tradicionales.

En esta tesis doctoral se ha conseguido validar un nuevo enfoque de desarrollar estudios de estabilidad predictiva acelerada (APS) capaces de proporcionar información útil para predecir la estabilidad a largo plazo de dispersiones sólidas amorfas. La herramienta ASAPprime facilita el

proceso de toma de decisiones de formulación haciéndolo más rápido y preciso. El modelado de la cinética de cristalización de fármacos es un desafío, pero el proceso se puede simplificar centrándose en una metodología APS.

Además, mediante un estudio APS se pudo identificar la mejor combinación de nifedipino, polímero y proceso de fabricación para generar dispersiones amorfas sólidas estables. Entre todas las formulaciones probadas, la dispersión amorfa secada por atomización de nifedipino y el copolímero PVP/VA exhibió el mejor equilibrio de estabilidad física y química y puede considerarse la mejor candidata para pasar a los ensayos clínicos. Así, la estabilidad predictiva acelerada ha demostrado ser una buena metodología para asegurar un proceso rápido de toma de decisiones para formulaciones farmacéuticas con incertidumbre reducida.

Summary

In-silico modelling and prediction of pharmaceutical stability

Pharmaceutical stability studies continue to be a key parameter in the development and manufacture of both drug substance and drug pruducts. The data collected from stability studies across the entire life cycle of drug development can be used to identify optimum formulation and manufacturing strategies, determine packaging and storage requirements, assign shelf-life or retest dates. Currently this information serves as both a key learning tool for industry as well as fulfilling a regulatory requirement for drug approval.

Predictive modelling tools such as Accelerated Predictive Stability (APS), Risk Based Predictive Stability (RBPS) and the Accelerated Stability Assessment Program (ASAP) have gained prominence in the pharmaceutical industry as a means to improve understanding of drug degradation mechanisms and other key stability characteristics.

Amorphous solid dispersions are currently one of the most common approaches utilised by the pharmaceutical industry to overcome solubility and dissolution issues when tackling the formulation of a poorly water-soluble drug for oral administration. Enhancing the solubility of hydrophobic drugs remains a challenge for oral delivery as their low solubility often results in reduced bioavailability being required for the administration of higher doses to ensure that a therapeutic dose is delivered to the target organ. Dispersing an active pharmaceutical ingredient (API) within an amorphous carrier – namely a polymer that controls drug release is one of the most common strategies to increase the dissolution rate of hydrophobic drugs. Several methods exist that may be used to produce amorphous solid dispersions but only a few, such as spray drying (SD) and hot melt extrusion (HME), are easily scalable.

To successfully design stable amorphous solid dispersions, there are several key considerations to bear in mind, such as the type of manufacturing process to use, the choice of suitable polymer, and the drug crystallisation kinetics, as the high tendency of an amorphous drug to recrystallise during storage is well known. It remains challenging to predict what type of manufacturing process

and which carrier will lead to the best amorphous solid dispersion of a particular drug, in terms of chemical and physical stability.

The overall aim of this project is to investigate the suitability of accelerated stability approaches to determine the physical and chemical stability of amorphous solid dispersions, whilst also identifying the relationship between active pharmaceutical ingredients and various excipients which may impact the critical quality attributes of a potential drug product during storage. These aims can be further categorised into several discrete objectives, outlined below.

1. To develop analytical and statistical methods to allow for the ageing, analysis, and modelling of both physical and chemical stability of a range of amorphous solid dispersions.
2. To prepare amorphous solid dispersions using selected BCS Class II active pharmaceutical ingredients (Budesonide, Ritonavir, Griseofulvin and Celecoxib) and polyvinylpyrrolidone K 90 (PVP K90) and hypromellose acetate succinate (HMPCAS) as common amorphous polymer carriers and to perform stability studies of both amorphous solid dispersions as free powders and compacts using an Accelerated Predictive Stability (APS) approach.
3. APS strategies applied to screening pharmaceutical formulation processes: A case study of spray dried and hot melt extruded nifedipine amorphous solid dispersions.
4. Validating all chemical and physical stability predictions against real time stability data collected under both traditional long term and accelerated stability storage conditions.

Results from this thesis have demonstrated that accelerated predictive stability (APS) approaches can provide useful information in predicting the long-term stability for amorphous solid dispersions. The ASAPprime tool facilitates the formulation decision making process making it faster and more accurate. The modelling of drug crystallisation kinetics is challenging but the process can be simplified by focusing on a time to failure approach methodology.

Additionally, a targeted APS study was able to identify the best combination of nifedipine: polymer: manufacturing process for the formulation of a novel amorphous dispersion. This APS approach was also able to successfully model both chemical and physical stability of each

formulation using ASAPprime. Amongst all the formulations tested, a spray dried amorphous dispersion of nifedipine and PVP/VA copolymer exhibited the best balance of both physical and chemical stability and may be considered to be the best candidate to move forward into clinical trials. Thus, accelerated predictive stability has been demonstrated to be a good methodology to ensure a fast decision-making process for pharmaceutical formulations with reduced uncertainty

Introduction

1. Introduction

1.1 Role of Stability

Stability plays important role in drug development Process. Stability studies are a prerequisite for the acceptance and approval of any pharmaceutical product and are key to maintaining product quality, safety, and efficacy throughout the shelf life. Stability is therefore often defined as the consistent product quality and therapeutic benefit over the product's shelf life under various environmental conditions[1]. Any successful pharmaceutical rug product stability program should identify the key process. Figure 1 illustrates how these factors contribute to improve the overall pharmaceutical product understanding.

These studies are required to be conducted in a planned way following the guidelines issued by ICH, WHO and or other agencies, these guidelines often act as the floor and not the ceiling in providing advice for carrying out stability studies. i.e. they outline the minimum requirements.[2],[3],[4],[5],[6]

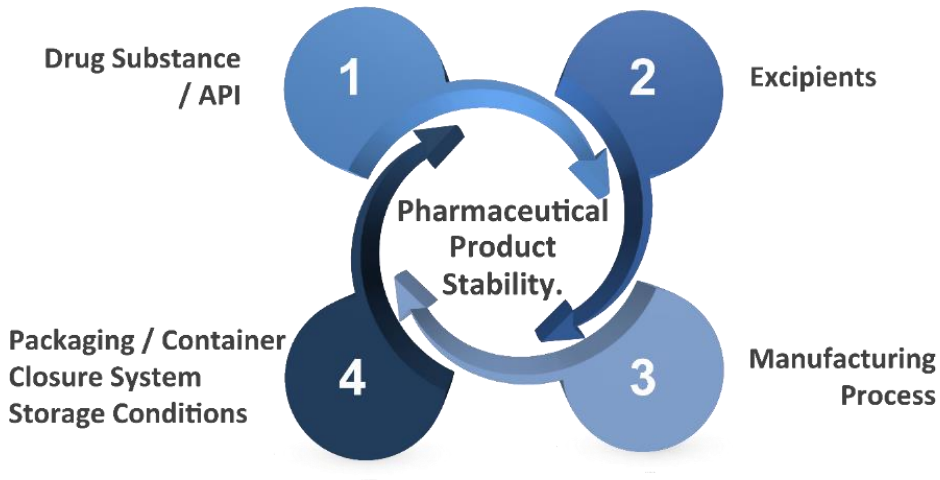

Figure 1: Factors impacting pharmaceutical stability.

However, due to the time-consuming nature of the drug discovery and development process, it can take up to 10-15 years to bring a new chemical entity (NCE) to the market. Within this period three distinct phases exist i. discovery/toxicology, ii. clinical development, and iii. commercialisation. Drug stability studies of some type are required at each of these stages and as

a result a comprehensive testing program to accommodate each stage requires a significant level of resources and expertise. In many cases, those involved in carrying out much of the stability program are not aware of the purposes of these studies and how these studies support the decision-making activities during the drug development process.[7]

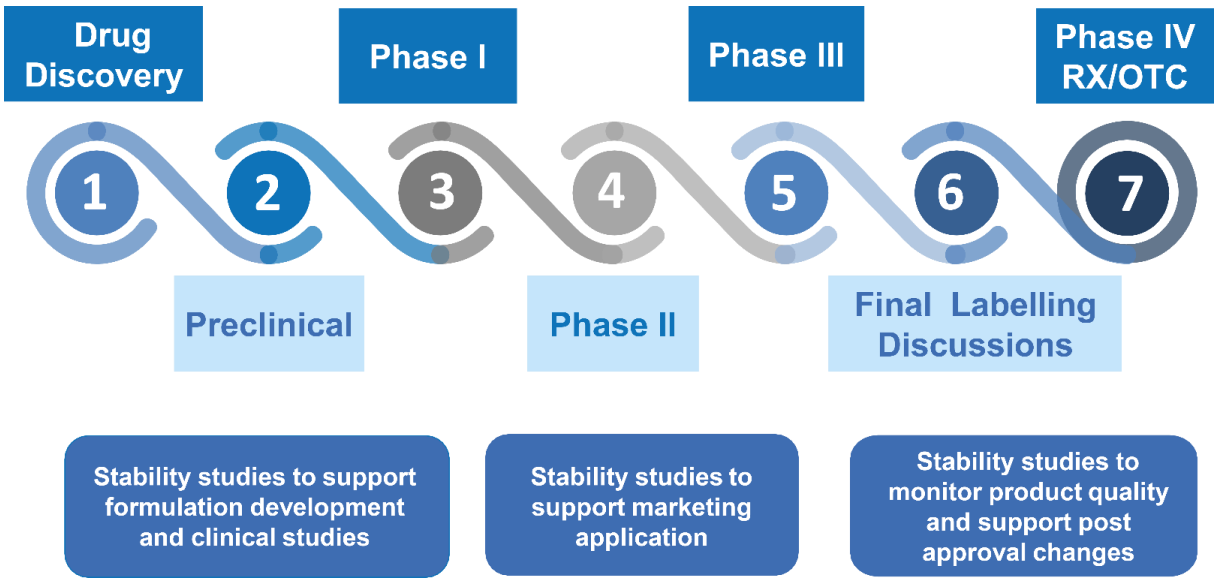

Figure 2:Stability Studies During Pharmaceutical Product Lifecycle.

1.2. Existing Stability Studies

1.2.1. Traditional Stability Studies

To assure that optimally stable molecules and products are designed, formulated, manufactured, packed, distributed and administered to the end user (typically patients), the regulatory authorities in several countries have made provisions in the drug regulations for the submission of stability data by the manufacturers. Its basic purpose was to bring in uniformity in testing from manufacturer to manufacturer. These guidelines include basic issues related to stability, the stability data requirements for application dossier and the steps for their execution. Such guidelines were initially issued in 1980s. These were later harmonized in the International Conference on Harmonization (ICH) in order to address the bottleneck to market and register the products in other countries. The ICH was a consortium formed with inputs from both regulatory and industry from European commission, Japan and the United States of America. In 1996 the World Health Organization (WHO) modified the guidelines to address the extreme climatic conditions found in many countries that were covered by the ICH guidelines and it only covered new drug substances

and products and not existing products that were already distributed in countries under the auspices of the WHO. The codes and titles covered under ICH guidance have been outlined in the Table 1-1.

Table 1-1: Codes and titles used in ICH Stability Guidelines. [2-6, 8]

ICH Guideline	Guideline Title
Q1A (R2)	Stability testing of new drug substances and drug products
Q1B	Photostability testing of new active substances and medicinal products
Q1C	Stability testing: requirements for new dosage forms
Q1D	Bracketing and matrixing designs for stability testing of drug substances and drug products
Q1E	Evaluation of stability data
Q1F	Stability data package for registration in climatic zones III and IV *(Subsequently Withdrawn)*
Q5C	Stability testing of biotechnological/biological products

In general, a drug substance should be evaluated under storage conditions (with appropriate tolerances) that test its thermal stability and, if applicable, its sensitivity to moisture. The storage conditions and the lengths of studies chosen should be sufficient to cover storage, shipment, and subsequent use.

The long-term testing should cover a minimum of 12 months' duration on at least three primary batches at the time of submission and should be continued for a period of time sufficient to cover the proposed re-test period. Additional data accumulated during the assessment period of the registration application should be submitted to the authorities if requested. Data from the accelerated storage condition and, if appropriate, from the intermediate storage condition can be used to evaluate the effect of short-term excursions outside the label storage conditions (such as might occur during shipping).

Long term, accelerated, and, where appropriate, intermediate storage conditions for drug substances are detailed in the sections below. The general case applies if the drug substance is not

specifically covered by a subsequent section. Alternative storage conditions can be used if justified.

Table 1-2: Typical ICH Storage Conditions for Zones 1 and 2 including Minimum Data Required.[2,3,4]

Study	Storage Condition	Minimum Time Period Covered by Data at Submission
Long Term	25°C ± 2°C / 60 % RH ± 5% RH or 30°C ± 2°C / 65 % RH ± 5% RH	12 Months
Intermediate	30°C ± 2°C / 65 % RH ± 5% RH	6 Months
Accelerated	40°C ± 2°C / 75 % RH ± 5% RH	6 Months

1.2.2. Accelerated Stability Studies

One of the primary benefits of forced degradation (stress testing) studies is to assist in developing stability-indicating analytical methods by providing an insight into the likely degradation products of any given drug substance or drug product. These studies when carried out on both the drug substance and product provide information of the degradation chemistry by producing "potential" degradation products that may or may not be formed under relevant storage conditions. These 'degradants' expose the degradation pathways available to the drug and facilitate the development of stability-indicating analytical methods. These methods are then used to assist in monitoring drug stability during long-term stability studies to determine which products typically form under room temperature and accelerated stability conditions and quantify these changes due to stability.[9]

During product development, accelerated stability tests are carried out to optimise the stability of a potential formulation (e.g., selection of excipients, pH, dosage form, and packaging type). Stability data from this part of the study can also be used to suggest suitable storage conditions and indicate a potential shelf-life for the product. Accelerated stability studies are, in general, performed at elevated temperatures and employ the Arrhenius equation to predict the shelf-life or retest period at room temperature or with respect to other potential storage conditions, such as in cases where the product is designed to be stored under refrigerated conditions.

To minimise the potential for further degradation between the initial stressing in accelerated stability studies and analysis samples are typically refrigerated after exposure to the stress or

accelerated ageing process. Furthermore, during the analytical sequence, the quantification of the of the unstressed starting test material is compared with stressed material within the same assay / analytical measurement and the stressed sample recovery is expressed as percent of unstressed sample recovery i.e. area normalisation.

The concept of accelerated stability testing is based upon the Arrhenius equation (1) and modified Arrhenius equation (2):

$$LnK = LnA - \frac{Ea}{RT} \quad (1)$$

where K is the degradation rate, A is the frequency particle collision factor, Ea is the activation energy (kJ/mol), R is the universal gas constant (1.987 cal/(mol K)) and T is the absolute temperature (expressed in Kelvin).

$$\log \frac{K2}{K1} = -\frac{Ea}{2.303\,R}\ \frac{1}{(T2-T1)} \quad (2)$$

where k1 and k2 are rate constants at temperatures T1 and T2 expressed in degree kelvins; Ea is the activation energy; R is the gas constant. These equations describe the relationship between storage temperatures and degradation rate. Using Arrhenius equation, projection of stability from the degradation rates observed at high temperatures for some degradation processes can be determined.

1.3. Chemical and Physical Stability

In physical stability, the physical states are significantly considered for the stability of drug products. The physical properties of drug such as appearance (size, shape,,and colour), uniformity, palatability, and dissolving and suspending ability should be maintained throughout the period of its shelf life. The physical changes depend upon the physical characteristics of the drug products such as particle size, texture, melting point, polymorphic behaviour, and morphology. The physical changes can have deleterious effects too. The physical evaluation of the solution is of particular importance for intrathecal, ocular and intra-arterial routes. A tablet may become soft and ugly or intra- arterial routes. A tablet may become soft and ugly, or it may become very hard and show very slow dissolution time as a result of which bioavailability may not be good, so physical stability studies are also essential. A more appropriate physical evaluation, using turbidimetry, particle size analysis, dynamic light scattering or microscopic

analysis, is particularly important for large molecules or protein based products to evaluate kinetic profiles of aggregation and degradation[10] (Fig. 3).

However, in addition to physical stability, instability resulting from chemical degradation can also be a problem for high-energy amorphous molecules. Previous work has suggested that Studies drug-excipient interactions can play a role in stabilising hot melt extruded amorphous products[11]. Similar work has also shown that including polymers such as HPMCAS and Soluplus® into an amorphous formulation can improve chemical stability when compared to the API alone.[12]

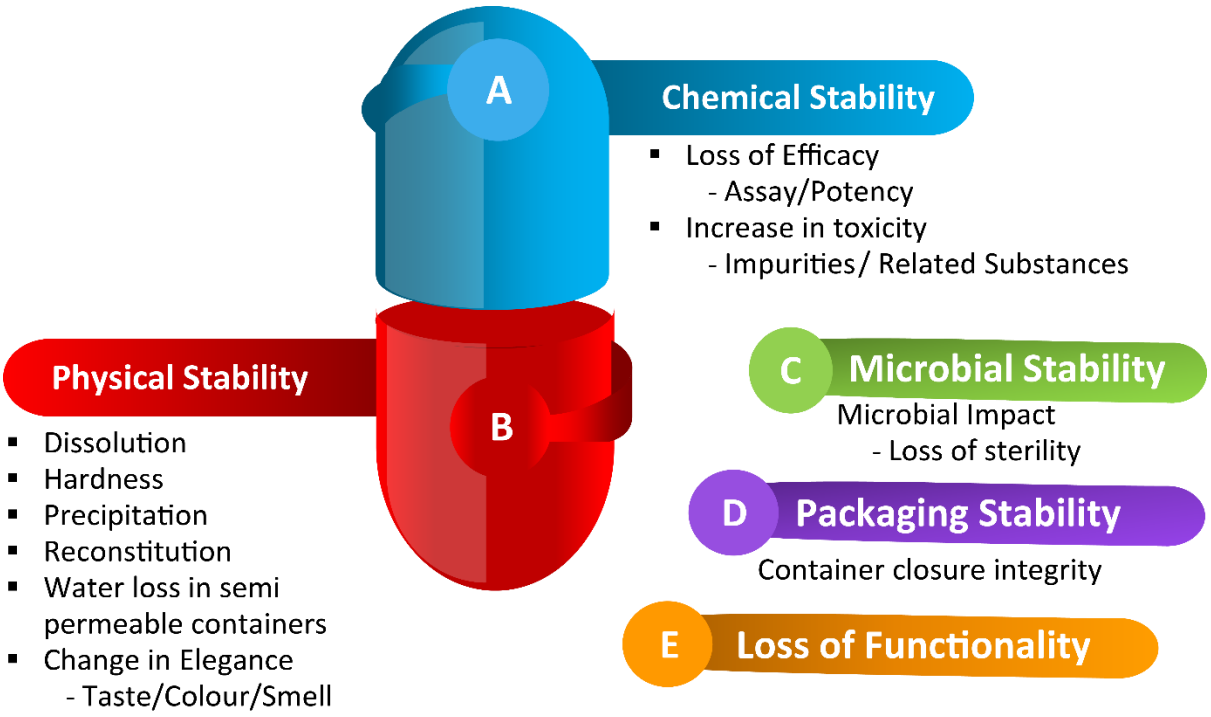

Figure 3: Stability Parameters.

1.4. Influence of Formulation on Stability

Amorphous formulations represent a promising approach to overcome limited bioavailability of poorly soluble drugs. However, the amorphous state is unstable, and there is a risk that an amorphous material will recrystallise during the typical shelf-life of a medicine (2-3 years), limiting the benefits of such formulations. In order to improve the stability of an active pharmaceutical ingredient (API) in the amorphous state, common strategies include co-processing it with a high glass transition (Tg) polymeric excipient to produce an amorphous dispersion. The

greater the temperature differential between the Tg and the storage temperature, the lower the likelihood of crystallisation. The components of a stable and robust amorphous dispersion must be carefully selected to optimise the solubility of the API in the polymer and thus reduce the risk of phase separation in the amorphous system. An important point to consider is that obtaining a one-phase system requires the two components to be thermodynamically miscible during processing. An understanding of drug-polymer thermodynamic phase diagrams which indicate not only the solubility of (crystalline) drug in the polymer but also the amorphous drug-polymer miscibility is important, due to the potential correlation of these parameters to the physical stability of the amorphous solid dispersion (Fig. 4).[10]

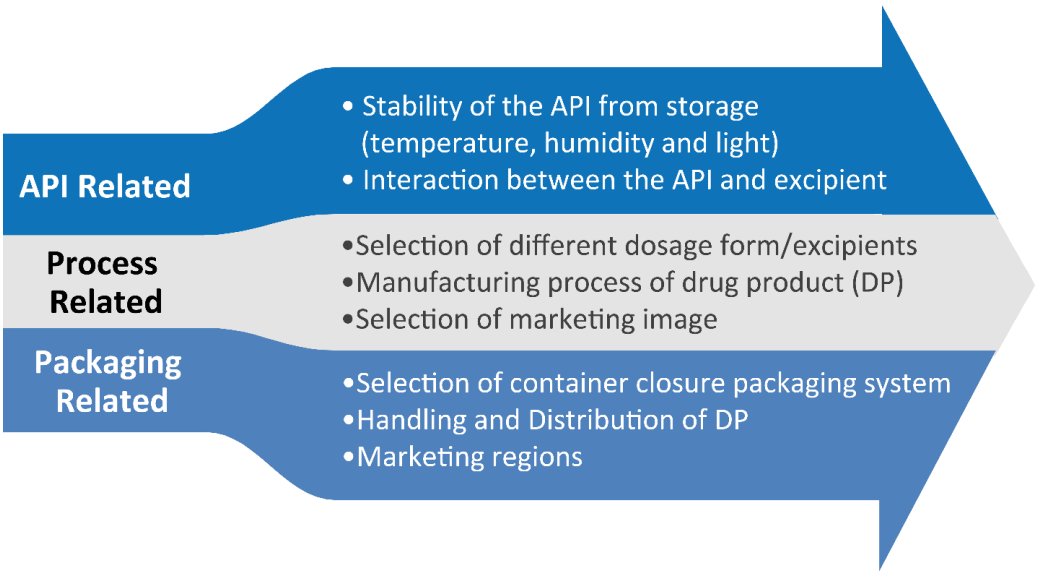

Figure 4: Factors affecting Pharmaceutical Stability.

1.5. Influence of Storage on Drug Product

Selection of appropriate packaging material plays an important role in the protection of any potential drug product. The primary role of packaging is to protect a drug substance or drug product from the influence of its environment, but the packaging material should not under any circumstances become a source for chemical or physical interaction with the product contained therein. Packaging-related interactions between the drug substances and products have had plenty of historical precedent and packaging selection should be considered as an important

component in the overall quality control strategy to ensure product quality safety and efficacy for the duration of the intended shelf-life of a product.

The moisture inside packaging equilibrates between headspace, drug products and desiccant if present. To measure moisture transfer is key to understand the importance to select a suitable primary packing material to prevent degradation and extend shelf-life when necessary (Fig. 5).

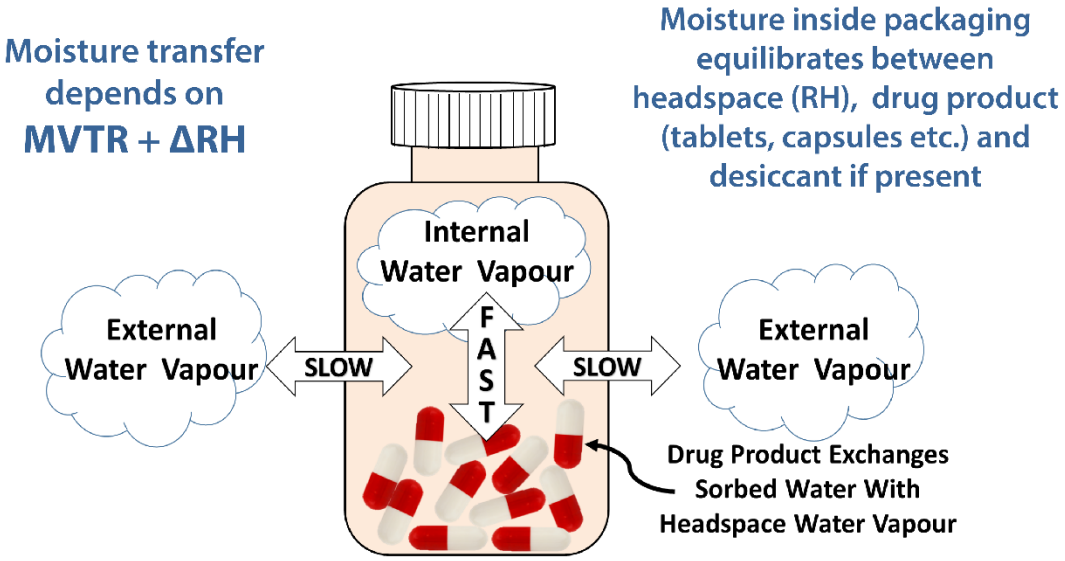

Figure 5: Role of Packaging in Drug Product Stability.

1.6. Modelling and Prediction

This accelerated predictive stability methodology, while often described as a modern approach to stability analysis but the key concepts are based on the works of Arrhenius in 1889[13] which when combined with material moisture sorption models[14] and the empirical experimentation by Genton and Kesselring[15] which took into account the effect of moisture on reaction kinetics resulting in Equation 3 below. Waterman advanced this reaction modelling by including the impact of other factors (e.g. packaging MVTR) to explore the protective effects of different packaging conditions.[16]. Most recently discussion have begun to investigate ways of formally incorporating accelerated approaches into updates of the ICH guidelines. [17]

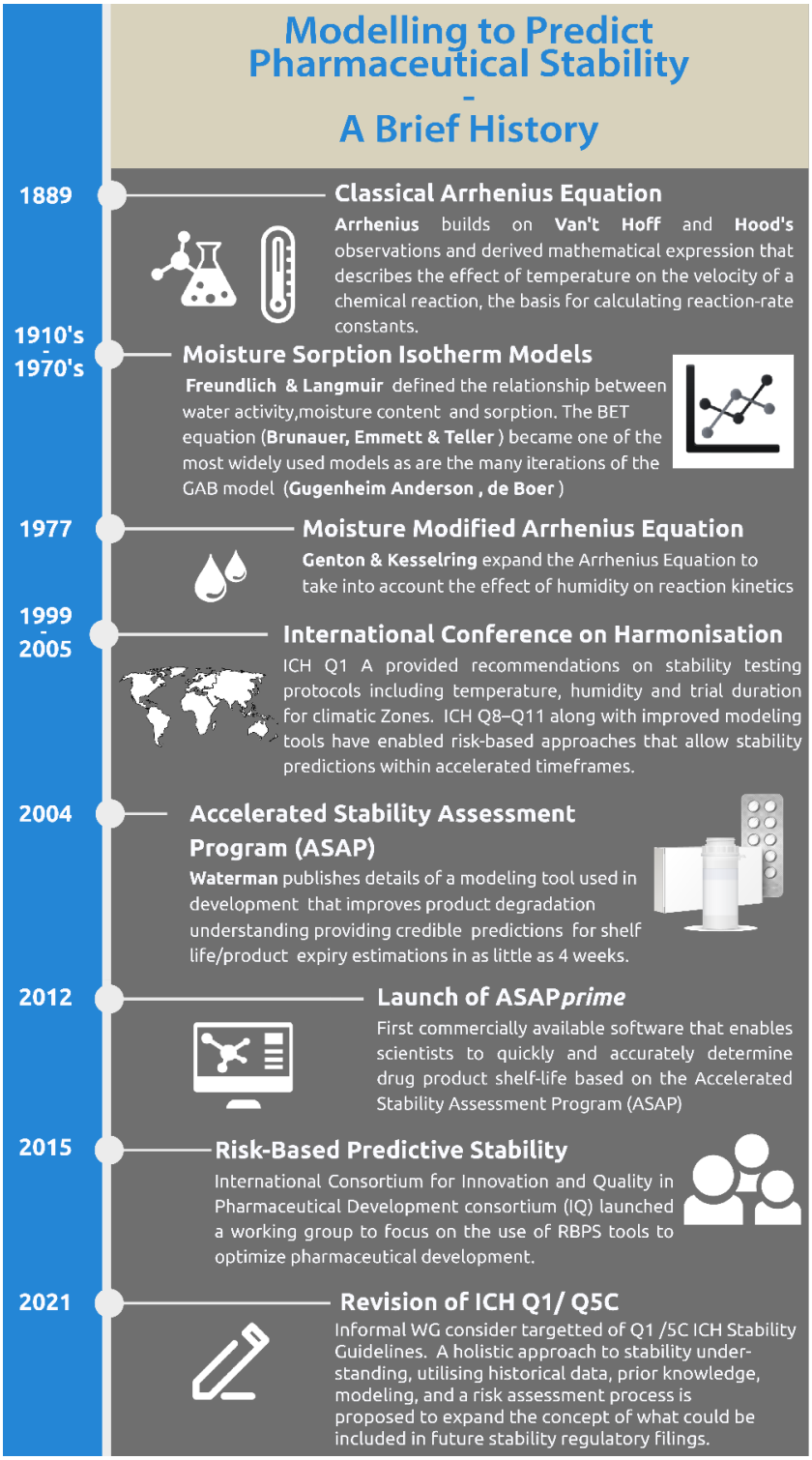

Figure 6: Key Dates in Development of APS Approaches

The modelling and stability predictions of the tested formulations can be performed using either standard statistical software programs (JMP Pro, SAS [18] [19]) or more recently commercial software applications e.g. ASAPprime® from Freethink Technologies, Branford, CT, USA [20] . This software package calculates the degradation rate at the isoconversion time (defined as the time when the percentage of crystallisation reaches the specification limit) for each temperature and relative humidity condition. A humidity-corrected Arrhenius equation is used to estimate the effect of temperature and relative humidity on the crystallisation rates of the amorphous solid dispersions (Eq.1).

$$lnK = lnA - \frac{Ea}{RT} + B\ (RH) \qquad \text{(Eq. 1)}$$

where k is the cyrstallisation rate (% crystallised drug/day), T is the temperature in Kelvin degrees, A is the collision factor, B is the moisture sensitivity factor, RH is the relative humidity, Ea is the activation energy in kcal mol^{-1}, and R is the gas constant. In order to calculate the degradation rate, the amount of crystallised drug at different time points should be fitted at each condition to different kinetic models such as zero-order, first-order, second-order, Avrami, and diffusion using the following equations (Eq. 2-6) [21]:

Zero-order: $[DC] = kt$ (Eq. 2)

1st order: $[DC]=[DC]_\infty[1-e^{(-kt)}]$ (Eq. 3)

2nd order: $[DC]=[DC]_\infty kt/ (1/[DC]_\infty + kt)$ (Eq. 4)

Diffusion: $[DC]=kt^{1/2}$ (Eq. 5)

Avrami: $[DC] = [DC]_\infty - e^{(-kt\wedge 2)}$ (Eq. 6)

where t is the time expressed in days, K is the crystallisation rate over time, and [DC] is the amount of crystalline drug expressed in percentage at each time point. To test the suitability of the models, the regression coefficient (R^2) is used. The Arrhenius equation is employed to estimate the activation energy and the effect of temperature on the degradation and/or crystallisation rate of each drug in each amorphous system. The predicted degradation rate at typical storage conditions can be extrapolated from the calculated Arrhenius equations (at accelerated ageing conditions) and compared with real-time data collected over the expected retest period or shelf-life to validate the predicted stability models.

1.6.1. Guide to Performing an APS Study

To perform an APS study, three stages are required: ageing, analysis and model building and stability prediction (Fig. 7).

Stage 1 (Sample Ageing): In this stage, the stability chambers are prepared based on the temperature and relative humidity conditions selected. Specific saturated salt solutions are introduced in each chamber to reach the desired relative humidity. Ideally, samples should not be introduced inside the chambers till the relative humidity and temperature have reached equilibrium, which should be confirmed with the corresponding sensor. Chambers with a small headspace tend to equilibrate faster than large containers. Once the stability chambers are ready, final dosage forms without packaging material are introduced in a glass vial within each chamber. Powder APIs can also be tested for which is recommended to weigh and introduce the same amount of material in each stability chamber. To minimise errors during the sample analysis at the stage 2, samples should be introduced sequentially in each chamber in such a way that at the end of the study all the samples are withdrawn and analysed in a single batch.

Stage 2 (Sample Analysis): the aged test material will typically be analysed using a stability indicating HPLC method. Depending on the set APS protocol, the percentage of degradants or the drug loss at different time points and conditions will be quantified (Other quantitative analytical techniques that measure degradation, change over time can also be used) . It is key to ensure a high reproducibility in the method to reduce the overall standard error of the experiment.

Stage 3 (Model Building and Stability Prediction): the data obtained in stage 2 will be used to build the corresponding degradation kinetic models. The degradation rate will be determined based on the theoretical model that fits better the experimental data points in all the conditions tested. At this point, the isoconversion time should be considered and the model with the best fitting around the specification limit should be selected. Those conditions that led to a high percentage of degradation should be removed as they are not relevant and can alter the selection of the most suitable degradation profile. Once the degradation rates (“k”) are calculated, the activation energy and b value can be calculated from the modified-Arrhenius equation. Based on this equation, the degradation rate at ICH conditions can be extrapolated, and hence, the long-term stability prediction can be obtained.

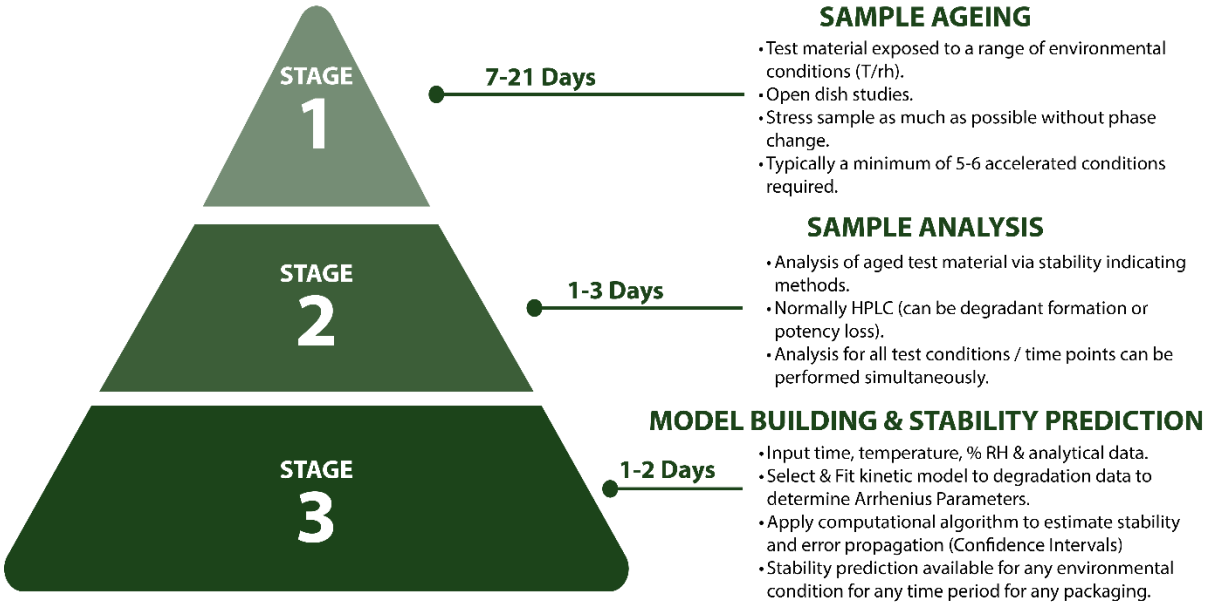

Figure 7: Steps required to perform an APS Study.

In conclusion APS approaches including Risk Based Predictive Strategies and the Accelerated Stability Assessment Program (ASAP) are routinely used within the pharmaceutical industry to quickly assess stability characteristics. The primary function of these studies is to determine product shelf life (Fig. 8) but one of the secondary benefits can be to provide key insights to understanding drug degradation pathways and kinetics. These tools can then provide a much more realistic prediction of the levels of degradation expected to be found in a pharmaceutical product rather than those suggested by traditional stress testing where new components (hydrochloric acid, hydrogen peroxide and sodium hydroxide) are often introduced and cause additional degradation products. The modelling tools can provide results within days or weeks when compared to the months or possibly years needed for traditional studies.

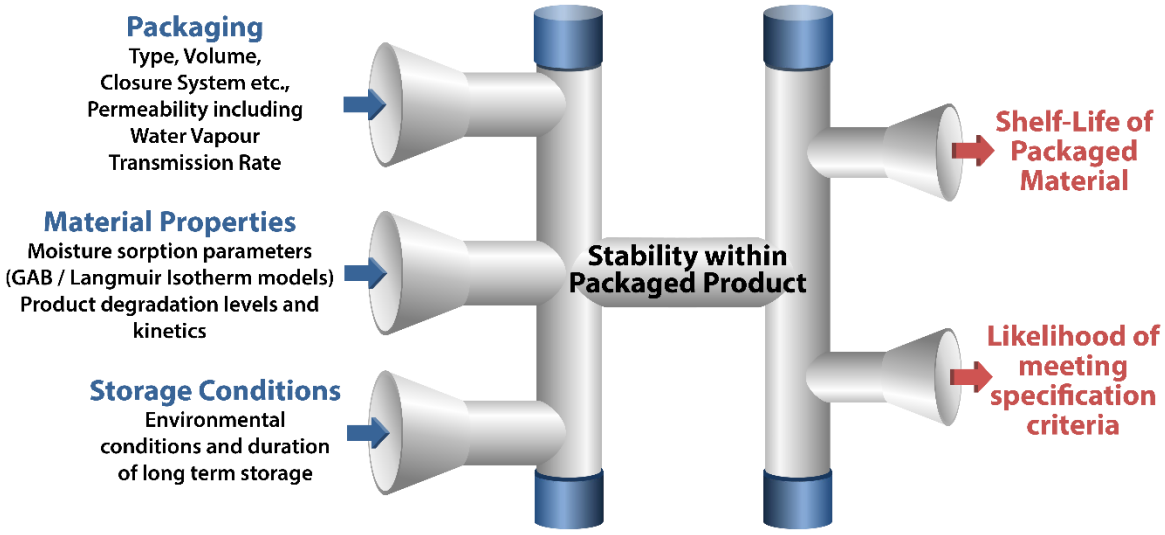

Figure 8: Typical Inputs and Outputs of an APS Study

References

(1) Buehler, G.; Huynh-Ba, K. Regulatory Perspectives on Product Stability. In *Pharmaceutical Stability Testing to Support Global Markets*, Huynh-Ba, K. Ed.; Springer New York, 2010; pp 9-13.

(2) International Council for Harmonisation of Technical Requirements for Pharmaceuticals for Human Use (ICH). Q1A (R2) Stability Testing of New Drug Substances and Products. 2003.

(3) International Council for Harmonisation of Technical Requirements for Pharmaceuticals for Human Use (ICH). Q1B Photostability Testing of New Drug Substances and Products. 1996.

(4) International Council for Harmonisation of Technical Requirements for Pharmaceuticals for Human Use (ICH). Q1C Stability Testing: Requirements for New Dosage Forms. 1996.

(5) International Council for Harmonisation of Technical Requirements for Pharmaceuticals for Human Use (ICH). Q1E Evaluation of Stability Data. 2003.

(6) International Council for Harmonisation of Technical Requirements for Pharmaceuticals for Human Use (ICH). Q5C Stability Testing of Biotechnological/Biological Products. 1995.

(7) Huynh-Ba, K. Introduction. In *Pharmaceutical Stability Testing to Support Global Markets*, Huynh-Ba, K. Ed.; Springer New York, 2010; pp 3-5.

(8) International Council for Harmonisation of Technical Requirements for Pharmaceuticals for Human Use (ICH). Q1D Bracketing and Matrixing Designs for Stability Testing of Drug Substances and Drug Products. 2002.

(9) Baertschi, S. W.; Hetrick, E. M.; Hoaglund Hyzer, C. S.; Pack, B. W.; Roberts, J. C.; Wolfe, C. N. Chapter 11 - Implementing an Accelerated Predictive Stability Program. In *Accelerated Predictive Stability*, Qiu, F., Scrivens, G. Eds.; Academic Press, 2018; pp 253-283.

(10) Caron, V.; Hu, Y.; Tajber, L.; Erxleben, A.; Corrigan, O. I.; McArdle, P.; Healy, A. M. Amorphous solid dispersions of sulfonamide/Soluplus® and sulfonamide/PVP prepared by ball milling. *AAPS PharmSciTech* **2013**, *14* (1), 464-474. DOI: 10.1208/s12249-013-9931-7 From NLM.

(11) Haser, A.; Cao, T.; Lubach, J. W.; Zhang, F. In situ salt formation during melt extrusion for improved chemical stability and dissolution performance of a meloxicam–copovidone amorphous solid dispersion. *Molecular pharmaceutics* **2018**, *15* (3), 1226-1237.

(12) Alshahrani, S. M.; Lu, W.; Park, J.-B.; Morott, J. T.; Alsulays, B. B.; Majumdar, S.; Langley, N.; Kolter, K.; Gryczke, A.; Repka, M. A. Stability-enhanced hot-melt extruded amorphous solid dispersions via combinations of Soluplus® and HPMCAS-HF. *AAPS PharmSciTech* **2015**, *16* (4), 824-834.

(13) Arrhenius, S. Über die Reaktionsgeschwindigkeit bei der Inversion von Rohrzucker durch Säuren. *Zeitschrift für Physikalische Chemie* **1889**, *4U*, 226 - 248.

(14) Zou, L.; Gong, L.; Xu, P.; Feng, G.; Liu, H. Modified GAB model for correlating multilayer adsorption equilibrium data. *Separation and Purification Technology* **2016**, *161*, 38-43. DOI: https://doi.org/10.1016/j.seppur.2016.01.026.

(15) Genton, D.; Kesselring, U. W. Effect of Temperature and Relative Humidity on Nitrazepam Stability in Solid State. *Journal of Pharmaceutical Sciences* **1977**, *66* (5), 676-680. DOI: https://doi.org/10.1002/jps.2600660517.

(16) Waterman, K. C.; Macdonald, B. C. Package Selection for Moisture Protection for Solid, Oral Drug Products. *Journal of Pharmaceutical Sciences* **2010**, *99* (11), 4437-4452. DOI: https://doi.org/10.1002/jps.22161.

(17) McMahon, M. E.; Abbott, A.; Babayan, Y.; Carhart, J.; Chen, C.-w.; Debie, E.; Fu, M.; Hoaglund-Hyzer, C.; Lennard, A.; Li, H.; et al. Considerations for Updates to ICH Q1 and Q5C Stability Guidelines: Embracing Current Technology and Risk Assessment Strategies. *The AAPS journal* **2021**, *23* (6), 107. DOI: 10.1208/s12248-021-00641-6.

(18) Clancy, D.; Hodnett, N.; Orr, R.; Owen, M.; Peterson, J. Kinetic Model Development for Accelerated Stability Studies. *AAPS PharmSciTech* **2017**, *18* (4), 1158-1176. DOI: 10.1208/s12249-016-0565-4 From NLM.

(19) Fu, M.; Perlman, M.; Lu, Q.; Varga, C. Pharmaceutical solid-state kinetic stability investigation by using moisture-modified Arrhenius equation and JMP statistical software. *Journal of Pharmaceutical and Biomedical Analysis* **2015**, *107*, 370-377. DOI: https://doi.org/10.1016/j.jpba.2015.01.014.

(20) Waterman, K. C. The application of the Accelerated Stability Assessment Program (ASAP) to quality by design (QbD) for drug product stability. *AAPS PharmSciTech* **2011**, *12* (3), 932-937. DOI: 10.1208/s12249-011-9657-3 From NLM Medline.

(21) Freethink Technologies, I. ASAPprime® user's guide. **2013**. Cerda, J. R.; Arifi, T.; Ayyoubi, S.; Knief, P.; Ballesteros, M. P.; Keeble, W.; Barbu, E.; Healy, A. M.; Lalatsa, A.; Serrano, D. R. Personalised 3D Printed Medicines: Optimising Material Properties for Successful Passive Diffusion Loading of Filaments for Fused Deposition Modelling of Solid Dosage Forms. *Pharmaceutics* **2020**, *12* (4). DOI: 10.3390/pharmaceutics12040345.

Hypothesis & Aims

2. Hypothesis & Aims

2.1 Hypothesis

In keeping with a Quality by Design (QbD) approach to improve pharmaceutical product design and formulation, there exists an opportunity to expand upon the current use of APS methodologies in predicting pharmaceutical stability. Heretofore, most APS techniques focussed on predicting chemical stability of small molecules. There is a shortage of research into the application of APS techniques with regard to physical stability, loss of stability is not always based on chemical changes, and therefore different kinetic models of drug degradation and the suitability of various analytical methods to evaluate physical stability should be explored. Therefore, we propose to expand upon current proven approaches to study the physical stability of pharmaceuticals and determine whether physical or chemical stability becomes the shelf life limiting parameter.

The hypothesis underpinning the current work is that APS testing and chemometrics can be applied simultaneously to determine the chemical and physical stability of amorphous solid dispersions prepared with different carriers and by different manufacturing technologies, to determine in a fast and efficient manner which process, and polymer is most suitable to stabilise an amorphous drug.

2.2 Aims

The aim of this project is to investigate the application of APS techniques for the assessment of physical and chemical stability, whilst also attempting to improve the understanding of the relationship between the different physical properties (mainly crystallisation) which may impact product performance during storage.

This aim can be divided into several discrete objectives, outlined below.

1. To develop analytical and statistical methods to allow for the ageing, analysis, and modelling of both physical and chemical stability of a range of amorphous solid dispersions.
2. APS strategies applied to screening pharmaceutical formulation processes: a case study of spray dried and hot melt extruded nifedipine amorphous solid dispersions. In this work, nifedipine has been selected as a model drug considering its high tendency to recrystallise and its poor aqueous solubility. Amorphous solid dispersions were prepared by either SD or HME utilising two different polymers: Soluplus® (SOL) consisting of polyvinyl caprolactam-polyvinyl acetate-polyethylene glycol graft copolymer or poly-vinylpyrrolidone vinyl acetate (PVPVA64). Full physicochemical characterisation of the formulations was performed. APS stability testing at a wide range of temperatures and RH was carried out. Samples were analysed at different time points by HPLC for chemical stability and by XRD and DSC for physical stability. NIR measurements were performed at the same time points in order to correlate the spectra with drug content and crystallisation using different chemometric tools. Modelling of stability data was developed for a deeper understanding of the crystallisation and degradation kinetics of nifedipine within an amorphous matrix to guide the ASD development decision-making process.
3. To prepare amorphous solid dispersions using selected BCS Class II active pharmaceutical ingredients (Budesonide, Ritonavir, Griseofulvin and Celecoxib) and polyvinylpyrrolidone K 90 (PVP K90) and hypromellose acetate succinate (HMPCAS) as common amorphous polymer carriers and to perform stability studies of both amorphous solid dispersions as free powders and compacts using an Accelerated Predictive Stability (APS) approach.
4. Validating all chemical and physical stability predictions against real time stability data collected under both traditional long term and accelerated stability storage conditions.

Chapter 3

3.0. Accelerated Predictive Stability (APS) strategies applied to screening pharmaceutical formulations: A comparison of spray dried and hot melt extruded nifedipine amorphous solid dispersions

Peter O'Connell[1,2,3], Joshua H. Yoon[4], Luke M. Geever[4], Nigel T. McSweeney[3], Anne Marie Healy[2]*, Dolores R. Serrano[1, 5*]

[1]Department of Pharmaceutics and Food Technology, School of Pharmacy, Universidad Complutense de Madrid, Plaza Ramon y Cajal s/n, 28040-Madrid, Spain.

[2]Synthesis and Solid State Pharmaceutical Centre (SSPC), School of Pharmacy and Pharmaceutical Sciences, Trinity College Dublin, Dublin 2, Ireland.

[3]Cuspor Limited, Dublin 2, Ireland

[4]Applied Polymer Technologies Gateway (APT), Athlone Institute of Technology, Dublin Road, Athlone, Co. Westmeath, Ireland.

[5]Instituto Universitario de Farmacia Industrial (IUFI), School of Pharmacy, Universidad Complutense de Madrid, Avenida Complutense, 28040 Madrid, Spain.

*Corresponding authors:

Anne Marie Healy

School of Pharmacy and Pharmaceutical Sciences, Trinity College Dublin, Dublin 2, Ireland.

Tel +353 1896 1444 Email healyam@tcd.ie

Dolores R. Serrano

Department of Pharmaceutics, School of Pharmacy, Universidad Complutense de Madrid, Plaza Ramon y Cajal SN, 28040, Spain,

Tel: +34913941620, Email: drserran@ucm.es

Abstract:

There are many challenges when designing or formulating stable amorphous solid dispersions (ASD). Difficulties arise when attempting to predict what type of manufacturing process and which excipients or carriers will lead to the optimum formulation. The decision-making process cannot rely solely on results from dissolution experiments, as physicochemical stability studies are also necessary. In this study, four different nifedipine amorphous solid dispersions (ASDs) were manufactured using scalable pharmaceutical techniques (hot melt extrusion and spray drying) and pharmaceutical grade polymers (Soluplus® and poly-vinylpyrrolidone vinyl acetate (PVPVA), Kollidon® VA64). An Accelerated Predictive Stability (APS) approach to determine stability was performed, using HPLC to quantify nifedipine degradation, and using PXRD and DSC to measure crystallisation kinetics. NIR measurements were also performed to develop PLS regression models to quantify physicochemical changes in a cost-effective and non-destructive manner. All four ASDs demonstrated similar improved drug dissolution rates compared to the crystalline drug alone. However, using APS, significant differences were found in the stability of the formulations. The spray dried powders exhibited greater physical stability than the extrudates, which showed two glass transition (T_g) temperatures, indicating phase separation. In contrast, formulations manufactured by HME were found to have superior chemical stability than spray dried powders, which demonstrated greater moisture sensitivity. The chemical degradation kinetics for both spray dried formulations were more complex than for the equivalent extruded materials. At less extreme conditions of temperature and relative humidity, spray dried systems followed Avrami-type kinetics, but under more extreme conditions, a shift from Avrami to diffusion kinetics was observed, which may be attributed to the miscibility of the degradation products and polymer chains. In conclusion, of all the formulations tested, the spray dried formulation with PVPVA64 exhibited the best balance between physical and chemical stability and would be the recommended candidate for further evaluation. Accelerated predictive stability combined with chemometrics has been demonstrated to be a good methodology to aid in the decision-making process for pharmaceutical amorphous formulations.

Keywords: Nifedipine, accelerated predictive stability, APS; amorphous solid dispersions, spray-drying, hot melt extrusion, NIR modelling, PLSR, chemometrics, physical stability.

Graphical abstract:

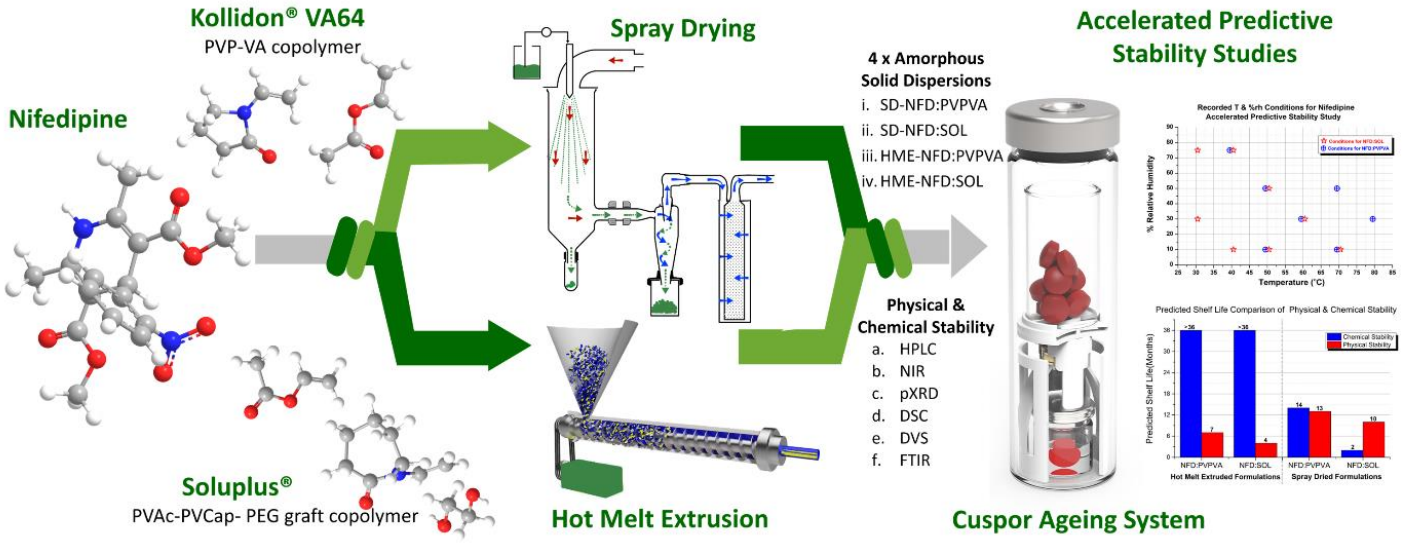

3.1 Introduction

Amorphous solid dispersions are currently one of the most common approaches utilised by the pharmaceutical industry to overcome solubility and dissolution issues when tackling the formulation of a poorly water-soluble drug for oral administration. There are a wide range of methods that may be used to produce amorphous solid dispersions but only a few, such as spray drying (SD) and hot melt extrusion (HME), are easily scalable [1].

SD is a bottom-up technique that allows fast solvent evaporation, triggering a rapid transformation of a drug-excipient solution into solid drug-excipient particles. The final physical structure of the particles will be dictated mainly by the solvent evaporation kinetics, but also by other formulation and process parameters such as solvent type, feed concentration, spray rate or gas flow rate, amongst others [1, 2]. In contrast, HME is a top-down strategy that involves pumping a solid mixture of drug and excipients, commonly with a rotating screw, at temperatures above their glass transition temperature (T_g) or their melting temperature (T_m) and forcing the feed material forward towards a die. The final physical structure of the extrudate will be highly dependent on the temperature selected and the degree of mixing of formulation components. Many formulation and process parameters play a role in the final characteristics of the product such as polymer type, rotating screw speed and presence of kneading and conveying elements [3].

To succeed when designing stable amorphous solid dispersions, there are several key considerations to bear in mind, such as the type of manufacturing process to use, the choice of suitable polymer, and the drug crystallisation kinetics, as the high tendency of an amorphous drug to recrystallise during storage is well known [4]. It remains challenging to predict what type of manufacturing process and which carrier will lead to the best amorphous solid dispersion of a particular drug, in terms of chemical and physical stability [5].

The ability to assess the stability profile at an early stage during the formulation development lifecycle is key for its success. However, stability testing using standard ICH conditions (25°C – 60% rh and 40°C - 75% rh) typically requires at least six months of laboratory data collection and uses a linear extrapolation of data derived from a very narrow range of temperatures [6]. The use of accelerated predictive stability (APS) testing, combining a significantly wider range of both temperature and relative humidity (RH) conditions, can make the decision-making process during

the development phase more accurate and faster and hence, more cost-efficient [7, 8]. However, to the best of our knowledge, there are a limited number of reports relating to the successful application of APS testing on amorphous solid dispersions, in terms of both chemical and physical stability assessment and prediction [9]. Also, very few attempts have been made to model degradation and crystallisation kinetics using chemometrics along with spectroscopic techniques.[10]

The hypothesis underpinning the current work is that APS testing and chemometrics can be applied simultaneously to determine the chemical and physical stability of amorphous solid dispersions prepared with different carriers and by different manufacturing technologies, to determine in a fast and efficient manner which process and polymer is most suitable to stabilise an amorphous drug.

In this work, nifedipine has been selected as a model drug considering its high tendency to recrystallise and its poor aqueous solubility [11]. Amorphous solid dispersions were prepared by either SD or HME utilising two different polymers: Soluplus® (SOL) consisting of polyvinyl caprolactam-polyvinyl acetate-polyethylene glycol graft copolymer or poly-vinylpyrrolidone vinyl acetate (PVPVA64). Full physicochemical characterisation of the formulations was performed. APS stability testing at a wide range of temperatures and RH was carried out. Samples were analysed at different time points by HPLC for chemical stability and by XRD and DSC for physical stability. NIR measurements were performed at the same time points in order to correlate the spectra with drug content and crystallisation using different chemometric tools. Modelling of stability data was developed for a deeper understanding of the crystallisation and degradation kinetics of nifedipine within an amorphous matrix to guide the ASD development decision-making process.

3.2 Materials and methods

3.2.1 Materials

Nifedipine (NFD) was purchased from Industria Chimica Italiana (Bergamo, Italia). Soluplus® (SOL) and Kollidon® VA64 (PVPVA64) were purchased from BASF (Darmsdat, Germany). Ethanol was supplied from Corcoran Chemicals (Ireland). Humidity capsules, dataloggers and stability chambers were provided by Cuspor Limited (Dublin, Ireland). All other chemicals were of reagent grade and were used as supplied. Solvents were of HPLC grade.

3.2.2 Methods

3.2.2.1 Spray drying

Spray drying was performed using a Büchi B-290 Mini Spray Dryer (Büchi, Flawil, Switzerland) operating in the open mode. Nitrogen (at 6 bar) was used as the drying and atomising gas in a co-current mode with the aspirator capacity set to maximum (100%). Solution concentrations of 2% (w/v) of nifedipine:polymer (1:1 weight ratio) were prepared using ethanol (200 ml). The solutions were delivered to a two-fluid nozzle (0.7-mm nozzle tip and a 1.5-mm diameter nozzle screw cap) using a peristaltic pump at a speed of 30% (9–10 ml/min). The flowmeter for the standard two-fluid nozzle was set at 473 NL/h. The inlet temperature was fixed at 78°C and the outlet temperature varied between 50°C and 57°C [12]. A high efficiency cyclone was used in order to improve the yield [13].

3.2.2.2 Hot melt extrusion

The weight ratio of nifedipine to polymer was 1:1 (w/w). HME was performed using a Prism twin-screw extruder (L/D 15:1 = 240 mm: 16 mm) (Thermo, Germany). The batch size used was 60 g for all extrusion studies. Conveying and kneading (30, 60, 90°) elements were assembled on the screw shafts. The screw speed was set at 100 rpm with a targeted feed rate of 0.5 kg/h. The extruder contained five heating zones, which were set at 30°C (feed throat), 55, 88, 130 and 150°C from the feeding zone to the exit die. An extruder soak-time of 30 minutes was employed to allow the extruder to heat and equilibrate fully before samples were extruded and collected. No visual sign of degradation inside the barrel was found.

3.2.2.3 Solid state characterisation

Powder X-ray diffraction (PXRD)

Powder X-ray analysis was performed in triplicate using a Miniflex II Rigaku diffractometer with Ni-filtered Cu Kα radiation (λ= 1.54 Å). The tube voltage and current used were 30 kV and 15 mA, respectively. Each sample was scanned over a 2Θ range of 5‑40º with a step size of 0.05 °/s [14].

Modulated temperature DSC (MTDSC)

MTDSC scans were recorded in triplicate on a QA-200 calorimeter (TA instruments, Elstree, UK) using nitrogen as the purge gas and indium as standard for calibration. Samples were weighed (4–6 mg) and sealed in closed aluminium pans with one pin-hole. A scanning rate of 5 °C/min, amplitude of modulation of 0.796 °C and modulation frequency of 1/60 Hz were employed. The temperature range was from 25 °C to 190 °C. The temperature of exothermic or endothermic events reported refers to the onset temperature. Glass transition temperatures were measured at the midpoint of the C_p shift.

Thermogravimetric analysis (TGA)

Analysis was performed using a TGA Q50 (TA instruments, Elstree, UK). Samples were placed into open aluminum pans (5−10 mg) and a heating rate of 10 °C/min was implemented in all measurements. Analysis was carried out in triplicate using a furnace under nitrogen purge and monitored by TA analysis software.

Fourier-transformed infrared Spectroscopy (FTIR)

FTIR spectra (n=6) of the four formulations were recorded in the range of 650-4000 cm^{-1} on a PerkinElmer Spectrum 1 FTIR Spectrometer equipped with a UATR and a diamond/ZnSe crystal accessory with a resolution of 4 cm^{-1}. Baseline correction and data normalization were performed using Spekwin32 version 1.71.6.1.

Dynamic vapour sorption (DVS)

Water sorption kinetic profiles were obtained using a DVS (Advantage, Surface Measurement Systems, Alperton, UK) at 25.0 ± 0.1 °C with water as the selected solvent. Samples were dried at 0% RH for 1 h and then subjected to step changes of 10% RH up to 90% RH, and the reverse for desorption. The sample mass was allowed to reach equilibrium, defined as dm/dt≤0.002 mg/min over 10 min, before the RH was changed [6, 18]. Sample weights were between 5 and 10 mg. The crystalline/amorphous nature of the systems was assessed by PXRD after every complete run. The percentage of vapour uptake in the first sorption cycle at the different steps of RH was used to calculate GAB parameters using ASAPprime software (FreeThink Technologies Inc.) [7].

Scanning electron microscopy (SEM)

Surface images of the four formulations were performed using a Zeiss Supra Variable Pressure Field Emission Scanning Electron Microscope (Germany) equipped with a secondary electron detector at 5 kV. Samples were glued onto aluminium stubs and sputter-coated with gold under vacuum prior to analysis [15].

3.2.2.4 Dissolution studies

Dissolution studies were performed in a Sotax AT-7 dissolution apparatus (Sotax, Wallbrunnstraße, Germany) using the USP Apparatus I method (Basket). To avoid the floating of the powders, a V-cap HMPC size 1 capsule was filled with 80 mg of the formulation (equivalent to 40 mg of nifedipine, which is comparable to the dosage available in marketed forms of nifedipine). For comparison purposes, unprocessed nifedipine and physical mixtures containing 1:1 weight ratio of nifedipine: polymer prepared in a mortar and pestle were also tested under the same conditions as the spray dried and hot melt extruded formulations. Hot melt extrudates were grinded in a mortar and pestle to reduce the particle size. A sieved fraction below 27 µm was collected and tested for all the systems. The dissolution studies were carried out in deionised water (900 ml) at 37 °C at a rotation speed of 100 rpm in triplicate for each formulation. Aliquots (5 ml) were withdrawn without volume replacement at appropriate intervals, filtered through a 0.45 µm PTFE hydrophilic filter (Fisher Scientific, Dublin, Ireland) and analysed using a UV spectrophotometer (Helios γ, Thermo Electro Corporation) connected to a Thermo Spectronic

single cell peltier at 37 °C at 230 nm. Statistical ANOVA followed by Tukey's test considering p-values for statistical significance < 0.05 was performed in Minitab® (Minitab Ltd, Coventry, UK). The dissolution data obtained was fitted to different kinetic equations (zero order, first order, Hixson–Crowell and Korsmeyer–Peppas) to investigate the differences observed in the release profile using DDsolver [12, 16].

3.2.2.5 Ageing of the samples

All the formulations were kept at a fixed temperature (25.33 ± 1.21 °C) in a desiccator containing silica gel (RH= 11.01 ± 1.64 % RH) prior to commencing the accelerated ageing/stability testing of the test material. The Cuspor Ageing System ™ was used to age each test material. The relevant humidity capsules were placed into the Cuspor chambers which were put inside the oven at the selected temperature in order to ensure that equilibrium RH was reached prior to the ageing of the formulations. A wireless Hygrochron datalogger (Maxim Integragrated, San Jose, USA) was placed inside each test chamber to monitor the temperature and relative humidity, and was set to record data at thirty minute intervals [17]. The mean temperature and relative humidity of exposure for every temperature/RH condition during the experiment were calculated using Thermotrack PC Software (Proges Plus, France), and this data was subsequently used in the prediction models described below. A schematic illustration of the Cuspor Ageing System can be found in supplementary material in Figure S1.

Considering the differences in T_g between the selected polymers (~69°C for Soluplus® and ~108°C for PVPVA64, (Figure. S2, Supplementary material)), exposure to milder temperatures was selected for those formulations containing Soluplus®. Hence, the nominal conditions used for sample ageing were the following : 30°C/30%rh, 30°C /75%rh, 40°C/10%rh, 40°C /75%rh, 50°C /10 %rh, 50°C /50%rh, 60°C /30 %rh, 70°C /10%rh for Soluplus® formulations and 40°C /75%rh, 50°C /10%rh, 50°C /50%rh, 60°C /30%rh, 70°C /10 %rh, 70°C /50%rh, 80°C /30%rh for PVPVA64 formulations. The unprocessed crystalline NFD was subjected to all the above conditions. The time-points were selected to vary according to the conditions employed. Longer time points (> 14 days) were established for milder conditions such as 50 °C and RH <30%.

Sample ageing conditions were selected to ensure there was not a linear relationship between temperature and relative humidity capable of introducing bias into the analysis, as otherwise it is

difficult to determine the independent effects of each variable [18] . A plot of the nominal stability testing conditions is shown in Figure 9.

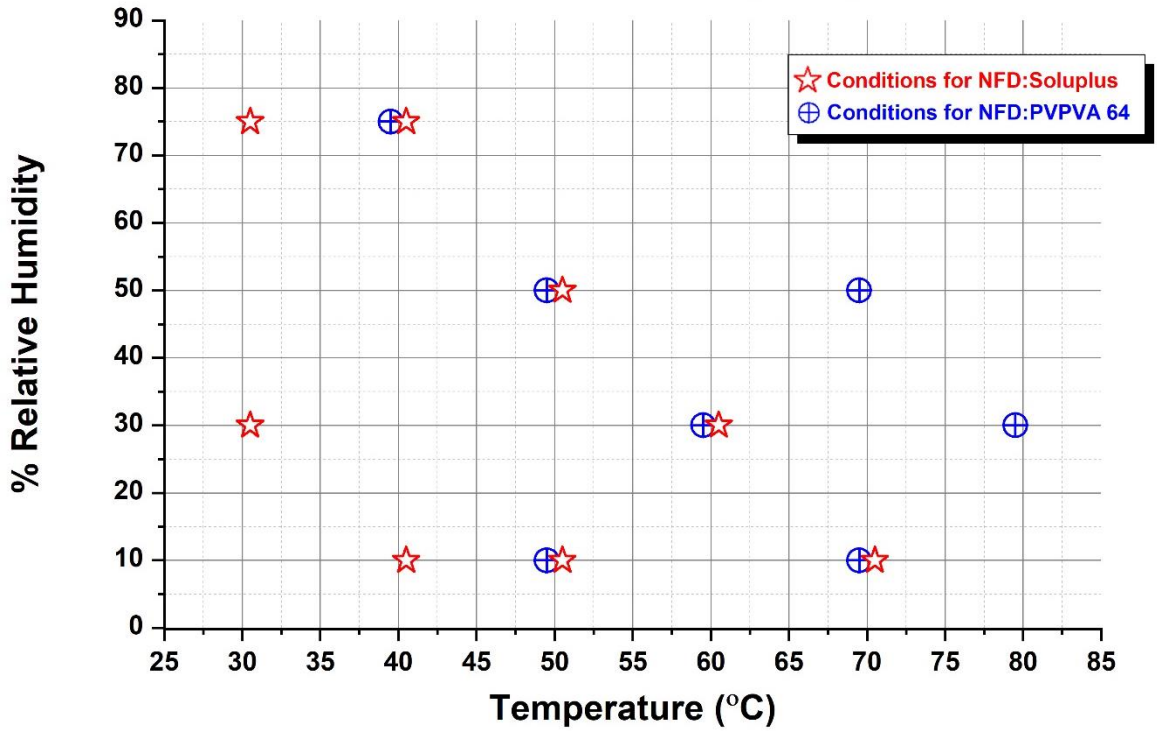

Figure 9: Sample Ageing conditions for APS of NFD amorphous solid dispersions.

Powdered aliquots of each formulation (ca. 20 mg) were weighed and placed into separate uncapped glass vials (11.6 mm x 32 mm) and introduced into the test chambers where they were exposed to different conditions of temperature and humidity. At different time points over a four-week period, samples were collected and analysed by HPLC for chemical stability and by PXRD and DSC for physical stability in order to quantify crystalline drug content. NIR measurements were also performed at the same times in order to construct prediction models, correlating chemical and physical degradation from the NIR spectra data.

3.2.2.6 Quantification of amorphous content

Calibration curves to quantify the amorphous content were prepared by mixing varying ratios of a 1:1 ratio (w/w) crystalline API:excipient (Xc) and ASD with a mortar and pestle. Different weight fractions of Xc (0.1, 0.25, 0.5, 0.75, 0.9) were mixed with ASDs (prepared by SD or HME as above described). The total mixed sample weight was 200 mg. Each set of reference standards

was analysed by PXRD and DSC for each weight fraction [19]. Calibration curves were produced in duplicate for each system and analytical method. The position of the PXRD peaks used for the quantification was at 8.15 and 16.25 2Θ degrees, which were selected due to the lack of interference with other peaks in the diffractogram. Rigaku Peak Integral software was used in the determination of peak intensity for each sample using the Sonnefelt-Visser background edit procedure. The first calibration curve using PXRD was constructed using the combined area of the two characteristic peaks for each weight fraction. The second calibration curve was constructed to determine the percent crystallinity of the sample via DSC using the enthalpy of fusion corresponding to the melting of NFD [20].

3.2.2.7 Quantification of nifedipine degradation

At different time points, samples were collected, diluted with mobile phase and analysed by HPLC to calculate the percentage of degraded nifedipine. HPLC analysis was performed using a Water Alliance HPLC with a Waters 2695 Separations module system and Waters 2996 Photodiode array detector. Separation was performed with a Thermo BDS Hypersil C18-reverse-phase column (200 x 4.6 mm, 5 µm) at 25º C and at a UV detection wavelength of 240 nm with an injection volume of 20 µL. The mobile phase consisting of methanol: water: acetonitrile (36:55:9, V:V:V) was pumped at a flow rate of 1 mL/min. Non-aged crystalline NFD was used as standard.

3.2.2.8 Accelerated Predictive Stability (APS) modelling

The modelling of chemical and physical stability of the four formulations was performed using ASAPprime®. A humidity-corrected Arrhenius equation was used to estimate the effect of temperature and RH on the chemical degradation and crystallisation rates of the amorphous solid dispersions (Eq.1) [21]:

$$\ln K = \ln A - \frac{Ea}{RT} + B\,(RH) \qquad \text{(Eq. 1)}$$

where K is the degradation rate (% drug degraded/day or crystallised/day), A is the collision factor, T is the absolute temperature in Kelvin, R is the gas constant (1.985 cal/mol/K), Ea is the activation energy in cal/mol, RH is the relative humidity and the B term is the moisture sensitivity factor [7]. The B term was calculated using the following equation:

$$B(RH)=\frac{\mathrm{Ln}(\frac{k_1}{k_2})}{RH_1-RH_2} \quad \text{(Eq. 2)}$$

where K1 and K2 are the degradation constants calculated at the same temperature but different relative humidity, RH1 and RH2, respectively. An average B term calculated at the different ageing temperatures was used.

The methods provided by the software which were used were "potency with RH" for the chemical stability/degradation of nifedipine and "degradation with RH" for the physical stability/percentage of crystallinity of the ASDs. Parameters selected for modelling were the following: limit of detection 0.5%, specification limit 10%, Monte Carlo simulations (MC) 2500 steps and calculated GAB parameters from DVS isotherm plots. Different fitting methods were assessed: zero order, first order, second order, diffusion and Avrami (Eq. 3-7) [22]. The mathematical form of these equations is shown below:

0-order: $[drug] = kt$ (Eq. 3)

1st order: $[drug]=[drug]_\infty[1-\exp(-kt)]$ (Eq. 4)

2nd order: $[drug]=[drug]_\infty kt/(1/[drug]_\infty + kt)$ (Eq. 5)

Diffusion: $[drug]=kt^{1/2}$ (Eq. 6)

Avrami: $[drug] = [drug]_\infty [1- \exp(-kt^2)]$ (Eq. 7)

Where, k is the degradation constant, t is the time, [drug] refers to nifedipine content via HPLC (chemical stability) or crystalline drug content (physical stability) and $[drug]_\infty$ is the nifedipine content (chemical stability) or the amorphous drug content (physical stability) at time zero. The isoconversion time was defined as the time when the percentage crystallinity or the percentage of nifedipine degraded reaches the specification limit, which was set to 10% and 95%, respectively in our study. An isoconversion point (time to failure) was calculated for each condition of temperature and RH. At the t = 0 timepoint the percent of drug degraded or crystalline NFD is assumed to be zero. In each case, ASAPprime® calculates the isoconversion point using the linearized form of the equations (Eqs. 3-7). For linear regressions, a least squares fit was done to calculate the slope and intercept of the regression line for each condition where:

Percent of degraded NFD or Percent of crystalline NFD = a * t + b (Eq. 8)

3.2.3Chemometric analysis of spectroscopic NIR data

NIR spectra were collected using a Büchi NIR (Flawil, Switzerland) with an NIR reflectance attachment. Spectra were collected with interleaved scans in the 10 000−4000 cm^{-1} range with a resolution of 8 cm^{-1}, using 32 co-added scans. Samples were repositioned between each measurement and measurements were performed in triplicate for each sample [23]. Multivariate data analysis was performed using Unscrambler® X software (CAMO Software, Norway). Pre-processing transformation (data normalisation) was used. Multiple Linear Regression (MLR), Support Vector Machine regression (SVR) and Partial Least Squares Regression (PLSR) were used to create calibration models for quantitative analysis of NFD content (chemical degradation) and crystalline levels of NFD (physical stability). The Kernel and NIPALS algorithms were used to compute the estimated regression coefficients for PLSR. The performance of the models was evaluated using the correlation coefficient (R^2) and the root mean- square error (RMSE) in order to estimate the fit of validation and calibration samples [24].

3.3 Results

3.3.1 Preparation and characterisation of NFD amorphous solid dispersions

Greater processing yields were obtained for HME (ca. 66%, with almost one third of the solid mass left inside the extruder) compared to spray drying (40% and 25% yield for PVPVA64 and Soluplus® respectively). SEM micrographs showed a completely different morphology for HME and spray dried systems. Spray dried formulations were comprised of spherical particles with sizes ranging between 1 and 10 µm. It is noteworthy that particles containing Soluplus® were more aggregated/fused than those prepared with PVPVA64, probably due to the lower T_g of Soluplus®, which also impacted on the yield. HME formulations before grinding exhibited a relatively smooth surface probably due to their amorphous nature (Figure. 10).

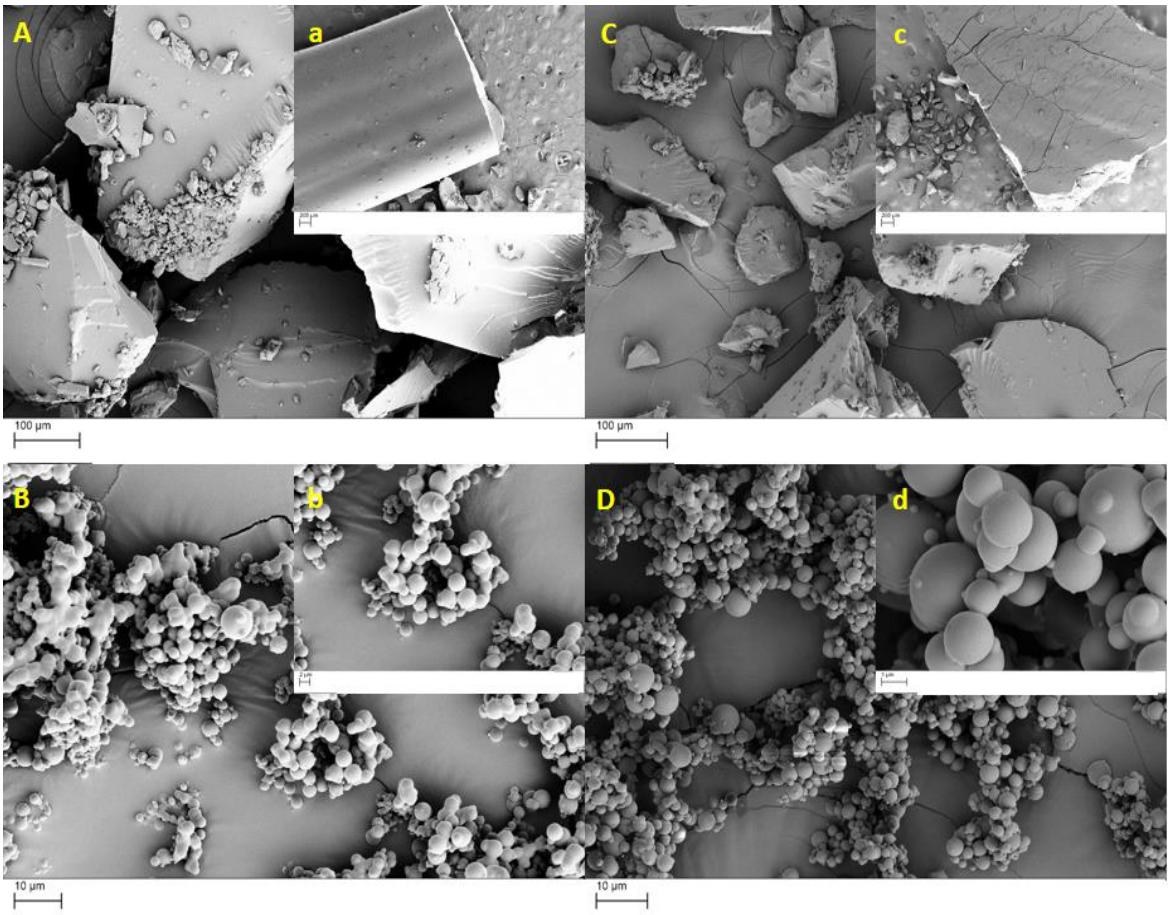

Figure 10: SEM micrographs of NFD amorphous solid dispersions.

Key: A) NFD-SOL-HME; B) NFD-SOL-SD; C) NFD-PVPVA-HME; D) NFD-PVPVA-SD. A micrograph of the same formulation at higher magnification is represented with a lower case.

Amorphous solid dispersions were obtained by both spray drying and HME methods when NFD was combined in a 1:1 weight ratio with Soluplus® and PVPVA64. Amorphous halos were clearly observed for the four systems in the PXRD (Figure. 11A). Crystalline NFD raw material showed a melting event with an onset at 168 °C and a heat of fusion of 106 J/g (Figure. 11Ba). In order to determine the T_g of NFD, the drug was melt-quenched. MTDSC analysis showed a T_g of 45 °C for amorphous NFD (Figure. S3, Supplementary data). Unprocessed amorphous Soluplus® and PVPVA64 were also analysed, and T_gs of 69 °C and 108 °C, respectively, were determined (Figure S2, Supplementary material). No melting events related to crystalline NFD were found in any of the processed formulations (Figure. 3B). A clear T_g was observed in the reversing heat flow signal for the four systems (72.6 ± 3.2 °C for NFD-PVPVA-HME, 70.5 ± 2.7 °C for NFD-PVPVA-SD, 46.7 ± 0.1 °C for NFD-SOL-HME and 48.9 ± 1.7 °C for NFD-SOL-SD), and was significantly higher ($p<0.05$) for those formulations containing PVPVA64 as polymer than those containing SOL (Figure 11B f-i). A desolvation peak from 25 to 100 °C was clearly evident in the total heat flow signal only in the spray dried formulations (Figure. 11B b-e). This is consistent with the content of unbound solvent remaining in the samples after processing, which was below 0.2% after HME and higher for spray dried systems (0.3% for NFD-PVPVA-SD and 0.59% for NFD-SOL-SD) (Figure S4, Supplementary material).

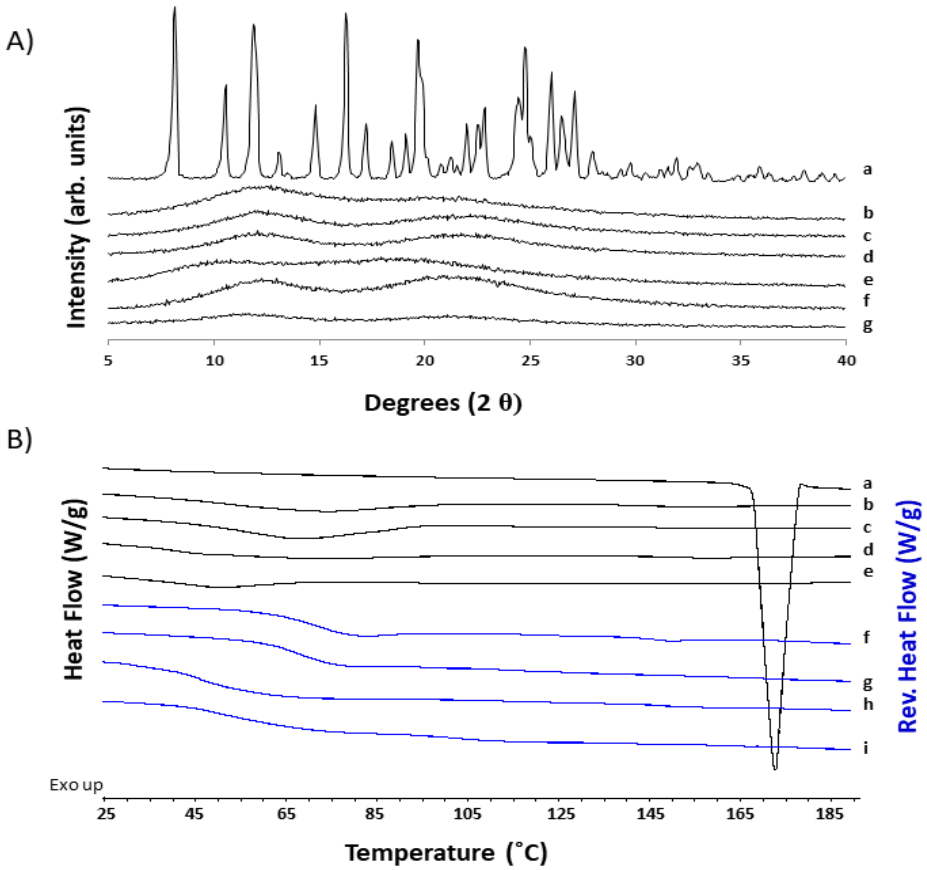

Figure 11: PXRD patterns and DSC thermograms of NFD systems.
A) PXRD patterns. Key: a) Unprocessed crystalline NFD; b) Unprocessed PVPVA64; c) NFD-PVPVA-HME; d) NFD-PVPVA-SD; e) Unprocessed Soluplus®; f) NFD-SOL-HME; g) NFD-SOL-SD.
B**) DSC thermograms.** Key: a) Unprocessed crystalline NFD; b) Total heat flow of NFD-PVPVA-HME; c) Total heat flow of NFD-PVPVA-SD; d) Total heat flow of NFD-SOL-HME; e) Total heat flow of NFD-SOL-SD; f) Reversing heat flow of NFD-PVPVA-HME; g) Reversing heat flow of NFD-PVPVA-SD; h) Reversing heat flow of NFD-SOL-HME; i) Reversing heat flow of NFD-SOL-SD.

FTIR measurements showed a strong H-bond interaction between the API and both polymers (Figure 12). A shift of 20-25 cm^{-1} was observed in the carbonyl group peak (C=O stretching at 1679 cm^{-1}) of NFD when co-processed by both HME and spray drying with both polymers. However, the shift was more prominent in those ASDs containing PVPVA64 (25 cm^{-1}) compared to those containing Soluplus® (20 cm^{-1}). Also, a shift in peaks attributed to the NO_2 (1350 cm^{-1}) and the C-O (1225 cm^{-1}) functional groups of NFD was observed after co-processing with Soluplus® and PVPVA64 using both methods. However, none of these shifts were observed in the physical mixtures (PM) prepared in a mortar and pestle. In addition, HME and spray dried

formulations showed broader bands in the FTIR, probably due to the amorphous nature of the systems when compared to the physical mixtures.

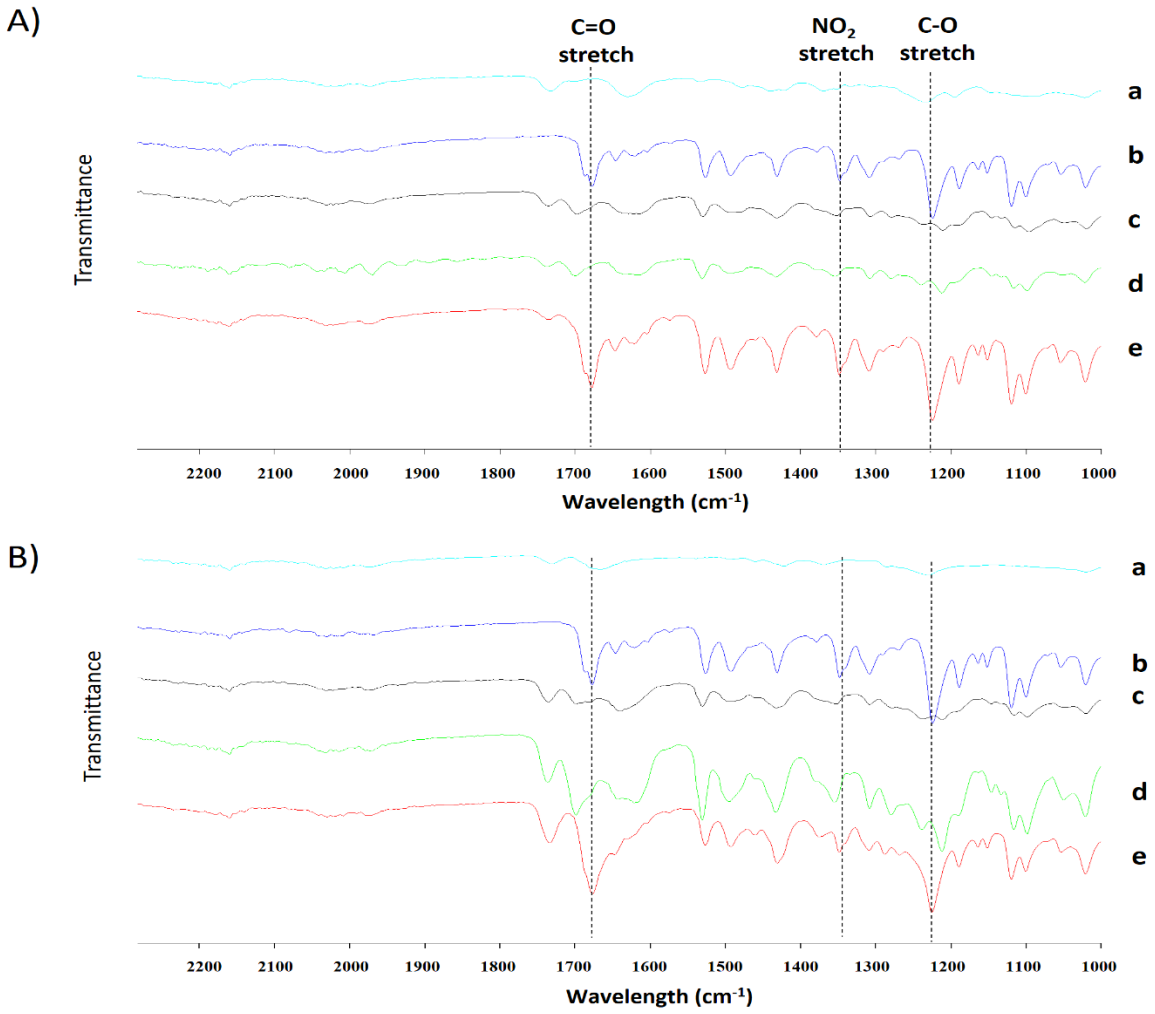

Figure 12: FTIR of NFD amorphous solid dispersions

Key: A) Soluplus® systems; a- unprocessed Soluplus®, b- Unprocessed NFD; c- NFD-SOL-HME formulation; d- NFD-SOL-SD formulation, e- PM NFD-SOL. **B) PVP/VA 64 systems**; a- unprocessed PVPVA64, b- Unprocessed NFD; c- NFD-PVPVA-HME formulation; d- NFD-PVPVA-SD formulation, e- PM NFD-PVPVA.

Moisture sorption isotherms are presented in Figure 13. Considering the impact that moisture has on chemical and physical stability of amorphous solid dispersions, an investigation of the sorption capacity of each system is key to understanding the degradation and crystallisation kinetics during accelerated stability studies. It should be noted that those formulations containing PVPVA64 sorbed much greater amounts of water vapour (between 1.5-3 fold) at high relative humidity compared to the Soluplus® systems. This can be related to the chemistry and hydrophilicity of each polymer but also to their molecular weight. Soluplus® has an average molar mass ranging from

90,000 to 140,000 g/mol while PVPVA 64 is only 65,000 g/mol [25]. It has been shown previously that high molecular weight hydroxypropyl cellulose exhibited a lesser amount of water sorption compared to other grades with lower molecular weight. Upon moisture saturation at the surface of the amorphous solid dispersion, a polymer-water mixture forms leading to varying viscosities. Higher molecular weight polymers with greater viscosities result in slower moisture adsorption rates when compared to similar polymers possessing lower molecular weights [26].

In addition, spray drying resulted in more hygroscopic formulations compared to their corresponding HME systems with higher water uptake (3-fold for Soluplus® and 1.8-fold for PVPVA64) at 90% relative humidity which can be attributed to the smaller particle size of the spray dried microparticles compared to ground HME composites [27]. Also, during the HME processing, drug and polymer mixture will soften and melt under high temperatures and high shear rates leading to materials with higher density and fewer small cavities and hence, lower moisture uptake [26]. However, HME systems showed a more pronounced hysteresis even at high relative humidity compared to spray dried systems, which can be indicative of small cavities and pores formed during the cooling of the extrudates where water can condense, retarding the desorption process. Even though mass loss events were not observed in any of the sorption cycles (which would be an indication of an amorphous to crystalline transition), samples were analysed by PXRD after DVS to inspect for any sign of crystallisation. Bragg peaks were observed only for Soluplus® systems produced by HME, indicating a lower physical stability compared to the other formulations (Figure S5, Supplementary material).

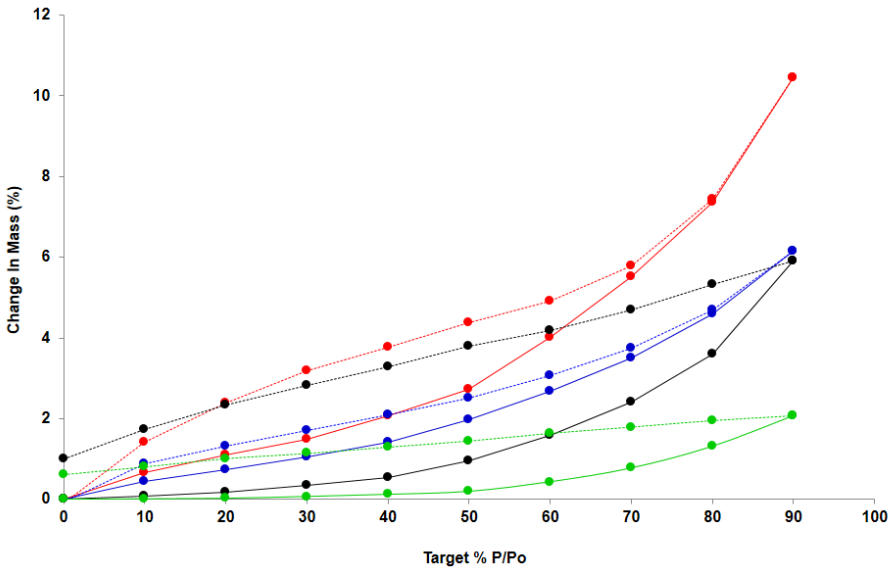

Figure 13: Moisture absorption isotherms for NFD amorphous solid dispersions.
Key: continuous line- sorption cycle; dotted line: desorption cycle; -●- NFD-SOL-HME; -●- NFD-PVPVA-HME; -●- NFD-SOL-SD; -●-NFD-PVPVA-SD.

3.3.2 Dissolution studies

Dissolution profiles of all four NFD amorphous solid dispersions were compared to physical mixtures and unprocessed crystalline NFD (Figure 14). All formulations showed a sustained release profile over 8 h and succeeded in significantly enhancing the dissolution of NFD in aqueous medium (5-6-fold higher) compared to the unprocessed drug. A sustained release is key for drugs like NFD considering that a fast dissolution profile can result in a quick oral bioavailability and high plasma concentrations which may lead to severe hypotension.

Surprisingly, the physical mixtures of both Soluplus® and PVPVA64 showed the fastest release at earlier time points (up to 2 h), indicating that just the presence of the polymer facilitates the dissolution process of the drug. However, both physical mixtures reached a plateau in the release profile after 2 h.

Regarding the four amorphous solid dispersions, NFD-SOL-SD exhibited the fastest release, similar to the one achieved by the physical mixtures; nevertheless over time the release rate was reduced which could potentially be due to the interaction between the polymer and adjacent water molecules leading to extensive swelling at 37 °C [27] and overall a retarded release at later time points. This is supported by the fact that it is the only formulation that follows a Korsmeyer-Peppas

release profile which is commonly applied to diffusion across hydrophilic matrices susceptible to swelling (R^2= 0.9825, Table S1, Supplementary material) [28]. The dissolution profile of NFD-PVPVA-SD was better explained by a first order kinetic rate equation while both HME formulations were the closest to achieving a zero order release. At 8 h, small differences were observed in terms of percentage of NFD dissolved amongst the different formulations.

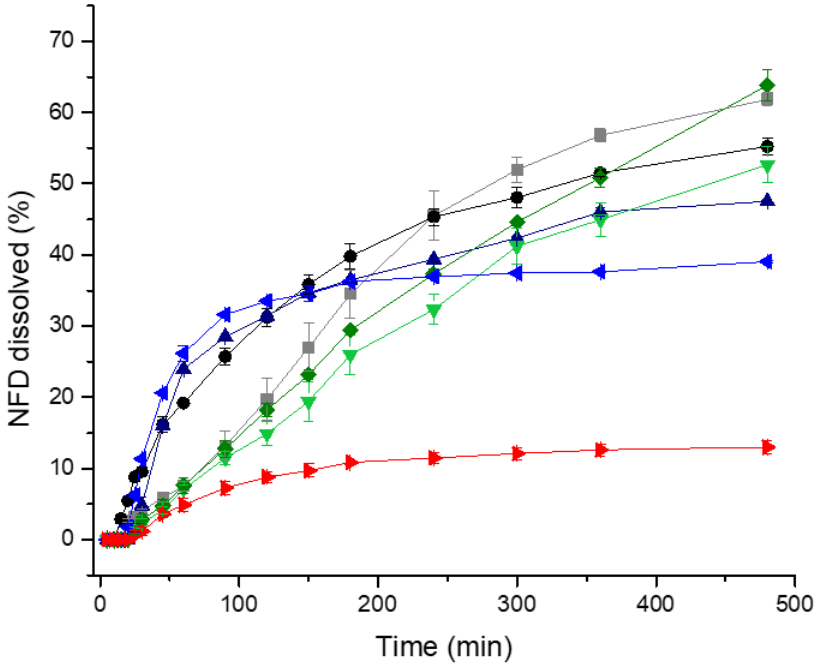

Figure 14:Dissolution profile of NFD amorphous solid dispersions and physical mixtures (PM).
Key: -▶- unprocessed NFD; -♦- NFD-SOL-HME; -▼- NFD-PVPVA-HME; -●- NFD-SOL-SD; -■-NFD-PVPVA-SD; -▲- PM NFD-SOL; -◀- PM NFD-PVPVA.

3.3.3 Accelerated Predictive Chemical and Physical Stability Studies

Unprocessed crystalline NFD exhibited good chemical stability, with a predicted shelf life above 3 years at storage conditions of 25 °C and 10% relative humidity respectively (Table 3-1). Zero order was the best fitting kinetic degradation model for crystalline NFD with an estimated activation energy of 23.381 ± 3.454 Kcal/mol and a low B value (RH sensitivity indicator) of 0.008 ± 0.003 [29]. The predicted chemical stability (% nifedipine content) at the nominated storage condition (open dish container 25 °C and 10% relative humidity) was compared to real time stability data of the test materials collected over 36 months (Figure 15.)

Table 3-1. Estimated Arrhenius equation parameters using the best fitting kinetic degradation model for chemical stability.

Key: Ea, activation energy and B, moisture sensitivity factor. Shelf life was estimated at a temperature of 25 °C and RH of 10%. The specification limit was set to 95%. Values are reported as mean ± standard deviation.

Sample	Degradation kinetic model	Ea (Kcal/mol)	B	Predicted shelf life (years)
Crystalline NFD	Zero order	23.381 ± 3.454	0.008 ± 0.003	> 3
NFD-SOL-HME	Diffusion	16.158 ± 3.023	0.011 ± 0.004	> 3
NFD-SOL-SD	Avrami/Diffusion	10.239 ± 0.64	0.018 ± 0.002	0.164
NFD-PVPVA-HME	Diffusion	18.921 ± 2.252	0.010 ± 0.001	> 3
NFD-PVPVA-SD	Avrami/Diffusion	15.627 ± 1.235	0.021 ± 0.004	1.131

All amorphous solid dispersions showed lower activation energy values and greater B terms, probably indicating their higher susceptibility to moisture due to their amorphous nature. Overall, formulations manufactured by HME demonstrated greater chemical stability and degraded following a diffusion process which resulted in longer shelf lives than spray dried powders which were greatly affected by humidity (almost 2-fold higher B values than for HME equivalent systems). The kinetics for the spray dried formulations were more complex. At less extreme conditions of temperature and RH, the Avrami kinetic model better explained the chemical degradation profile, while at more extreme conditions experimental data was better fitted to the diffusion model (Figure. 9, Table S2 Supplementary material). These observations can be explained by analysis of the physical stability of the formulations. Faster crystallisation of the HME systems resulted in more chemically stable formulations than equivalent SD systems. HME formulations were evidently less physically stable than spray dried powders with a predicted shelf life at a temperature and RH of 25 °C/10% well below 6 months (Table 3-2). The predicted physical stability (% crystalline content) at the nominated storage condition (open dish container 25 °C and 10% relative humidity) was also compared to real time stability data of the test materials collected over 12 months (Figure 8.)

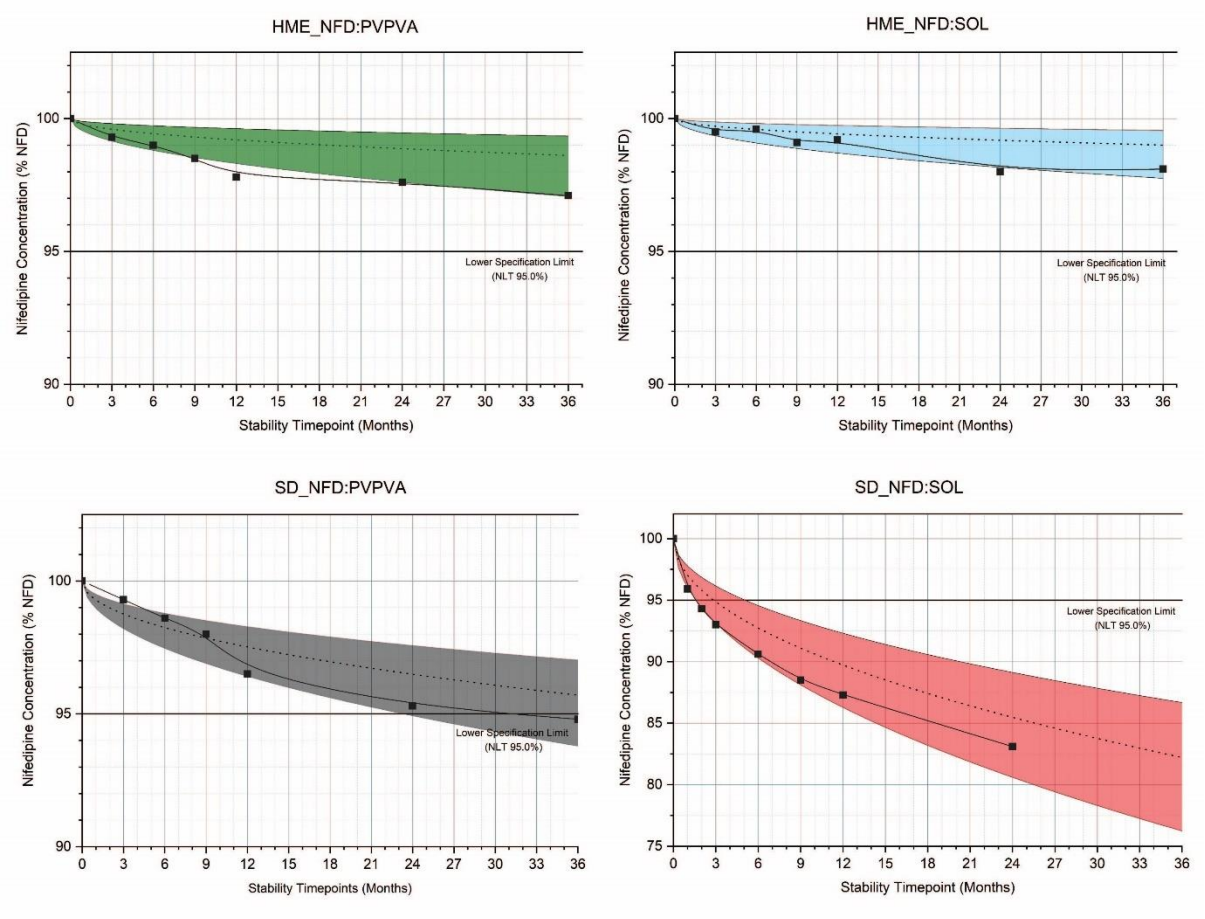

Figure 15: Comparison of predicted and long-term chemical stability of NFD amorphous solid dispersions for materials stored at 25°C / 10% relative humidity

-■- Long term stability data, ---- Mean predicted stability, shaded regions reflect the confidence interval of predicted stability data

Table 3-2. Estimated Arrhenius equation parameters using the best fitting kinetic crystallisation model.

Crystallisation kinetics were calculated based on DSC data. Results from percent of crystallisation were more consistent by DSC than XRD (which exhibited higher variability). Key: Ea, activation energy and B, moisture sensitivity factor. Shelf life was estimated at a temperature of 25°C and RH of 10%. The specification limit was set to 10%. Values are reported as mean ± standard deviation.

Sample	Crystallisation kinetic model	Ea (Kcal/mol)	B	Shelf life (years)
NFD-SOL-HME	Diffusion	5.626 ± 1.503	0.024 ± 0.003	0.371
NFD-SOL-SD	Avrami	12.643 ± 0.471	0.028 ± 0.001	0.789
NFD-PVPVA-HME	Diffusion	7.465 ± 0.968	0.015 ± 0.003	0.556
NFD-PVPVA-SD	Avrami	10.11 ± 1.319	0.023 ± 0.04	1.057

In contrast, spray dried formulations exhibited a 2-fold greater physical shelf life than their composition equivalent HME formulations, with reduced activation energies. However, the higher physical stability of amorphous spray dried systems makes them more susceptible to moisture compared to HME formulations which translates to a decrease in chemical stability. One of the reasons for the high chemical stability of unprocessed NFD is due to its low water uptake compared to the amorphous dispersions and hence, reduced degradation. The crystallisation model that best fit the experimental data was diffusion for HME formulations and Avrami for spray dried powders (Figure. 8, Table S3, Supplementary data). The PVPVA64 polymer was better at forming more physically stable amorphous solid dispersions than Soluplus®, which can be explained by the stronger H-bonding and the higher T_gs for the PVPVA64-containing ASDs, which were both above 70°C, compared to both Soluplus® formulations which exhibited a T_g below 50 °C.

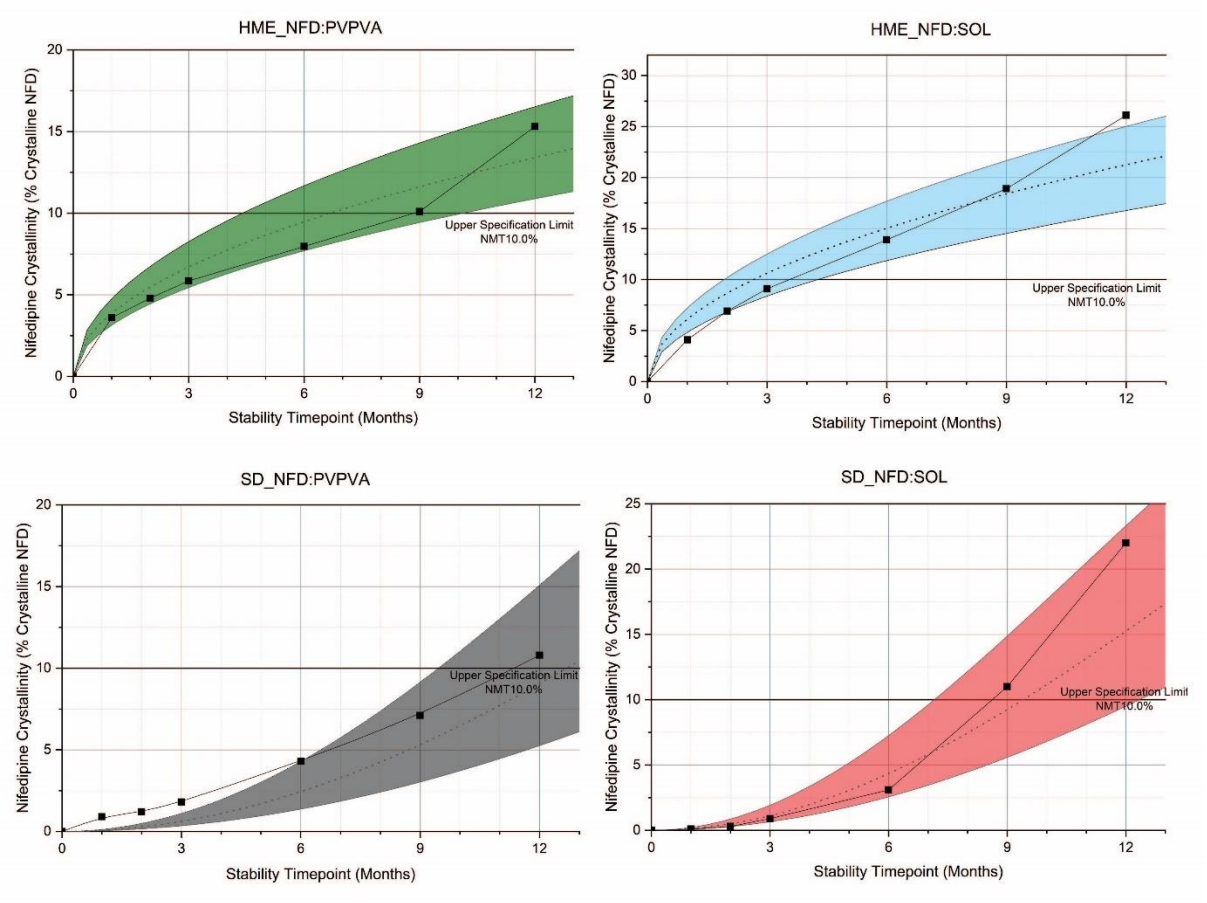

Figure 16: Comparison of predicted and long-term physical stability of NFD amorphous solid dispersions for materials stored at 25°C / 10% relative humidity.

-■- Long term stability data, ---- Mean predicted stability, shaded regions reflect the confidence interval of predicted stability data.

3.3.4 Spectroscopic NIR correlation with chemical and physical stability

PLSR models were the most accurate amongst all the regression models used to evaluate the chemical and physical degradation data of the four NFD formulations using NIR spectra (Figure 17 and 18). Prediction models developed for the NFD content (chemical degradation) were better than those models developed to predict percentage crystallinity (based on R^2 and RMSE values). Also, models for formulations containing Soluplus® as a polymer exhibited greater R^2 values (> 0.68) compared with those prepared using PVPVA64 (R^2 values < 0.68). This can be explained by the rationale that PVPVA64 can sorb larger amounts of water molecules compared to Soluplus® (based on the DVS moisture sorption isotherm) and therefore, the water uptake can interfere with the accuracy of the model generated. The greatest correlation was found for the NFD-SOL-HME system, showing R^2 values of 0.75 and 0.83 for chemical and physical stability respectively. In contrast, the correlation observed between the percentage crystallinity of NFD in the NFD-PVPVA-SD formulation and its NIR spectra was poor by PLSR (R^2= 0.27). This may be due to the greater physical stability of the formulation and hence, the model was constructed with a limited number of samples that exhibited some extent of crystallisation at the storage conditions tested. SVR improved greatly the correlation by increasing the correlation coefficient 2-fold and reducing the RMSE by half.

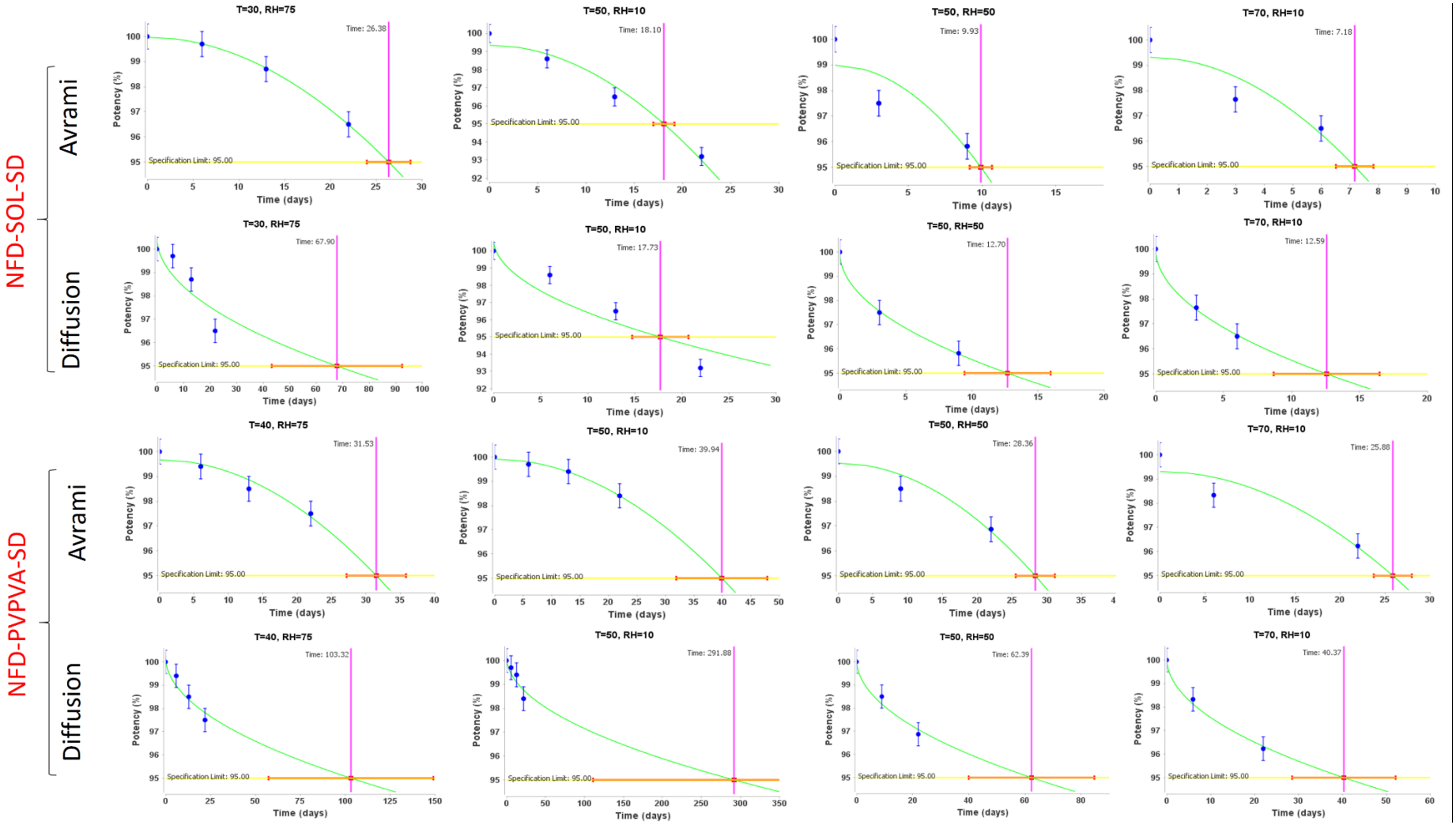

Figure 17: Accelerated chemical stability studies. The potency (NFD remaining in the formulation expressed in %) is illustrated at different time points and different conditions for the two spray dried formulations.

The isoconversion time is shown in each individual graph and represents the time when the potency falls below the specification limit which was set at 95%.

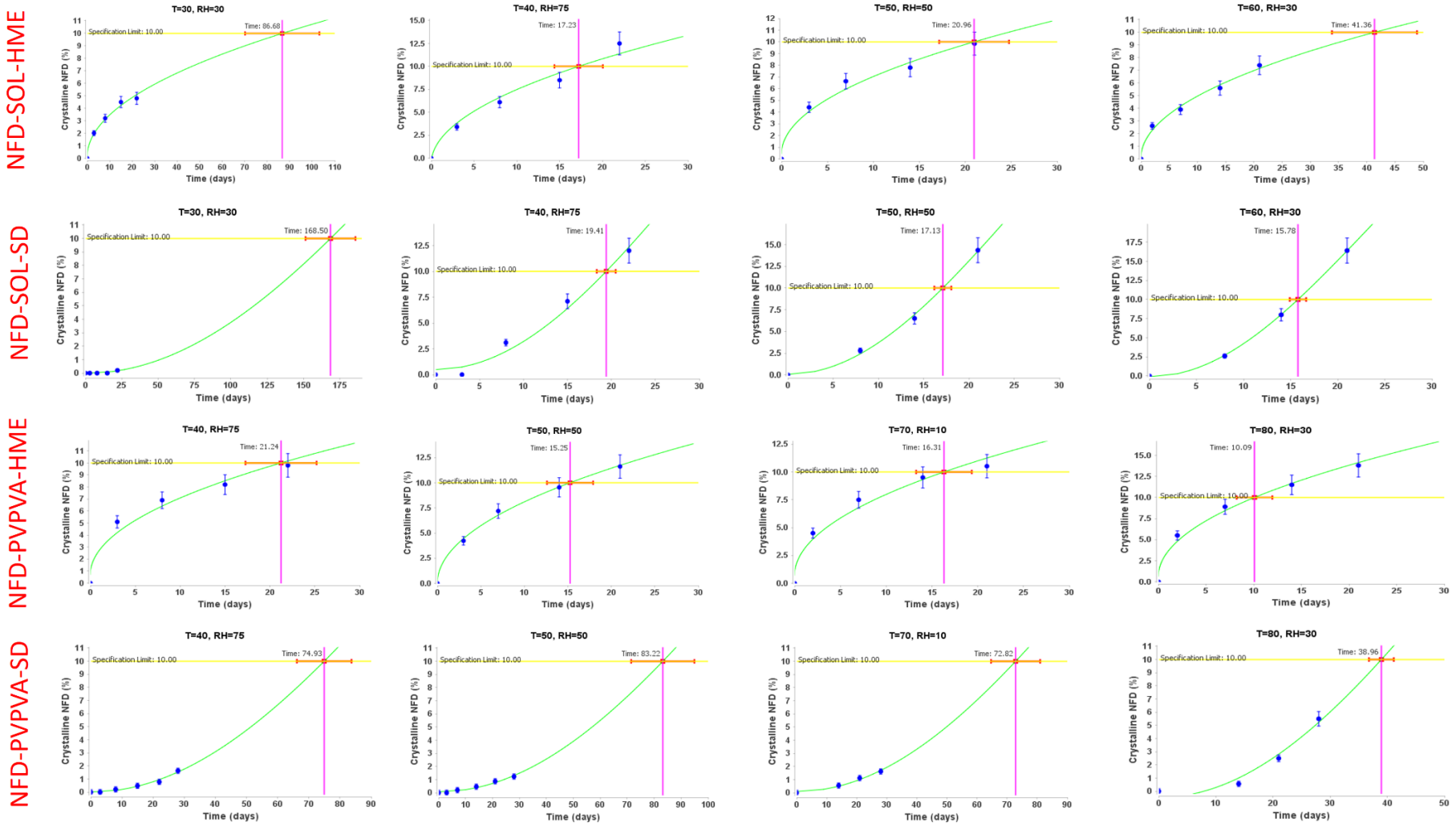

Figure 18: Accelerated physical stability studies. The percentage of crystalline NFD is expressed at different time points and different conditions for the four formulations.

The isoconversion time is shown in each individual graph and represents the time when the percentage of crystalline NFD reaches the specification limit which was set at 10%.

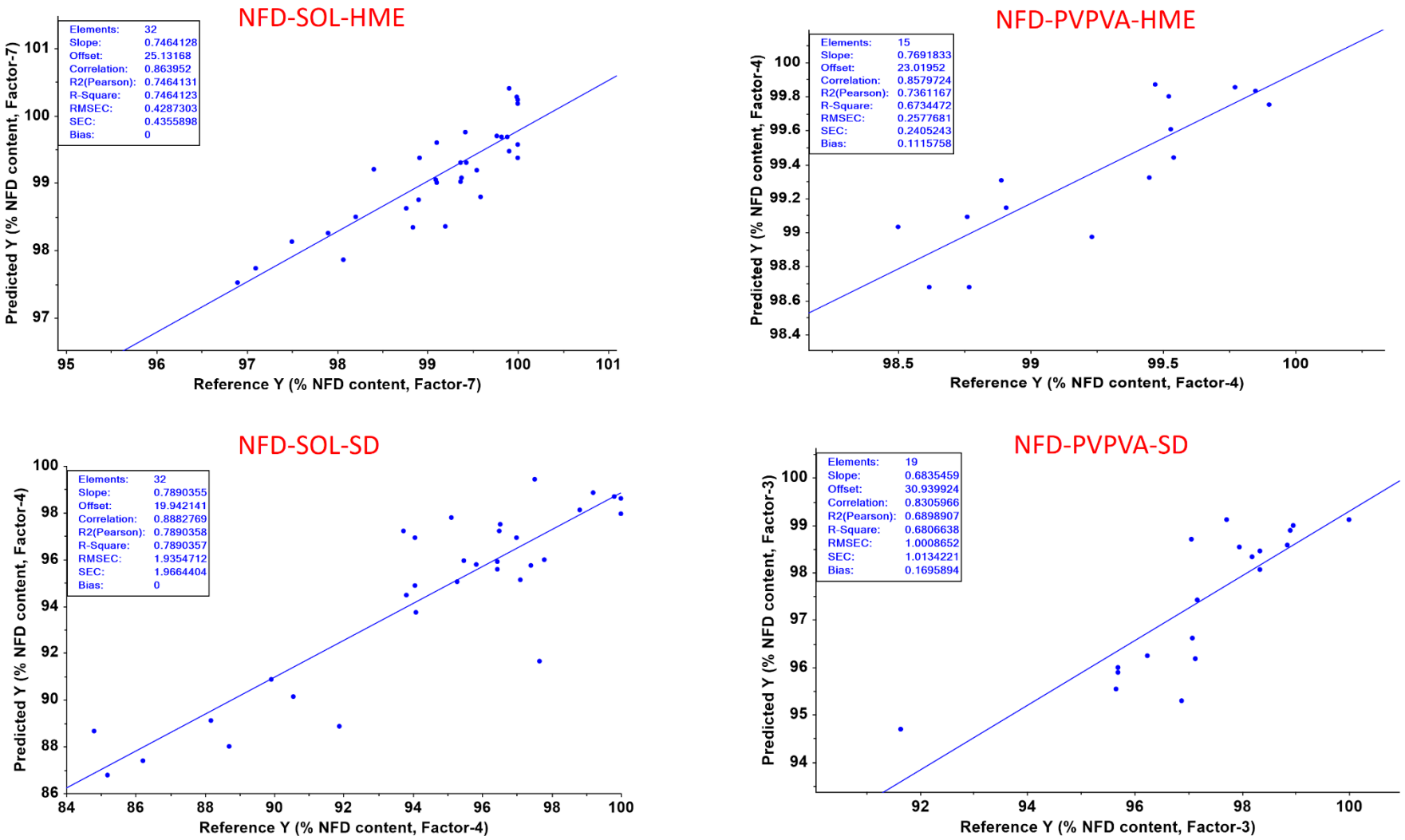

Figure 19:. PLSR correlation model between NIR spectra and drug content of the four NFD formulations.

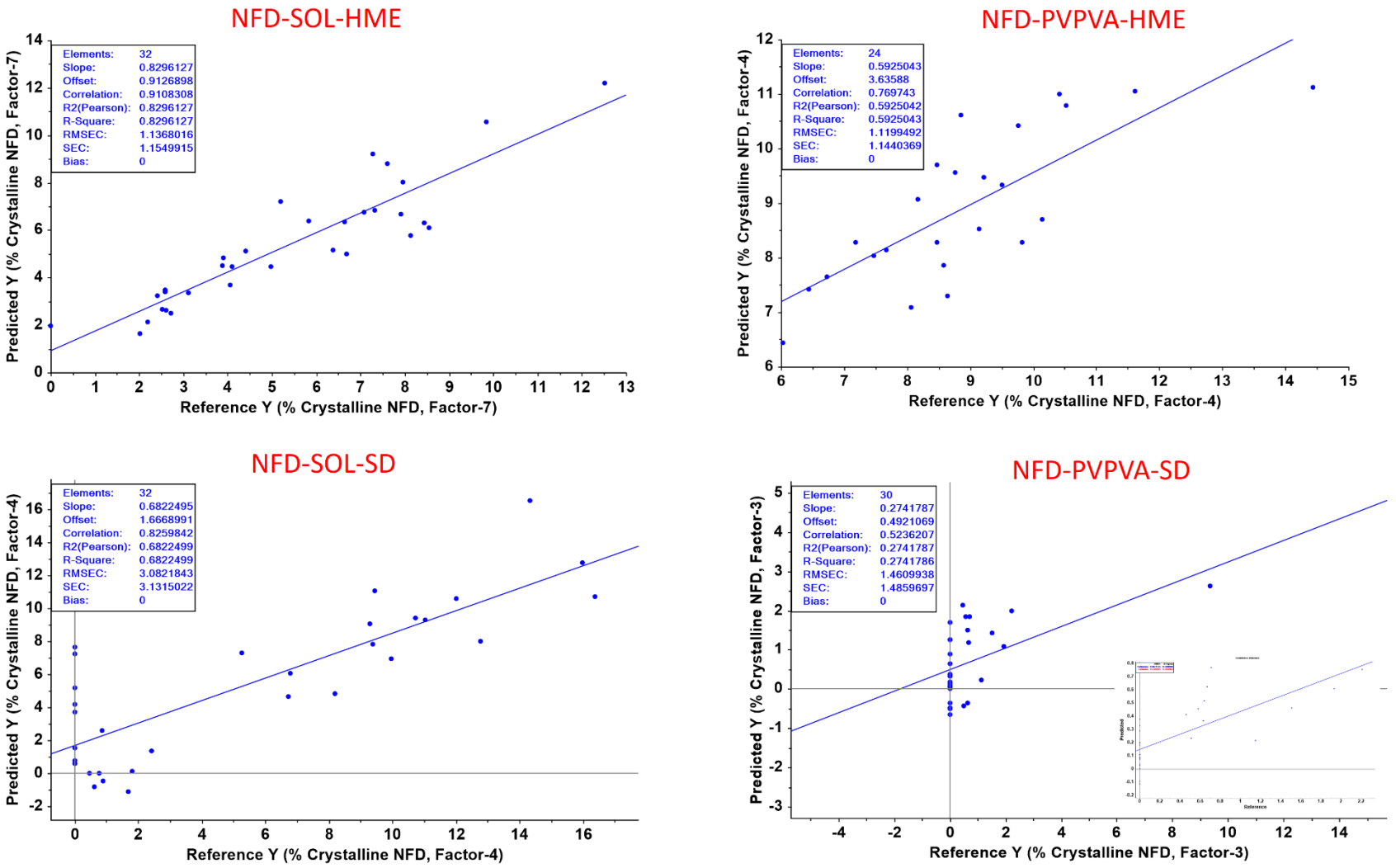

Figure 20: PLSR correlation model between NIR spectra and crystalline NFD content of the four NFD formulations.

SVR for NFD-PVPVA-SD is shown also in a smaller scale.

3.4 Discussion

Four different nifedipine ASDs were manufactured using scalable pharmaceutical techniques. Soluplus® and PVPVA64 were selected as excipients for two main reasons, first, their T_g is not very high, which facilitates the HME process, taking into account the temperature above which nifedipine will degrade (< 220 °C) and secondly, both excipients have a similar Hansen Solubility Parameter (19.4 and 19.7 $MPa^{1/2}$ for Soluplus® and PVPVA64 respectively) to nifedipine (17.9 $MPa^{1/2}$), which is a good indicator of miscibility [1].

In terms of dissolution, the four systems exhibited a significantly improved dissolution/faster dissolution rate compared to the crystalline drug itself. Nevertheless, the uncertainty about which is the best formulation to move forward into clinical trials is high and hence, the decision-making process cannot rely solely on results from dissolution experiments, but must also be based on stability studies, which are key to ensuring that the enhanced dissolution profile is maintained over time, and that the selected formulation will meet the pharmacopeial requirements over the whole shelf life of the product. Considering all the physicochemical parameters of the four formulations, it is worth highlighting that those systems which contain PVPVA64 have a single T_g (>70 °C) which is significantly higher than that of the Soluplus® formulations (< 50 °C). The T_g of the Soluplus® formulations is just few degrees above the T_g of amorphous nifedipine prepared by melt quenching (45 °C) (Figure. S3, Supplementary material). Based on this, amorphous solid dispersions with PVPVA64 are potentially better candidates to ensure physical stability on storage at 25 °C. However, based on moisture sorption results, those formulations prepared with PVPVA64 had a higher tendency to take up water, which can act as a plasticizer, decreasing the physical stability of the systems [2].

Combined chemical and physical stability studies are crucial to understand which formulation has the best long term performance. HME formulations exhibited greater chemical stability, while spray drying resulted in more physically stable systems. Looking closer into the thermodynamics and crystallisation kinetics of the four systems, it is important to note, that over time for most conditions, two T_gs were found in the NFD-PVPVA-HME and NFD-SOL-HME formulations (Figure. S6, Supplementary material), indicating a progression into a heterogeneous solid dispersion with different domains. This phase separation can explain the poorer physical stability

compared to the equivalent spray dried systems, (2-fold lower predicted shelf life than NFD-PVPVA-SD and NFD-SOL-SD) and also the data fit to the diffusion kinetic model in which, prior to drug nucleation and crystal growth, diffusion of drug molecules takes places, resulting in domains rich in drug or in polymer (Figure 21).

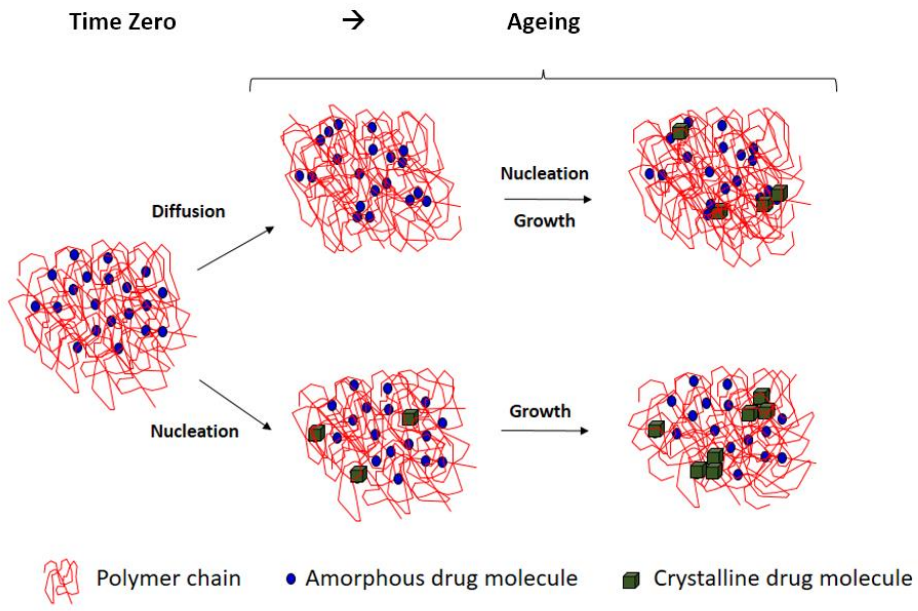

Figure 21: Graphical representation of diffusion and Avrami crystallisation models.

The physical stability of spray dried formulations was better predicted by an Avrami kinetic model. In this type of kinetic model, nucleation takes places first followed by crystal growth. If the drug is well-stabilised within the polymer, the initial nucleation step is delayed and the stability is overall enhanced [3].

The formulation that exhibited the greatest physical stability performance was NFD-PVPVA-SD. For those samples stored under low relative humidity ageing conditions, a relaxation enthalpy was observed (Figure S7, Supplementary material). This phenomenon occurs in materials that are in a nonequilibrium state when maintained at temperatures below their T_g. This can explain why a relaxation enthalpy was only observed in the NFD-PVPVA-SD system and not in the NFD-SOL-SD system, due the latter's lower T_g.

Spray drying is a fast process in which the polymer chains are rapidly fixed into high-energy conformations compared to HME where the extrudates cool slower allowing the polymer chains to find energetically more favourable orientations. Relaxation towards equilibrium (in the form of

molecular rearrangements) can take place over extended periods of time at room temperature. Nevertheless, this relaxation time is significantly reduced by increasing the temperature to near, but not exceeding the T_g [4]. A clear relaxation enthalpy was observed for samples stored at 70 °C and 10% RH in the NFD-PVPVA-SD formulation, which was accompanied by an increase in C_p and T_g (Figure 14). The extent of material relaxation (Φ_t) at day 2 was 26%. This value was calculated using the following equation [2]:

$$\Phi_t = 1-(\Delta H_t / \Delta H\alpha) \qquad \text{(Eq. 8)}$$

where ΔHt is the measured enthalpy recovery at a particular condition and ΔHα is the maximum enthalpy change needed for a glass to relax to a supercooled liquid state calculated as follows:

$$\Delta H\alpha = \Delta Cp\ (Tg - Ta) \qquad \text{(Eq. 9)}$$

where ΔCp is the change in the heat capacity at Tg and Ta is the storage temperature. However, crystallisation of the formulation started after 14 days when stored at this condition, resulting in a decrease in the relaxation enthalpy, probably due to a new arrangement of the polymer chains.

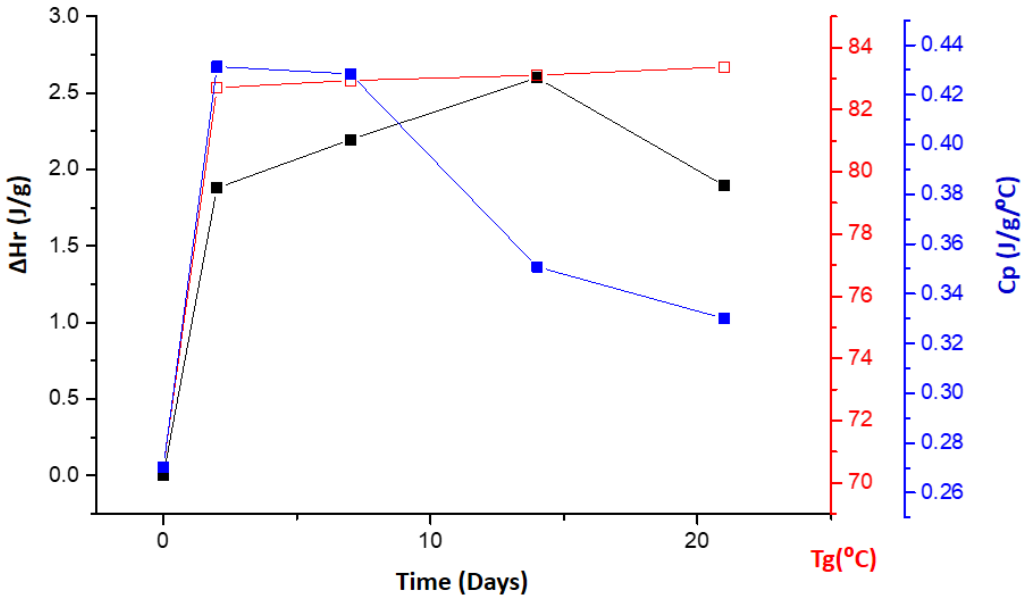

Figure 22: Graphical representation of relaxation enthalpy (ΔHr), heat capacity (Cp) and mild temperature glass transition (Tg) of NFD-PVPVA-SD system storage at 70°C /10 %rh

.

The enhanced physical stability of spray dried formulations resulted in faster chemical degradation. Even though the percentage of crystallinity in HME systems was relatively low (< 15%), it had the effect of stabilising the formulation against chemical degradation pathways such as hydrolysis and oxidation. At less extreme conditions of temperature and relative humidity, spray dried systems followed Avrami kinetics, similar to the degradation model found for physical stability, but under more extreme conditions, a shift from Avrami to a diffusion kinetic model was observed. This may be explained by the different miscibility between the polymer chains and the degradation products, which may be able to diffuse with higher molecular mobility within the polymer matrix.

Regarding chemometric analysis using NIR spectra and chemical and physical stability data, it is worth noting that analysis is far less time consuming compared to HPLC or XRD/DSC analysis. Allied to this is the fact that NIR analysis is a non-destructive technique meaning less test material is required for the overall stability study. Correlation in terms of percentage of drug degraded and crystallinity was good for those systems with less propensity for water sorption (NFD-SOL-HME). Compared to Raman, the interference with water molecules reduces the sensitivity and accuracy of this methodology. Further research should be performed to take into account the percentage of water uptake at each time point and hence, correct the prediction models.

3.5 Conclusions

Four different nifedipine amorphous solid dispersions were manufactured using scalable pharmaceutical techniques by HME and spray drying. In terms of dissolution, the four systems exhibited significantly enhanced dissolution compared to the crystalline drug itself. The uncertainty about which is the best formulation to move forward into clinical trials is high and hence, the decision-making process cannot rely solely on results from dissolution experiments, but combined physicochemical stability studies are also necessary. The spray dried powders were more stable from a physical point of view than extrudates, reflected in the appearance of two T_gs in the NFD-PVPVA-HME and NFD-SOL-HME formulations, indicating phase separation which correlates with a diffusion kinetic model. In contrast, formulations manufactured by HME exhibited a greater chemical stability, resulting in longer predicted shelf lives than spray dried

powders which were greatly affected by humidity. The chemical degradation kinetics for both spray dried formulations was more complex. At less extreme conditions of temperature and relative humidity, spray dried systems followed an Avrami kinetic model but under more extreme conditions, a shift from Avrami to diffusion kinetics took place, which may be due to a change in miscibility between the degradation products and the polymer chains.

In conclusion, amongst all the formulations tested, NFD-PVPVA-SD exhibited the best balance of both physical and chemical stability and may be considered to be the best candidate to move forward into clinical trials. Thus, accelerated predictive stability has been demonstrated to be a good methodology to ensure a fast decision-making process for pharmaceutical formulations with reduced uncertainty.

Acknowledgements

This work was supported by Science Foundation Ireland grants co-funded under the European Regional Development Fund (SFI/12/RC/2275 and SFI/12/RC/2275_P2) provided to Prof. A. M. Healy. The authors would like to thank Dr. Elaine Kenny of Applied Polymer Technologies Gateway (APT) for her assistance in producing HME samples.

References

(1) Lamy, B.; Tewes, F.; Serrano, D. R.; Lamarche, I.; Gobin, P.; Couet, W.; Healy, A. M.; Marchand, S. New aerosol formulation to control ciprofloxacin pulmonary concentration. Journal of controlled release : official journal of the Controlled Release Society 2018, 271, 118-126. DOI: 10.1016/j.jconrel.2017.12.021.

(2) Garcia-Castillo, I.; Fernandez-Mayo, L.; Serrano-Drozdowskyij, E.; Carmona, R.; Martin-Calvo, M. J.; Ovejero, S.; Millan, I.; Garcia, F.; Baca-Garcia, E. [Early detection of hypomania episodes in patients with affective disorder]. Revista de psiquiatria y salud mental 2012, 5 (2), 89-97. DOI: 10.1016/j.rpsm.2011.12.002.

(3) Maniruzzaman, M.; Boateng, J. S.; Snowden, M. J.; Douroumis, D. A review of hot-melt extrusion: process technology to pharmaceutical products. ISRN pharmaceutics 2012, 2012, 436763. DOI: 10.5402/2012/436763.

(4) Mugheirbi, N. A.; O'Connell, P.; Serrano, D. R.; Healy, A. M.; Taylor, L. S.; Tajber, L. A Comparative Study on the Performance of Inert and Functionalized Spheres Coated with Solid Dispersions Made of Two Structurally Related Antifungal Drugs. Molecular pharmaceutics 2017, 14 (11), 3718-3728. DOI: 10.1021/acs.molpharmaceut.7b00482. Laitinen, R.; Lobmann, K.; Strachan, C. J.; Grohganz, H.; Rades, T. Emerging trends in the stabilization of amorphous drugs. International journal of pharmaceutics 2013, 453 (1), 65-79. DOI: 10.1016/j.ijpharm.2012.04.066.

(5) Dedroog, S.; Huygens, C.; Van den Mooter, G. Chemically identical but physically different: a comparison of spray drying, hot melt extrusion and cryo-milling for the formulation of high drug loaded amorphous solid dispersions of naproxen. European journal of pharmaceutics and biopharmaceutics : official journal of Arbeitsgemeinschaft fur Pharmazeutische Verfahrenstechnik e.V 2018. DOI: 10.1016/j.ejpb.2018.12.002.

(6) Waterman, K. C.; Carella, A. J.; Gumkowski, M. J.; Lukulay, P.; MacDonald, B. C.; Roy, M. C.; Shamblin, S. L. Improved protocol and data analysis for accelerated shelf-life estimation of solid dosage forms. Pharmaceutical research 2007, 24 (4), 780-790. DOI: 10.1007/s11095-006-9201-4.

(7) Waterman, K. C. The application of the Accelerated Stability Assessment Program (ASAP) to quality by design (QbD) for drug product stability. AAPS PharmSciTech 2011, 12 (3), 932-937. DOI: 10.1208/s12249-011-9657-3 From NLM Medline.

(8) Qiu, F.; Scrivens, G. Accelerated Predictive Stability. Fundamentals and Pharmaceutical Industry Practices; Elsevier, 2018.

(9) Liu, B.; Theil, F.; Lehmkemper, K.; Gessner, D.; Li, Y.; van Lishaut, H. Crystallization Risk Assessment of Amorphous Solid Dispersions by Physical Shelf-Life Modeling: A Practical Approach. Molecular pharmaceutics 2021, 18 (6), 2428-2437. DOI: 10.1021/acs.molpharmaceut.1c00270 From NLM.

(10) Raina, S. A.; Alonzo, D. E.; Zhang, G. G.; Gao, Y.; Taylor, L. S. Impact of polymers on the crystallization and phase transition kinetics of amorphous nifedipine during dissolution in aqueous media. Molecular pharmaceutics 2014, 11 (10), 3565-3576. DOI: 10.1021/mp500333v.

(11) Serrano, D. R.; O'Connell, P.; Paluch, K. J.; Walsh, D.; Healy, A. M. Cocrystal habit engineering to improve drug dissolution and alter derived powder properties. The Journal of pharmacy and pharmacology 2016, 68 (5), 665-677. DOI: 10.1111/jphp.12476.

(12) Maury, M.; Murphy, K.; Kumar, S.; Shi, L.; Lee, G. Effect of process variables on the powder yield of spray dried trehalose on a laboratory spray-drier. European Journal of Pharmaceutics and Biopharmaceutics 2005, 59 (3), 565-573.

(13) Grossjohann, C.; Serrano, D. R.; Paluch, K. J.; O'Connell, P.; Vella-Zarb, L.; Manesiotis, P.; McCabe, T.; Tajber, L.; Corrigan, O. I.; Healy, A. M. Polymorphism in sulfadimidine/4-aminosalicylic acid cocrystals: solid-state characterization and physicochemical properties. Journal of pharmaceutical sciences 2015, 104 (4), 1385-1398. DOI: 10.1002/jps.24345.

(14) Serrano, D. R.; Persoons, T.; D'Arcy, D. M.; Galiana, C.; Dea-Ayuela, M. A.; Healy, A. M. Modelling and shadowgraph imaging of cocrystal dissolution and assessment of in vitro antimicrobial activity for sulfadimidine/4-aminosalicylic acid cocrystals. European journal of pharmaceutical sciences : official journal of the European Federation for Pharmaceutical Sciences 2016, 89, 125-136. DOI: 10.1016/j.ejps.2016.04.030.

(15) Zhang, Y.; Huo, M.; Zhou, J.; Zou, A.; Li, W.; Yao, C.; Xie, S. DDSolver: an add-in program for modeling and comparison of drug dissolution profiles. The AAPS journal 2010, 12 (3), 263-271. DOI: 10.1208/s12248-010-9185-1.

(16) Serrano, D. R.; Walsh, D.; O'Connell, P.; Mugheirbi, N. A.; Worku, Z. A.; Bolas-Fernandez, F.; Galiana, C.; Dea-Ayuela, M. A.; Healy, A. M. Optimising the in vitro and in vivo performance of oral cocrystal formulations via spray coating. European journal of pharmaceutics and biopharmaceutics : official journal of Arbeitsgemeinschaft fur Pharmazeutische Verfahrenstechnik e.V 2018, 124, 13-27. DOI: 10.1016/j.ejpb.2017.11.015.

(17) Williams, H. Predictive Stability Testing Utilizing Accelerated Stability Assessment Program (ASAP) Studies. In Methods for Stability Testing of Pharmaceuticals, Bajaj, S., Singh, S. Eds.; Springer New York, 2018; pp 213-232.

(18) Curtin, V.; Amharar, Y.; Gallagher, K. H.; Corcoran, S.; Tajber, L.; Corrigan, O. I.; Healy, A. M. Reducing mechanical activation-induced amorphisation of salbutamol sulphate by co-processing with selected carboxylic acids. International journal of pharmaceutics 2013, 456 (2), 508-516. DOI: 10.1016/j.ijpharm.2013.08.025.

(19) Gill, P.; Moghadam, T. T.; Ranjbar, B. Differential scanning calorimetry techniques: applications in biology and nanoscience. Journal of biomolecular techniques : JBT 2010, 21 (4), 167-193.

(20) Yoshioka, S.; Stella, V. J. Stability of Drugs and Dosage Forms. Plenum, New York, 2000, 108-113.

(21) Freethink Technologies, I. ASAPprime® user's guide. 2013.

(22) Curtin, V.; Amharar, Y.; Hu, Y.; Erxleben, A.; McArdle, P.; Caron, V.; Tajber, L.; Corrigan, O. I.; Healy, A. M. Investigation of the capacity of low glass transition temperature excipients to minimize amorphization of sulfadimidine on comilling. Molecular pharmaceutics 2013, 10 (1), 386-396. DOI: 10.1021/mp300529a.

(23) Dea-Ayuela, M. A.; Serrano, D. R. New Drugs and Therapeutic/Diagnostic Targets for Fungal and Parasitic Diseases - Part II. Current topics in medicinal chemistry 2018, 18 (16), 1357. DOI: 10.2174/1568026618161811071421 30.

(24) Skiba, M.; Skiba, M.; Milon, N.; Bounoure, F.; Fessi, H. Preparation and characterization of amorphous solid dispersions of nimesulide in cyclodextrin copolymers. Journal of nanoscience and nanotechnology 2014, 14 (4), 2772-2779.

Paudel, A.; Geppi, M.; Van den Mooter, G. Structural and dynamic properties of amorphous solid dispersions: the role of solid-state nuclear magnetic resonance spectroscopy and relaxometry. Journal of pharmaceutical sciences 2014, 103 (9), 2635-2662. DOI: 10.1002/jps.23966.

(25) Feng, X.; Vo, A.; Patil, H.; Tiwari, R. V.; Alshetaili, A. S.; Pimparade, M. B.; Repka, M. A. The effects of polymer carrier, hot melt extrusion process and downstream processing parameters on the moisture sorption properties of amorphous solid dispersions. The Journal of pharmacy and pharmacology 2016, 68 (5), 692-704. DOI: 10.1111/jphp.12488.

(26) Kelleher, J. F.; Gilvary, G. C.; Madi, A. M.; Jones, D. S.; Li, S.; Tian, Y.; Almajaan, A.; Senta-Loys, Z.; Andrews, G. P.; Healy, A. M. A comparative study between hot-melt extrusion and spray-drying for the manufacture of anti-hypertension compatible monolithic fixed-dose combination products. International journal of pharmaceutics 2018, 545 (1-2), 183-196. DOI: 10.1016/j.ijpharm.2018.05.008.

(27) Colombo, P.; Bettini, R.; Santi, P.; Peppas, N. A. Swellable matrices for controlled drug delivery: gel-layer behaviour, mechanisms and optimal performance. Pharmaceutical science & technology today 2000, 3 (6), 198-204.

(28) Cerda, J. R.; Arifi, T.; Ayyoubi, S.; Knief, P.; Ballesteros, M. P.; Keeble, W.; Barbu, E.; Healy, A. M.; Lalatsa, A.; Serrano, D. R. Personalised 3D Printed Medicines: Optimising Material Properties for Successful Passive Diffusion Loading of Filaments for Fused Deposition Modelling of Solid Dosage Forms. Pharmaceutics 2020, 12 (4). DOI: 10.3390/pharmaceutics12040345.

(29) Ponnammal, P.; Kanaujia, P.; Yani, Y.; Ng, W. K.; Tan, R. B. H. Orally Disintegrating Tablets Containing Melt Extruded Amorphous Solid Dispersion of Tacrolimus for Dissolution Enhancement. Pharmaceutics 2018, 10 (1). DOI: 10.3390/pharmaceutics10010035. Kolter, K.; Karl, M.; Grycke, A. Hot Melt Extrusion with Basf Pharma Polymers, 2nd ed.; BASF: Ludwigshafen, Germany. 2012.

(30) Chawla, G.; Bansal, A. K. Molecular Mobility and Physical Stability of Amorphous Irbesartan Scientia Pharmaceutica 2008, 77, 695-709.

(31) Ruiz, G. N.; Romanini, M.; Barrio, M.; Tamarit, J. L.; Pardo, L. C.; Macovez, R. Relaxation Dynamics vs Crystallization Kinetics in the Amorphous State: The Case of Stiripentol. Molecular pharmaceutics 2017, 14 (11), 3636-3643. DOI: 10.1021/acs.molpharmaceut.7b00399.

(32) Parker, M. J. Test Methods, Nondestructive Evaluation, and Smart Materials. In Comprehensive Composite Materials, Kelly, A., Zweben, C. Eds.; Elsevier, 2000.

Supplementary Material

Accelerated Predictive Stability (APS) strategies applied to screening pharmaceutical formulations: A case study of spray dried and hot melt extruded nifedipine amorphous solid dispersions

Peter O'Connell[1,2,3], Joshua H. Yoon[4], Luke M. Geever[4], Nigel T. McSweeney[3], Anne Marie Healy[2]*, Dolores R. Serrano[1, 5*]

[1]Department of Pharmaceutics and Food Technology, School of Pharmacy, Universidad Complutense de Madrid, Plaza Ramon y Cajal s/n, 28040-Madrid, Spain.

[2]Synthesis and Solid State Pharmaceutical Centre (SSPC), School of Pharmacy and Pharmaceutical Sciences, Trinity College Dublin, Dublin 2, Ireland.

[3]Cuspor Limited, Dublin 2, Ireland

[4]Applied Polymer Technologies Gateway (APT), Athlone Institute of Technology, Dublin Road, Athlone, Co. Westmeath, Ireland.

[5]Instituto Universitario de Farmacia Industrial (IUFI), School of Pharmacy, Universidad Complutense de Madrid, Avenida Complutense, 28040 Madrid, Spain.

*Corresponding authors:

Anne Marie Healy

School of Pharmacy and Pharmaceutical Sciences, Trinity College Dublin, Dublin 2, Ireland.

Tel +353 1896 1444 Email healyam@tcd.ie

Dolores R. Serrano

Department of Pharmaceutics, School of Pharmacy, Universidad Complutense de Madrid, Plaza Ramon y Cajal SN, 28040, Spain,

Tel: +34913941620, Email: drserran@ucm.es

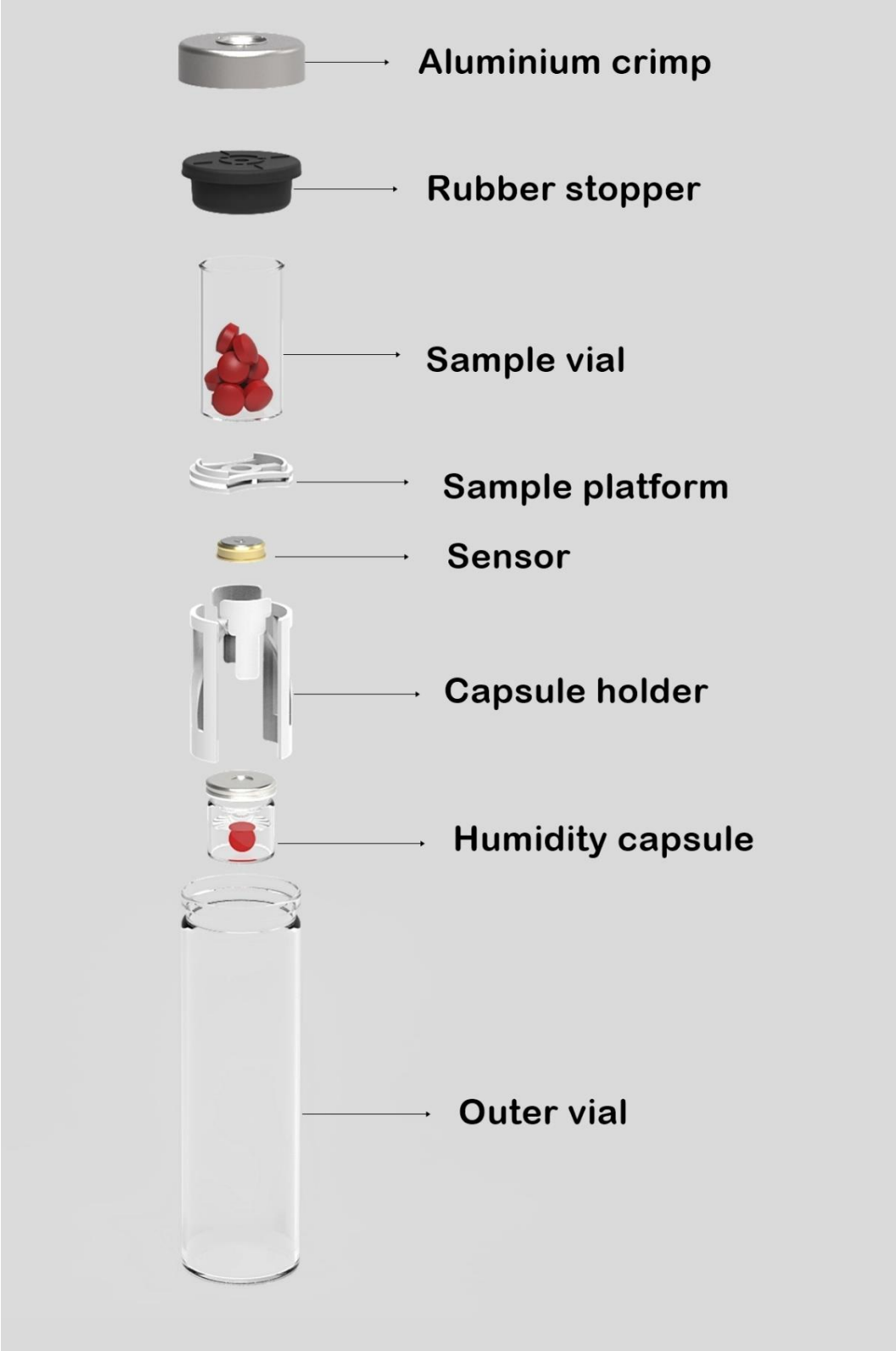

Figure S1. Schematic illustration of Cuspor Ageing System used in APS study.

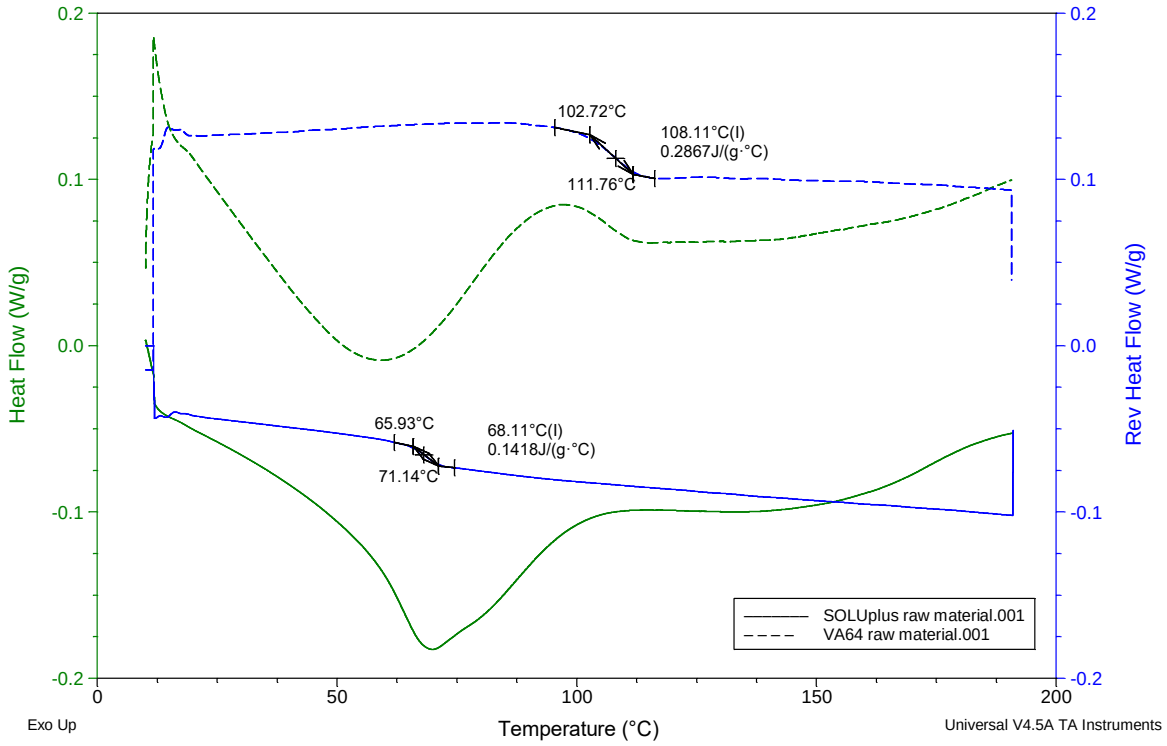

Figure S2. **MTDSC of unprocessed Soluplus® and PVPVA64.** A scanning rate of 5°C/min, amplitude of modulation of 0.796°C and modulation frequency of 1/60Hz were then employed from 10°C to 190°C.

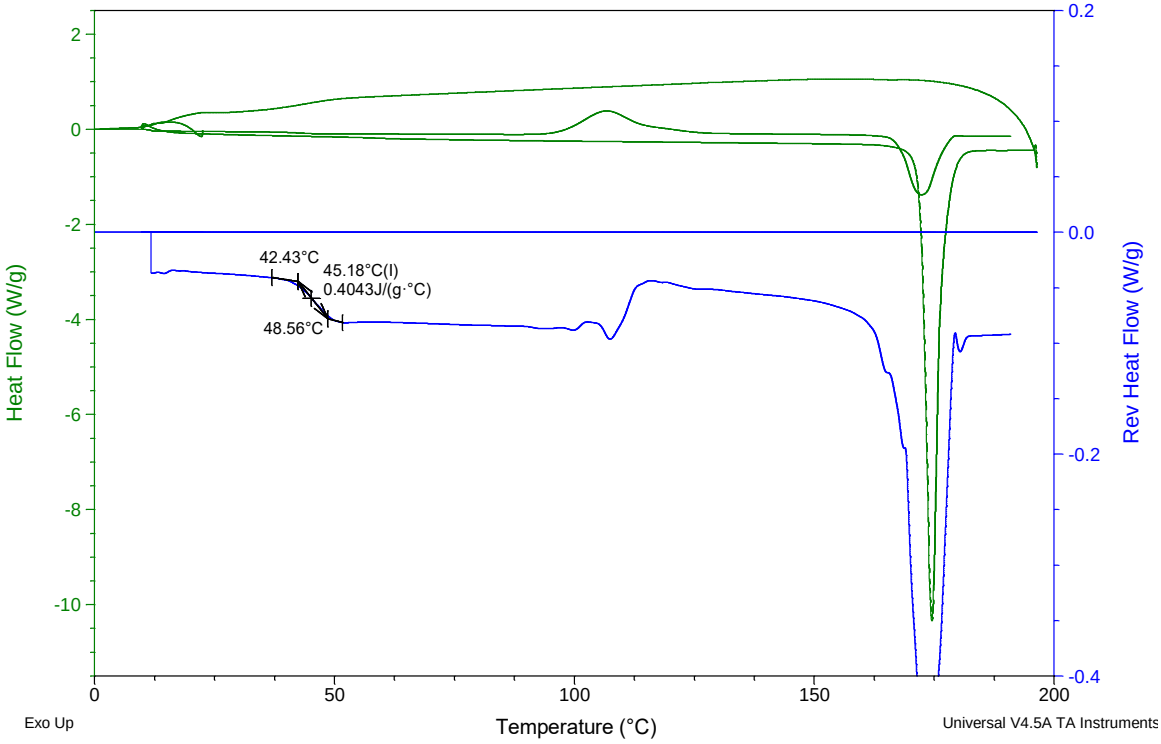

Figure S3. MTDSC of melt quenched NFD. The following method was used to obtain amorphous NFD: the sample was heated at 20 °C/min to 190 °C and then quickly cooled down to 10 °C. A scanning rate of 5°C/min, amplitude of modulation of 0.796°C and modulation frequency of 1/60Hz were then employed from 10°C to 190°C.

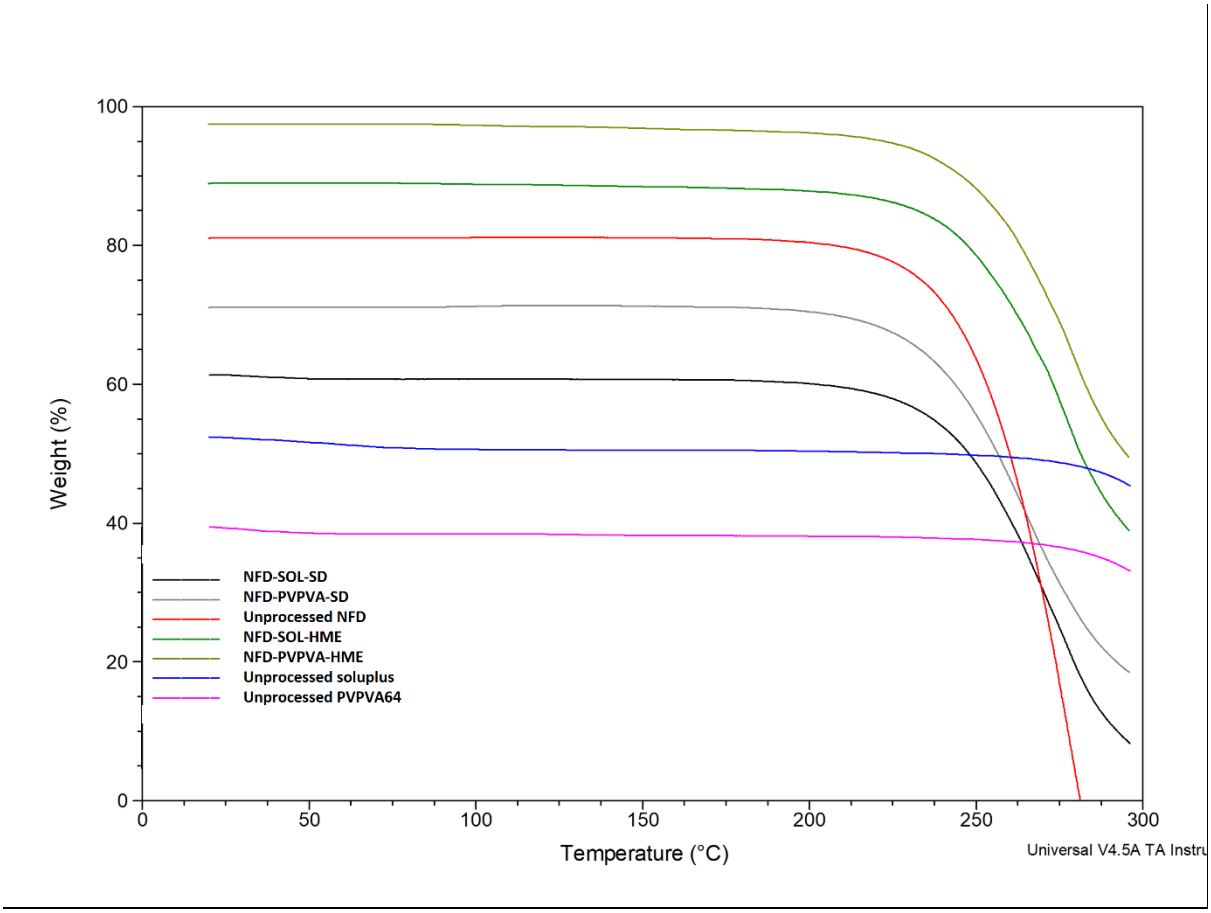

Figure S4. Thermogravimetric analysis of unprocessed NFD, unprocessed polymers and the four amorphous solid dispersions.

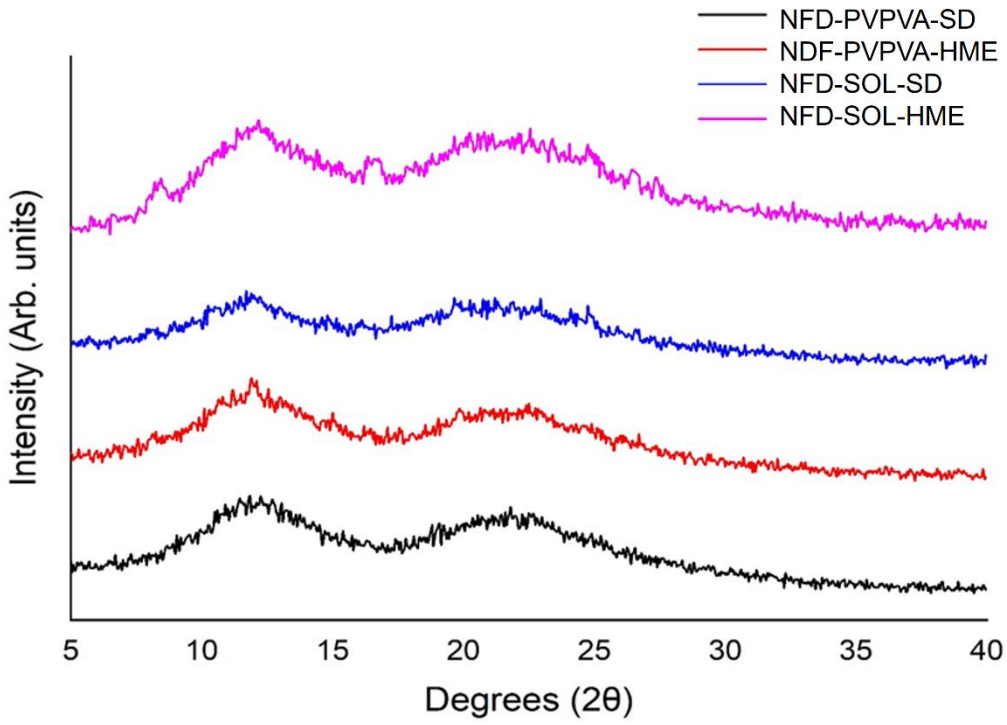

Figure S5. PXRD diffractograms post-DVS analysis of the four formulations.

Table S1. Determination coefficient values (R^2) in the analysis of the dissolution data using the following kinetic equations: first order, Hixson–Crowell and Korsmeyer–Peppas.

Formulation	Zero order	First order	Hixon-Crowell	Korsmeyer-Peppas
PVPVA-HME	0.9890	0.9939	0.9925	0.9927
PVPVA-SD	0.9736	0.9838	0.9809	0.9832
SOL-HME	0.9930	0.9973	0.9961	0.9956
SOL-SD	0.9364	0.9557	0.9498	0.9825

Table S2. Averaged determination coefficient values (R^2) for chemical stability.

Sample	Zero order	First order	Second order	Diffusion	Avrami
Crystalline NFD	0.894	0.892	0.891	0.868	0.892
NFD-SOL-HME	0.813	0.814	0.814	0.92	0.616
NFD-SOL-SD	0.920	0.919	0.918	0.818	0.941
NFD-PVPVA-HME	0.867	0.867	0.868	0.895	0.721
NFD-PVPVA-SD	0.916	0.917	0.919	0.969	0.805

Table S3. Averaged regression coefficients values for physical stability.

Sample	Zero order	First order	Second order	Diffusion	Avrami
NFD-SOL-HME	0.939	0.937	0.936	0.924	0.948
NFD-SOL-SD	0.907	0.912	0.915	0.86	0.935
NFD-PVPVA-HME	0.883	0.885	0.886	0.877	0.889
NFD-PVPVA-SD	0.99	0.99	0.991	0.991	0.989

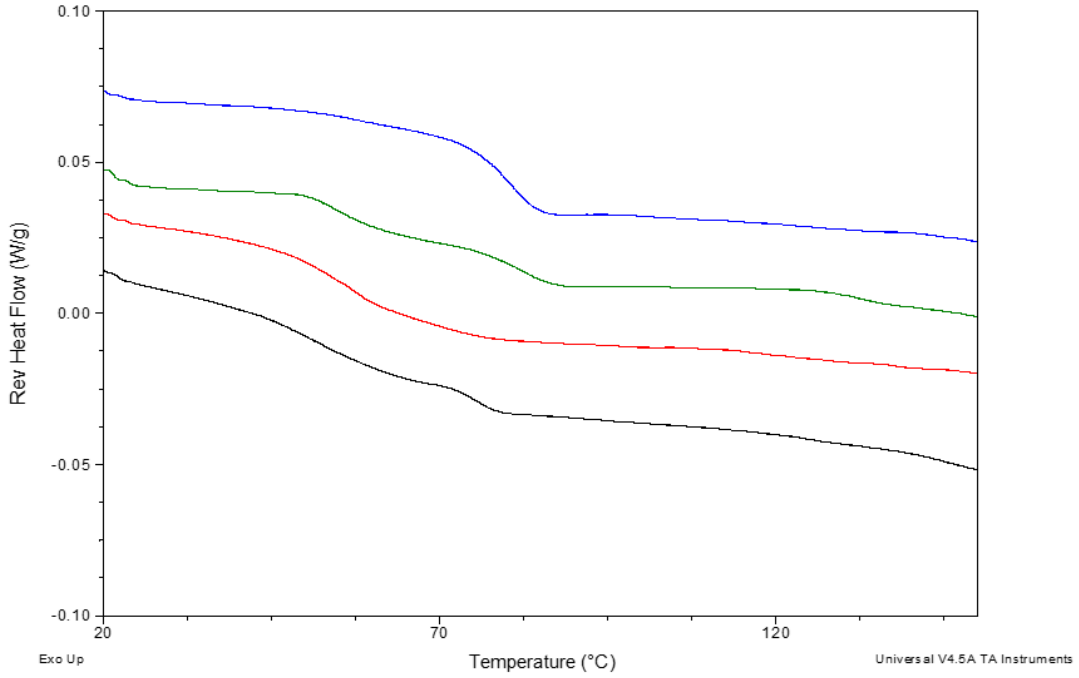

Figure S6. Reversing heat flow signal of the fours formulations after aging at different conditions of temperature and RH. Key: blue, NFD-PVPVA-SD, Green, NFD-PVPVA-HME, red, NFD-SOL-SD, black, NFD-SOL-HME.

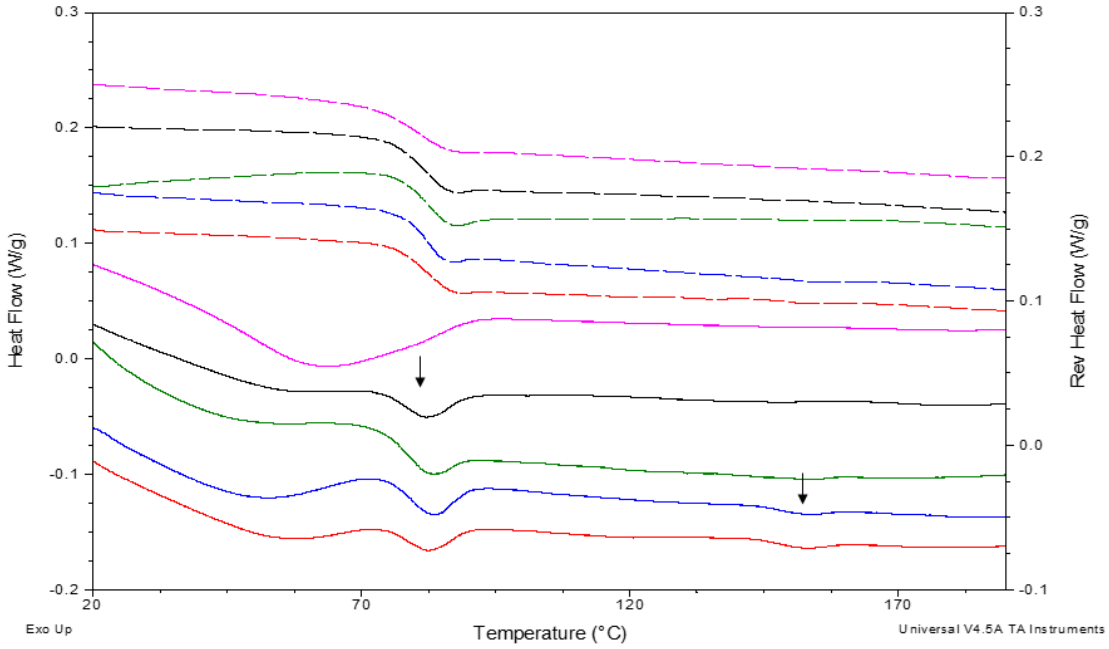

Figure S7. MTDSC of NFD-PVPVA-SD at different time points when exposed to 70 °C and 10% RH. Solid lines represent total heat flow and long dash are referred to reversing heat flow signal. Key: Fucsia, time zero; black, day

2; green, day 7; blue, day 14 and red, day 21. Arrows are pointing to relaxation enthalpy at the glass transition (left) and enthalpy of fusion (right).

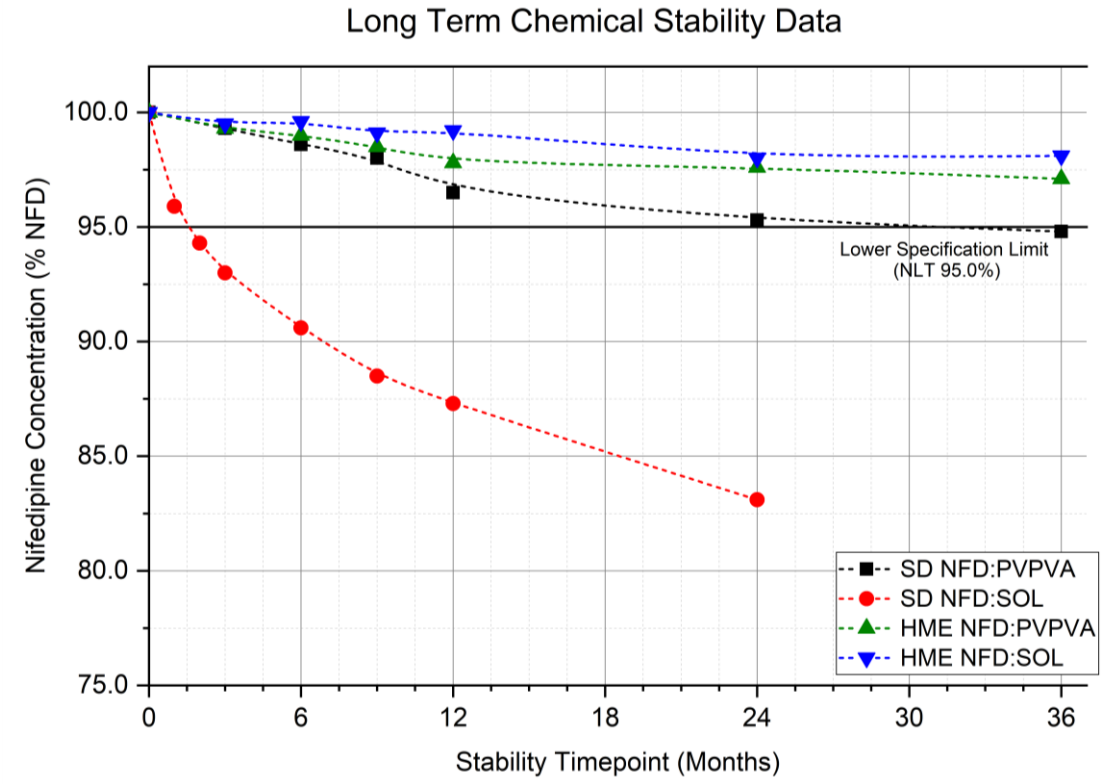

Figure S8. Predicted chemical stability of test materials stored at 25 °C and 10% RH.

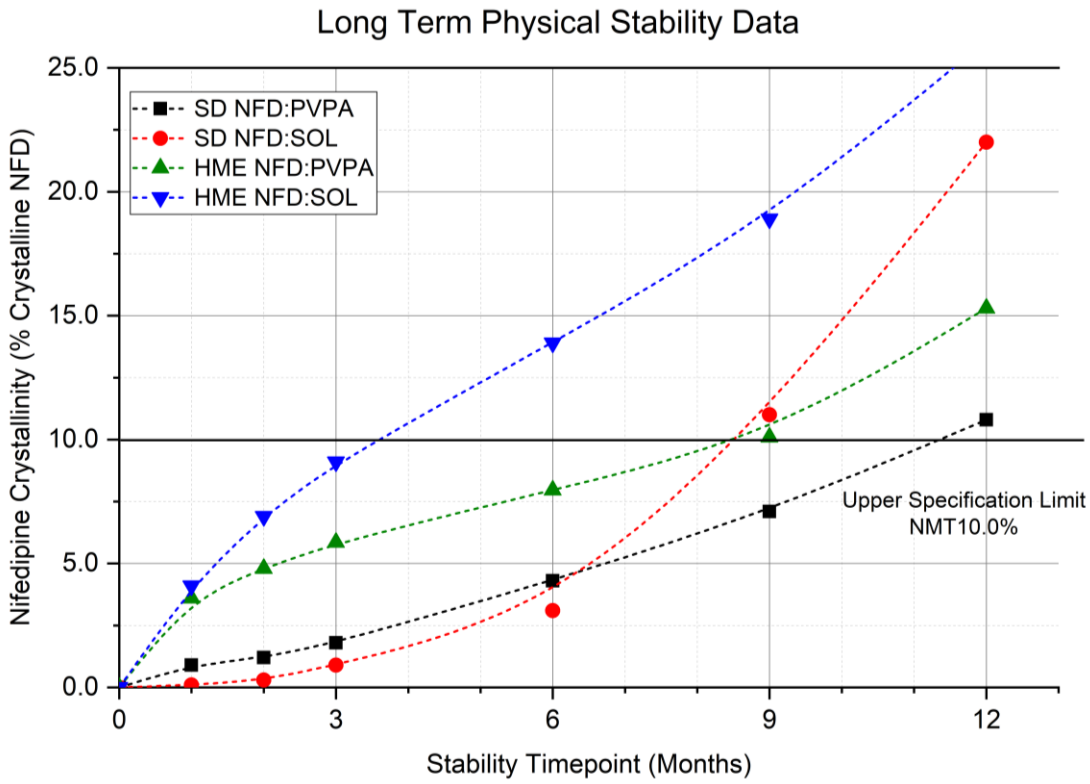

Figure S9. Predicted physical stability of test materials stored at 25 °C and 10% RH.

Chapter 4

4.0. Physical Accelerated Predictive Stability of Amorphous Solid Dispersions

Peter O'Connell[1,2,3], Dolores R. Serrano[2], Anne Marie Healy[1]*

[1]Synthesis and Solid State Pharmaceutical Centre (SSPC), School of Pharmacy and Pharmaceutical Sciences, Trinity College Dublin, Dublin 2, Ireland.

[2]Department of Pharmaceutics and Food Technology and Instituto Universitario de Farmacia Industrial (IUFI), School of Pharmacy, Universidad Complutense de Madrid, Plaza Ramon y Cajal s/n, 28040-Madrid, Spain.

[3]Cuspor Limited, Dublin 2, Ireland

*Corresponding author:
Anne Marie Healy
School of Pharmacy and Pharmaceutical Sciences
Trinity College Dublin
Dublin 2, Ireland.
Tel +353 1896 1444
Email healyam@tcd.ie

Abstract:

Predicting the physical stability of amorphous solid dispersions is a challenging task taking into account the complex kinetics involved in the process. A novel accelerated predictive stability based approach is proposed in this work to predict physical by determining the time to failure (isoconversion the time when the percentage of drug crystallisation reaches a set specification limit) for a selection of amorphous systems when exposed to a range of elevated temperature and relative humidity conditions. A humidity-corrected Arrhenius equation was then used to determine the crystalisation kinetic profile and estimate the effect of temperature and relative humidity on the crystallisation rates of several amorphous solid dispersions containing budesonide, griseofulvin, ritonavir or celecoxib formulated with HMPC AS or PVP K90. In budesonide-PVP K90 and griseofulvin-HMPC AS solid dispersions, the diffusion model predicted more accurately the physical stability than the Avrami model implying that drug molecules have to migrate through the matrix before nucleation takes place. However, an Avrami kinetic model was the most accurate in the long-term physical stability prediction for the budesonide-HPMC AS formulation which exhibited the highest stability which may be linked to the higher capacity to form hydrogen bonds with the drug, reducing further its molecular mobility making the diffusion process extremely slow. An acceptable prediction of long-term physical stability of amorphous solid dispersions was successful demonstrated using this methodology which can assist in the formulation decision making process making it faster and more accurate.

Keywords: physical stability, accelerated predictive stability, APS, ASAP, amorphous solid dispersions, in-silico modelling

Graphical abstract:

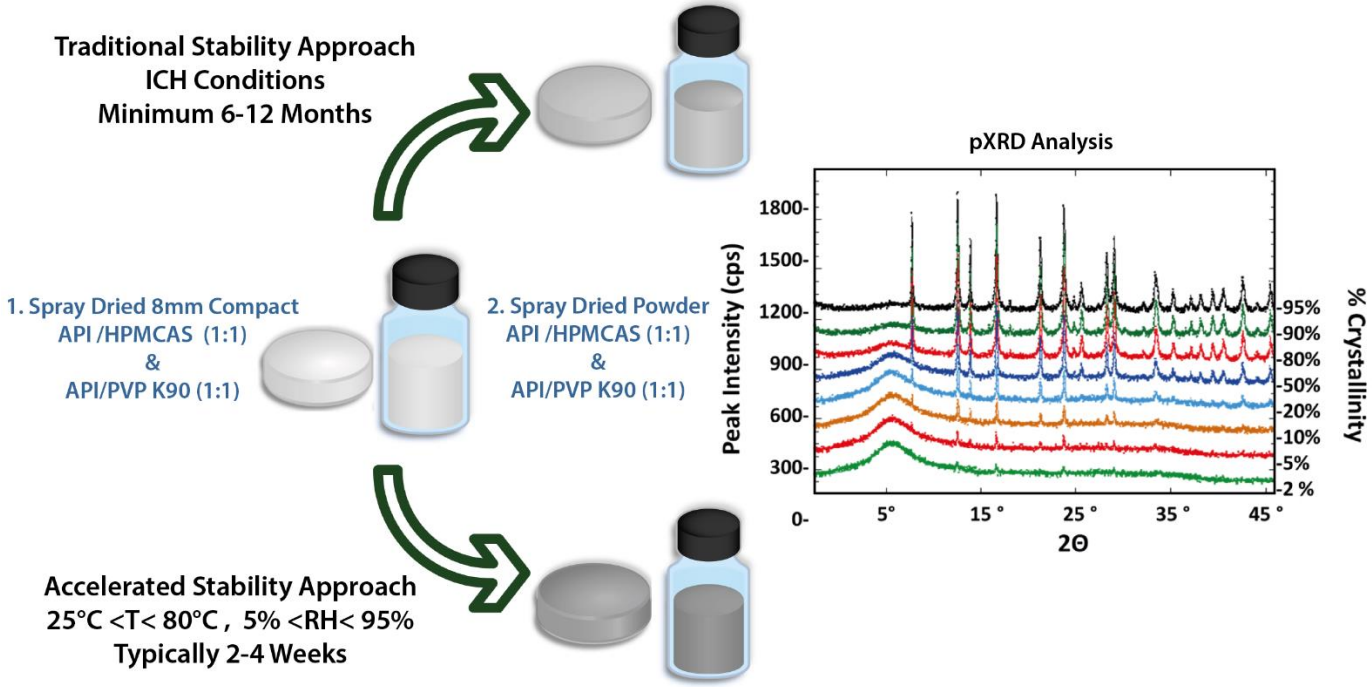

4.1 Introduction

Enhancing the solubility of hydrophobic drugs remains a challenge for oral delivery [1] as their low solubility often results in reduced bioavailability being required for the administration of higher doses to ensure that a therapeutic dose is delivered to the target organ [2]. Dispersing an active pharmaceutical ingredient (API) within an amorphous carrier [3, 4] – namely a polymer that controls drug release is one of the most common strategies to increase the dissolution rate of hydrophobic drugs[5].

Based on the molecular interactions between drug and carrier, amorphous solid dispersions can be classified in one of three ways:

i) amorphous solid solutions when drug and carrier are miscible and soluble originating a homogeneous molecular interaction and thereafter only one phase is present;
ii) amorphous solid suspensions which are formed when the drug has limited solubility or an extremely high melting point resulting in a dispersion composed of two phases without a molecularly homogeneous structure and
iii) a mixture of both of them when the drug is both dissolved and suspended in the carrier originating a heterogeneous structure with mixed properties of amorphous solid solutions and suspensions [4, 6].

Nevertheless, the tendency of amorphous drugs to recrystallise during storage limits their use, being critical to assess their stability profile at an early stage during the formulation development phase. Stability testing using standard ICH conditions (Typical long term condition of 25°C / 60% RH and accelerated condition of 40°C / 75% RH) typically requires at least six months of laboratory data collection and uses a linear extrapolation of data derived from a very narrow range of temperatures. Using a commercially available software application ASAPprime® (Accelerated Stability Assessment Programme), the chemical stability of drugs can be gathered in two to four weeks based on utilising a significantly wider range of temperature and relative humidity conditions. Currently, this modeling tool is widely utilised by pharmaceutical companies to support pharmaceutical formulation and establishing expiry dates / retest periods [7]. However, modeling of the physical stability of amorphous materials using ASAPprime® has not been documented but offers a potential to obtain a deeper and fast insight into the physical stability of amorphous solid dispersion during formulation development, screening and preclinical phases.

This work aims to prepare amorphous systems (either raw drug or drug formulated with different excipients) and assess the capability of ASAPprime® to predict the physical stability of different amorphous systems across a range of temperature and relative humidity conditions. Accurate measurements of temperature and relative humidity are crucial to obtain a reliable prediction, thus, the Cuspor ageing system has been used for the ageing of all the formulations as it incorporates a wireless datalogger into each environmental test chamber . Physical stability will be monitored by calculating the % crystalline content at various timepoint using a combination of pXRD, DSC and NIR analysis. The model drugs or drug/excipient formulations were selected based on their ability to be amorphised to track changes in crystallisation over a certain period and avoid a very fast crystallisation. Budesonide and griseofulvin which are poorly-soluble drugs that belong to Class II in the Biopharmaceutics Classification System (BCS) were selected as model API because their amorphous form is relatively stable with a glass transition (T_g) of 87-88 °C. Ritonavir with a lower T_g of 51 °C has also been studied as ritonavir amorphous solid dispersions are already in the market (Kaletra®, anti-HIV). T_g plays a key role in the physical stability of amorphous drugs [8]. To ensure the stability of amorphous materials, there are two logical approaches:

i) to store the amorphous API at temperatures well below the T_g ($T_{storage} = T_g - 50$ °C)[9] as the molecular mobility is limited or

ii) to co-process the API with high Tg excipients to obtain a miscible molecular system with higher T_g composite than the amorphous API by itself, then increasing the storage temperature at which the molecular mobility is still limited [10].

Polyvinylpyrrolidone K 90 (PVP K90) and Hypromellose acetate succinate (HMPC AS) have been selected as amorphous carriers to prepare the solid dispersions due to their spread use in formulations and their capacity to form hydrogen bonds to enhance the physical stability of amorphous solid dispersions.

4.2 Materials and Methods

4.2.1 Materials

Ritonavir and budesonide were purchased from Kemprotec Limited (Cumbria, UK). Griseofulvin and celecoxib were purchased from Sigma-Aldrich (Dublin, Ireland) with a purity ≥ 97%. HMPC AS LG was supplied by Shin-Etsu Chemical Co (Tokyo, Japan), and PVP K90 was a gift from BASF (Darmstadt, Germany). Ethanol and acetone were supplied from Fisher Scientific (Loughborough, United Kingdom). Humidity capsules and stability chambers were purchased from Cuspor Limited (Dublin, Ireland).

4.2.2 Methods

4.2.2.1 Preparation of amorphous systems

4.2.2.1.1 Amorphous budesonide

Ball milling

Milling was carried out in a Retsch PM100 planetary ball mill (Restch, Hope Valley, UK) using three stainless steel balls (Ø=20 mm) in each milling jar (50 ml). Crystalline budesonide (2.5 g) was used. The rotation speed of the sun wheel was set to 400 rpm. The total milling time was 18 h. A pause period of 10 min was made after 20 min of milling to avoid high temperature in the jar and thus the risk of crystallisation. The powder obtained was sieved through 300 µm stainless steel sieves to homogenize the particle size before performing the stability studies.

Spray-drying

Budesonide was dissolved at a concentration of 1% (w/v) in a mixture of ethanol: water (95:5, v:v). Spray-drying was carried out using a Büchi B-290 Mini Spray Dryer (Buchi, Flawil, Switzerland) operating in the open mode with an inlet temperature of 78°C and outlet temperature of 58°C, a pump speed of 30%, an aspirator at 100%, a nitrogen flow rate set at 473 Nl/h and a pressure of 6 bars [11].

4.2.2.2 Amorphous budesonide solid dispersions

Budesonide was dissolved at a concentration of 0.5 % (w/v) in a 300 ml mixture of ethanol: water (95:5, v:v). Thereafter, either PVP K90 or HMPC AS LG at 0.5% (w/v) was added to the solution. Sonication was required to obtain a completely transparent solution or slightly cloudy dispersion for PVP K90 and HMPC AS-LG respectively. Spray-drying was carried out using a Büchi B-290 Mini Spray Dryer operating in the open mode (inlet temperature 78°C, outlet temperature 58°C, pump speed 20%, aspirator 100%, nitrogen flow rate 473 Nl/h and a pressure of 6 bars)[11].

4.2.2.3 Griseofulvin amorphous solid dispersions

Griseofulvin was dissolved at a concentration of 0.5 % (w/v) in acetone (1.5 g in 300 ml). Thereafter, 1.5 g of HMPC AS LG (0.5 %, w/v) was added to the solution. Sonication was required to obtain a slightly cloudy dispersion. Spray-drying was carried out using a Büchi B-290 Mini Spray Dryer operating in the close mode (inlet temperature 60°C, outlet temperature 41°C, pump speed 30%, aspirator 100%, nitrogen flow rate 473 Nl/h and a pressure of 6 bars). The formulation with PVP K90 was prepared as follows: PVP K90 (1.5 g) was dissolved in 120 ml of miliQ H_2O and griseofulvin (1.5 g) was dissolved in acetone (180 ml). Under sonication, acetone (180 ml) containing dissolved griseofulvin (1.5 g) was poured slowly onto the PVP solution obtaining a clear solution that was spray-dried. The final solution that was spray-dried was consisting of PVP (0.5%, w/v), Griseofulvin (0.5%, w/v) dissolved in a mixture (300 ml) of H_2O/acetone (40/60). The spray-drying was carried out in a Büchi B-290 Mini Spray Dryer operating in the close mode (inlet temperature 85°C, outlet temperature 51°C, pump speed 30%, aspirator 100%, nitrogen flow rate 473 Nl/h and a pressure of 6 bars).

4.2.2.4 Ritonavir amorphous solid dispersions

Ritonavir was dissolved at a concentration of 0.5 % (w/v) in a mixture of ethanol: water (95:5, v:v). Thereafter, either PVP K90 or HMPC AS LG at 0.5% (w/v) was added to the solution. Sonication was required to obtain a completely transparent solution or slightly cloudy dispersion for PVP K90 and HMPC AS-LG respectively. Spray-drying was carried out using a Büchi B-290 Mini Spray Dryer operating in the open mode (inlet temperature 78°C, outlet temperature 58°C, pump speed 20%, aspirator 100%, nitrogen flow rate 473 Nl/h).

The second experiment was performed in a drug: excipient mass ratio of 2:1. Ritonavir was dissolved at 0.67 % (w/v) in a mixture of ethanol: water (95:5, v:v). Thereafter, either PVP K90 or HMPC AS LG at 0.33% (w/v) was added to the solution. The spray-dried conditions were the same as the above described.

4.2.2.5 Celecoxib amorphous solid dispersions

Celecoxib was dissolved at 0.75 % (w/v) in ethanol. Thereafter, either PVP K90 or HMPC AS LG at 0.75% (w/v) was added to the solution. Sonication was required to obtain a completely transparent solution or slightly cloudy dispersion for PVP K90 and HMPC AS-LG respectively. Spray-drying was carried out using a Büchi B-290 Mini Spray Dryer operating in the close mode (inlet temperature 78°C, outlet temperature 58°C, pump speed 20%, aspirator 100%, nitrogen flow rate 473 Nl/h).

4.2.3 Solid-state characterisation

4.2.3.1 Powder X-ray diffraction (PXRD)

Powder X-ray analysis was performed using a Rigaku Miniflex II diffractometer (Rigaku, Tokyo, Japan) with Ni-filtered Cu Kα radiation (λ= 1.54 Å). The tube voltage and tube current used were 30 kV and 15 mA, respectively. Each sample was scanned over a 2 theta range of 5‑40° with a step size of 0.05°/s [12]. PXRD patterns were recorded at least in duplicate.

4.2.3.2 Differential scanning calorimetry (DSC)

Differential scanning calorimetry was performed on a QA-200 TA Instruments (TA Instruments, United Kingdom) calorimeter using nitrogen as a purge gas. Sample powders (3-5 mg) were placed in aluminum pans, sealed, pierced to provide one vent hole and heated at a rate of 10 °C/min in the temperature range of 25–300 °C, 25–250 °C, 25–180 °C, and 25–180 °C for budesonide, griseofulvin, ritonavir, and celecoxib respectively. The calibration of the instrument was carried out using indium as standard. The temperature of exothermic or endothermic events was referred to as the onset temperature. Glass transition temperatures were measured at the midpoint of the specific-heat capacity (Cp) shift.

4.2.3.3 Near-Infrared Spectroscopy (NIR)

NIR spectra were collected using a Buchi NIR (Flawil, Switzerland) with a NIR reflectance attachment. Spectra were collected with interleaved scans in the 10 000−4000 cm^{-1} range with a resolution of 8 cm^{-1}, using 32 co-added scans. Samples were repositioned between each measurement in triplicate. NIR data analysis was carried out using the NIRCal Chemometric software (Flawil, Switzerland). Preprocessing methods (standard normal variate) transformation was used. Partial least-squares (PLS) regression was used to create calibration models for quantitative analysis, and its performance was evaluated using the correlation coefficient (R^2) and the root mean-square error (RMSE) [8].

4.2.3.4 Dynamic vapour sorption (DVS)

Sorption isotherms and kinetic profiles of the formulations were obtained using SMS Advantage (Surface Measurement Systems, Alperton, UK). Water was used as the probe vapour and the temperature was set at 40 °C. Samples were subjected to step changes of 10% RH up to 90% RH and the reverse for desorption [13]. The second sorption cycle isotherms were also determined. The sample mass was allowed to reach equilibrium defined as $dm/dt \leq 0.002$ mg/min over 10 min before the RH was changed. Sample weights were between 8 and 12 mg. The crystalline nature of the systems was confirmed by PXRD after every complete run. The percentage of vapour uptake in the first sorption cycle at the different steps of RH was used to calculate GAB parameters necessary for the modelling with the ASAPprime® software.

4.2.4 Quantification of amorphous content

Different weight fractions of crystalline API (Xc) (Xc= 0.1, 0.25, 0.5, 0.75, 0.9) were mixed with the relevant quantities of amorphous API (total mixed sample weight 200 mg) using an agate mortar and pestle. The calibration curves containing one of the polymers as excipient were prepared as follows: it was prepared initially a physical mixture of crystalline drug and excipient in a mass ratio 1:1 (w/w) in a mortar and pestle. Different weight fractions of the mixture crystalline API- excipient (Xc= 0.1, 0.25, 0.5, 0.75, 0.9) were mixed with the relevant quantities of amorphous solid dispersion (total mixed sample weight 200 mg) using an agate mortar and pestle. Calibration curves were produced in duplicate. Each set of reference standards was analysed by PXRD, DSC, and NIR for each weight fraction [13].

The position of the PXRD peak used for the quantification was at 6.2, 10.85, 21.7 ,and 19.7 2 theta degrees for budesonide, griseofulvin, ritonavir, and celecoxib respectively which were selected due to the lack of interference with other peaks in the diffractogram. Rigaku Peak Integral software was used in the determination of peak intensity for each sample using the Sonnefelt-Visser background edit procedure. A calibration curve was constructed using the area of the characteristic peak for each weight fraction for each formulation. Another calibration curve was constructed for determining the crystallinity percent of the sample via DSC using either the heat of crystallisation (ΔH_c) or the enthalpy of fusion (ΔH_f) when no crystallisation peak was observed in the thermograms [14]. The calibration curve for NIR was performed as above described. The crystalline content was calculated as the average value obtained from NIR, PXRD, and DSC measurements (Table 4-1).

Table 4-1. Techniques employed to quantify amorphous content in each amorphous system.

Amorphous system	Quantification technique
Milled budesonide	PXRD (6.2 thetha) / DSC (ΔHc)/ NIR
Spray dried budesonide	PXRD (6.2 thetha) / DSC (ΔHc)/ NIR
Spray dried budesonide:HMPC AS	PXRD (6.2 thetha) / DSC (ΔHc)/ NIR
Spray dried budesonide: PVP K90	PXRD (6.2 thetha) / DSC (ΔHc)
Spray dried griseofulvin:HMPC AS	PXRD (10.85 thetha) / DSC (ΔHc)/ NIR
Spray dried ritonavir:HMPC AS	PXRD (21.7 thetha) / DSC (ΔHf)
Spray dried ritonavir: PVP K90	PXRD (21.7 thetha) / DSC (ΔHf)
Spray dried celecoxib: HMPC AS	PXRD (19.7 thetha) / DSC (ΔHf)
Spray dried celecoxib: PVP K90	PXRD (19.7 thetha) / DSC (ΔHf)

4.2.5 Ageing of the samples

All the formulations were kept at room temperature (26.33 ± 1.21 °C) in a desiccator containing silica gel (RH= 11.51 ± 1.64 %) prior to the ageing. The corresponding humidity capsules were placed into the Cuspor chambers which were put inside the oven at the selected temperature to ensure that the equilibrium of the RH was reached before the ageing of the formulations. A sensor was introduced in each chamber to collect the temperature and humidity during the whole ageing process. The conditions used in the experiments are summarised in Table 4-2. The average temperature and relative humidity in every condition during the experiment were calculated and were used in the prediction models below described.

The formulations (40 mg) were placed in uncapped HPLC vials and introduced in the test chambers being exposed to different conditions of temperature and humidity. At different time points, samples were collected and analysed by PXRD, DSC, and NIR to quantify crystalline content.

Long-term stability studies were performed at 25 °C/10% RH, 25 °C/50% RH and 40 °C/75% RH. Samples were analysed by pXRD, DSC and NIR at different time points. Real time stability data for materials stored at these conditions was compared with the values obtained from the tability spreadiction models.

Table 4-2. Protocol for the accelerated screening of SD budesonide and amorphous solid dispersions.
Key * The celecoxib formulations and ritonavir:excipient 2:1 formulations were the only ones tested at 60°C / 90% RH but not at 60°C /10% RH.

SD budesonide		Amorphous solid dispersions	
Temperature (°C)	Relative humidity (%)	Temperature (°C)	Relative humidity (%)
25	75	40	75
40	17	50	15
40	30	50	50
40	75	60	10
50	15	60	30
50	50	60	60
60	30	60*	90*
60	75	70	11
70	11	70	65
70	75	80	25
80	11	80	50
80	50	-	-

4.2.6 Modelling of physical stability

The modelling of physical stability of the tested formulations was performed using ASAPprime® software (Freethink Technologies, Branford, CT, USA). This software calculates the degradation rate at the isoconversion time (defined as the time when the percentage of crystallisation reaches the specification limit 10% in our study) for each temperatre and relative humidity condition. A humidity-corrected Arrhenius equation was used to estimate the effect of temperature and relative humidity on the crystallisation rates of the amorphous solid dispersions (Eq.1).

$$lnK = lnA - \frac{Ea}{RT} + B\ (RH) \qquad \text{(Eq. 1)}$$

where k is the cyrstallisation rate (% crystallised drug/day), T is the temperature in Kelvin degrees, A is the collision factor, B is the moisture sensitivity factor, RH is the relative humidity, Ea is the activation energy in kcal mol^{-1}, and R is the gas constant (0.00198 kcal K^{-1} mol^{-1}). The method used was focused on the percentage of crystallisation with variation in temperature and relative humidity. Parameters selected for modelling were the following: limit of detection 1%, specification limit 10%, Montecarlo simulations 2500 steps, and calculated GAB parameters were obtained from DVS isotherm plots. In order to calculate the degradation rate, the amount of cyrstallised drug at different time points was fitted at each condition to the following kinetic models: zero-order, first-order, second-order, Avrami, and diffusion using the following equations (Eq. 2-6) [15, 16]:

Zero-order: $[DC] = kt$ (Eq. 2)

1st order: $[DC]=[DC]_\infty[1-e^{(-kt)}]$ (Eq. 3)

2nd order: $[DC]=[DC]_\infty kt/ (1/[DC]_\infty + kt)$ (Eq. 4)

Diffusion: $[DC]=kt^{1/2}$ (Eq. 5)

Avrami: $[DC] = [DC]_\infty - e^{(-kt\wedge 2)}$ (Eq. 6)

where t is the time expressed in days, K is the crystallisation rate over time, and [DC] is the amount of crystalline drug expressed in percentage at each time point. To test the suitability of the models, the regression coefficient (R^2) was used. The Arrhenius equation was employed to estimate the activation energy and the effect of temperature on the crystallisation rate of each drug in each

amorphous system. The percentage of crystallisation at 25 °C/10% RH, 25 °C/50% RH, and 40 °C/75% RH was extrapolated from the calculated Arrhenius equations and was compared with the long-term data to validate the accelerated physical stability models.

4.3 Results

4.3.1 Preparation and characterisation of the formulations

The yield of the formulation was significantly increased when the API was co-spray dried in the presence of the excipient (Table 4-3). A higher yield (between 10-30% depending on the API) was obtained when HMPC was used.

Table 4-3. Characteristics of the tested amorphous systems.

Drug Tg (°C)/ LogP	Excipient	Mass ratio drug:excipient	Process	Yield (%)	Amorphous drug after processing
Budesonide **87-88°C / 1.9**	-	-	Milling (18 h)	87	Yes
	-	-	Spray drying	45	Yes
	HPMC AS LG	1:1	Spray drying	74	Yes
	PVP K90	1:1	Spray drying	65	Yes
Griseofulvin **88-89°C / 2.2**	HPMC AS LG	1:1	Spray drying	72	Yes
	PVP K90	1:1	Spray drying	44	No
Ritonavir **45-49°C / 3.9**	HPMC AS LG	1:1	Spray drying	75	Yes
	PVP K90	1:1	Spray drying	67	Yes
	HPMC AS LG	2:1	Spray drying	75	Yes
	PVP K90	2:1	Spray drying	66	Yes
Celecoxib **51-52°C / 3.9**	HPMC AS LG	1:1	Spray drying	88	Yes
	PVP K90	1:1	Spray drying	62	Yes

Apart from griseofulvin-PVP system (Fig. 1E b), all the other co-spray dried systems resulted in the formation of an amorphous solid dispersion characterised by the presence of a characteristic amorphous halo as shown in the pXRD patterns (Fig. 23). No differences in the pXRD were observed between spray dried and milled budesonide. However, the DSC thermograms of milled budesonide showed a double exotherm event a 77.4°C and 100.6°C whereas spray dried budesonide exhibited a single crystallisation peak at a higher temperature (109.2°C) (Fig. 2A). The exotherm was preceded by a glass transition with the midpoint at ~88.9°C which is in good agreement with the observation of Tabjer et al. [11]. The co-spray dried budesonide:HPMC AS exhibited a single T_g at 92.1°C and higher onset of crystallisation (149.4°C) (Fig. 2B). A melting

event at 232.6°C was also observed. However, the co-spray dried budesonide:PVP K90 system displayed an endothermic event at temperatures below 100 °C probably indicating dehydration of the polymer not being evident the presence of a T_g composite (Fig. 24B). Both ritonavir:HMPC AS systems (1:1 and 2:1 weight ratio) exhibited a higher Tg composite at 60.1°C and 62.2°C respectively (Fig. 24C and 24D) than the Tg from the amorphous API alone (about 45°C - 49°C)[17]. No melting event was observed in any of the amorphous systems.

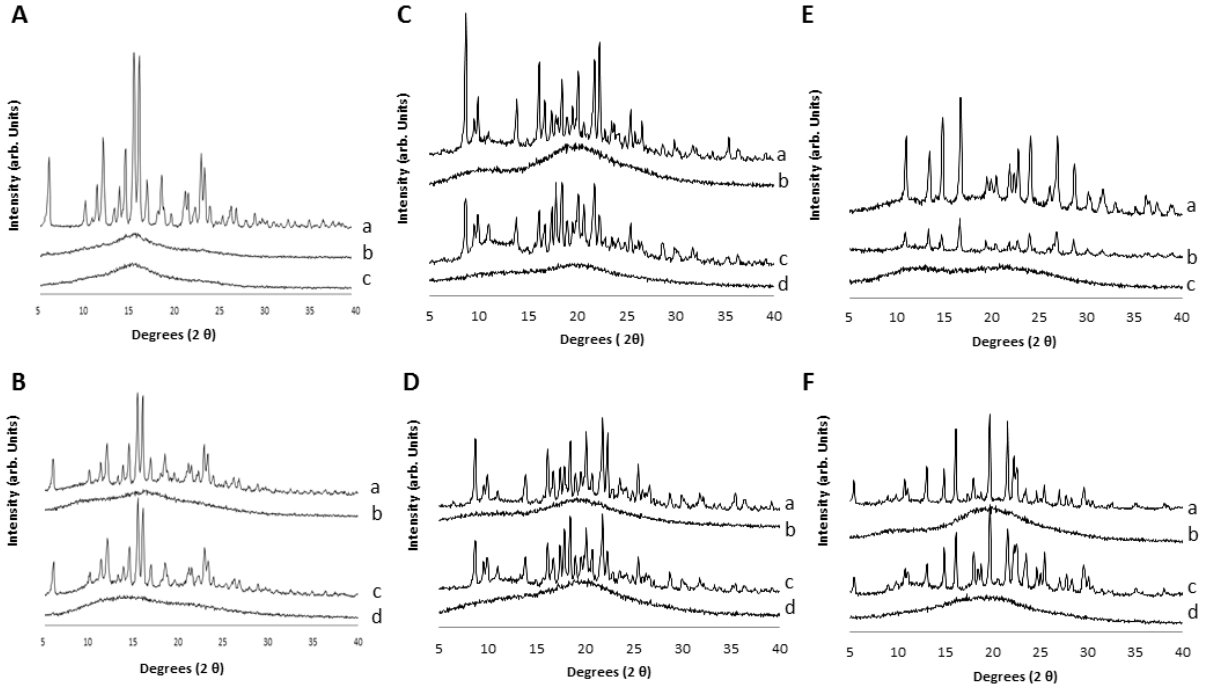

Figure 23: pXRD patterns budesonide, ritonavir, griseofulvin, celecoxib

A) Budesonide. Key: a) Crystalline budesonide, b) milled budesonide, c) spray dried budesonide; **B) Co-spray dried budesonide formulations**. Key: a) a physical mixture of crystalline budesonide and HPMC AS (1:1, w/w), b) spray dried budesonide-HPMC AS (1:1, w/w), c) a physical mixture of crystalline budesonide and PVP K90 (1:1, w/w) and d) spray dried budesonide- PVP K90 (1:1, w/w). **C) Co-spray dried ritonavir formulations (1:1 weight ratio)**. Key: a) a physical mixture of crystalline ritonavir and HPMC AS (1:1, w/w), b) spray dried ritonavir-HPMC AS (1:1, w/w), c) a physical mixture of crystalline ritonavir and PVP K90 (1:1, w/w) and d) spray dried ritonavir- PVP K90 (1:1, w/w); **D) Co-spray dried ritonavir formulations (2:1 weight ratio)**. Key: a) a physical mixture of crystalline ritonavir and HPMC AS (2:1, w/w), b) spray dried ritonavir-HPMC AS (2:1, w/w), c) a physical mixture of crystalline ritonavir and PVP K90 (2:1, w/w) and d) spray dried ritonavir- PVP K90 (2:1, w/w); **E) Co-spray dried griseofulvin formulations**. Key: a) a physical mixture of crystalline griseofulvin and HPMC AS (1:1, w/w), b) spray dried griseofulvin-PVP K90 (1:1, w/w) and c) spray dried griseofulvin-HPMC AS (1:1, w/w); **F) Co-spray dried celecoxib formulations**. Key: a) a physical mixture of crystalline celecoxib and HPMC AS (1:1, w/w), b) spray dried celecoxib-HPMC AS (1:1, w/w), c) a physical mixture of crystalline celecoxib and PVP K90 (1:1, w/w) and d) spray dried celecoxib- PVP K90 (1:1, w/w).

Ritonavir:PVP K90 systems (1:1 and 2:1 ratio) exhibited a Tg composite at 59.7°C and 65.1 °C respectively (Fig. 3 and 4). No melting event was observed. Griseofulvin:HMPC AS formulation showed a glass transition at 86.9°C similar to what other authors have reported for the amorphous

drug itself [18]. A melting event ocurred at 203.4°C which is observed also in the physical mixture with the polymer (Fig. 24E). Co-spray dried celecoxib formulations were characterised by the absence of a melting event (Fig. 24F). The Tg composite at 73.1 °C was observed in the celecoxib:HPMC AS formulation which was around 20°C higher than the Tg of amorphous celecoxib alone reported by other authors [19].

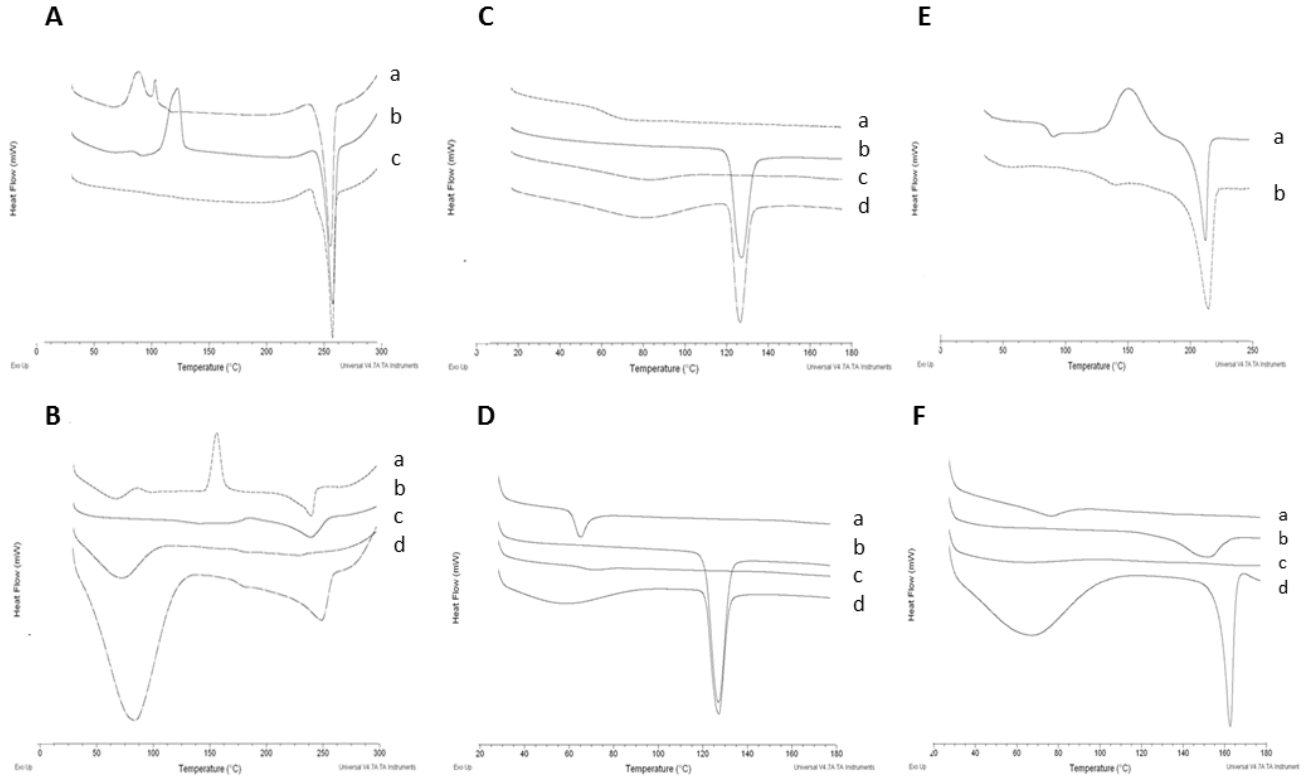

Figure 24: DSC thermograms budesonide, ritonavir, griseofulvin, celecoxib

A) Budesonide. Key: a) milled, b) spray dried and c) crystalline budesonide; **B) Co-spray dried budesonide formulations**. Key: a) spray dried budesonide-HPMC AS (1:1, w/w), b) a physical mixture of crystalline budesonide and HPMC AS (1:1, w/w), c) spray dried budesonide- PVP K90 (1:1, w/w) and d) a physical mixture of crystalline budesonide and PVP K90 (1:1, w/w); **C) Co-spray dried ritonavir formulations (1:1 ratio)**. Key: a) spray dried ritonavir-HPMC AS (1:1, w/w), b) a physical mixture of crystalline ritonavir and HPMC AS (1:1, w/w), c) spray dried ritonavir- PVP K90 (1:1, w/w) and d) a physical mixture of crystalline ritonavir and PVP K90 (1:1, w/w); **D) Co-spray dried ritonavir formulations (2:1 ratio)**. Key: a) spray dried ritonavir-HPMC AS (2:1, w/w), b) a physical mixture of crystalline ritonavir and HPMC AS (2:1, w/w), c) spray dried ritonavir- PVP K90 (2:1, w/w) and d) a physical mixture of crystalline ritonavir and PVP K90 (2:1, w/w); **E) Co-spray dried griseofulvin formulations**. Key: a) spray dried griseofulvin-HPMC AS (1:1, w/w), b) a physical mixture of crystalline griseofulvin and HPMC AS (1:1, w/w); **F) Co-spray dried celecoxib formulations**. Key: a) spray dried celecoxib-HPMC AS (1:1, w/w), b) a physical mixture of crystalline celecoxib and HPMC AS (1:1, w/w), c) spray dried celecoxib- PVP K90 (1:1, w/w) and d) a physical mixture of crystalline celecoxib and PVP K90 (1:1, w/w).

4.3.2 Modelling of physical stability

Both milled budesonide and spray-dried budesonide showed complete crytallisation after 24 hours at extreme conditions of temperature and relative humidity. To predict the stability of the amorphous budesonide, less stressful temperature and relative humidity conditions (25°C and 40 °C) were included in a modified ageing protocol. Milled budesonide recrystallised rapidly at all the tested conditions and as a result physical stability could not be modelled. On the contrary, celecoxib and ritonavir mixed with HPMC AS or PVP K90 in a 1:1 weight ratio were physically stable in almost all the range of ageing conditions not having enough data to create any model. At least five conditions (of temperature and RH) are necessary to build a statistically accurate model with a minimum of three degrees of freedom. The ageing protocol for the remaining amorphous systems (co-spray dried budesonide, co-spray dried ritonavir:excipient, 2:1 weight ratio, and co-spray dried griseofulvin-HPMC AS) was amenable to modelling of crystallisation kinetic behaviour.

Prior to modelling, the moisture sorption isotherms for each system were analysed and the Guggenheim-Anderson-de Boer (GAB) parameters were calculated taking into account the percentage of vapour uptake at every RH step (Table 4-4, Fig. S1 in Supplementary material). The GAB isotherm discriminates between multilayer and condensate properties of molecules sorbed on top of the first molecule at a site, being C, K and W_m the three main parameters [20, 21]. C measures the strength of binding of water to the primary binding sites and can be represented as the ratio between the partition function of the first molecule sorbed on a site and the molecules sorbed beyond the first molecule in the multilayer. The greater the C parameter, the stronger water is bound in the monolayer, and the larger the differences in enthalpy between the molecules at the monolayer and multilayer [22]. W_m represents the number of molecules forming the monolayer or the monolayer moisture content, in other words, the availability of active sites for water sorption by the material. K is a constant in the GAB sorption equation that corrects the properties of the multilayer molecules relative to the bulk liquid. The more the sorbed molecules in the multilayer, the lower the value for K is. When K value is close to 1, the difference is minimum between multilayer molecules and liquid molecules because the vapour molecules beyond the monolayer are not structured in a multilayer but exhibit similar characteristics to the molecules in the bulk liquid [20].

Table 4-4. GAB parameters of the different formulations.
Co-spray dried celecoxibformulation were not modelled as no crystallisation was observed in any of theconditions tested.

System	W_m	C	K
Milled budesonide	0.13	2.5	0.748
Spray dried budesonide	4.265	0.795	0.613
Co-spray dried budesonide:HMPC AS (1:1 w/w)	1.914	2.809	0.781
Co-spray dried budesonide: PVP K90 (1:1 w/w)	4.487	4.701	0.934
Co-spray dried griseofulvin:HMPC AS (1:1 w/w)	1.064	3.536	0.869
Co-spray dried ritonavir:HMPC AS (1:1 w/w)	3.067	1.346	0.711
Co-spray dried ritonavir: PVP K90 (1:1 w/w)	5.708	2.247	0.9
Co-spray dried ritonavir:HMPC AS (2:1 w/w)	4.429	0.868	0.638
Co-spray dried ritonavir: PVP K90 (2:1 w/w)	4.881	1.428	0.887

The spray dried budesonide demonstrated a much greater vapour uptake (higher Wm value) than the milled drug (Table 4). Spray dried formulations containing HMPC AS sorbed a lower amount of vapour water than the ones containing PVP K90. This could affect considerably the physical stability of the amorphous systems at higher RH conditions and then these parameters were taken into account in the model of physical stability.

4.3.2.1 Spray dried budesonide

The crystalline content was quantified at several time points at the different ageing conditions (Table S1, Supplementary material). Among all the assessed fitting models, Avrami showed the best fitting with a good correlation coefficient value (R^2>0.99) and an acceptable residual plot (Fig. S2, Supplementary material). The residual plot shows the quality of the fit of the moisture-modified Arrhenius equation to the isoconversion data, defined as the time when the percentage of crystalline content equals the specification limit (set at 10% in our study). A good fit of the Avrami- model is evident as the majority of the experimental data points are lying near the zero residual [15]. The crystallisation plots using the Avrami model showed also good correlation with the experimental data point (Fig. S2, Supplementary material). However, the predicted activation energy was extremely high (82.38 ± 10.91 Kcal/mol) which may be a sign that there is a phase transition occurring at higher temperatures [15]. Zero-order was the second fitting model with the greatest correlation coefficient value (R^2), also exhibiting a good match with the experimental data at all tested conditions (Fig. 25).

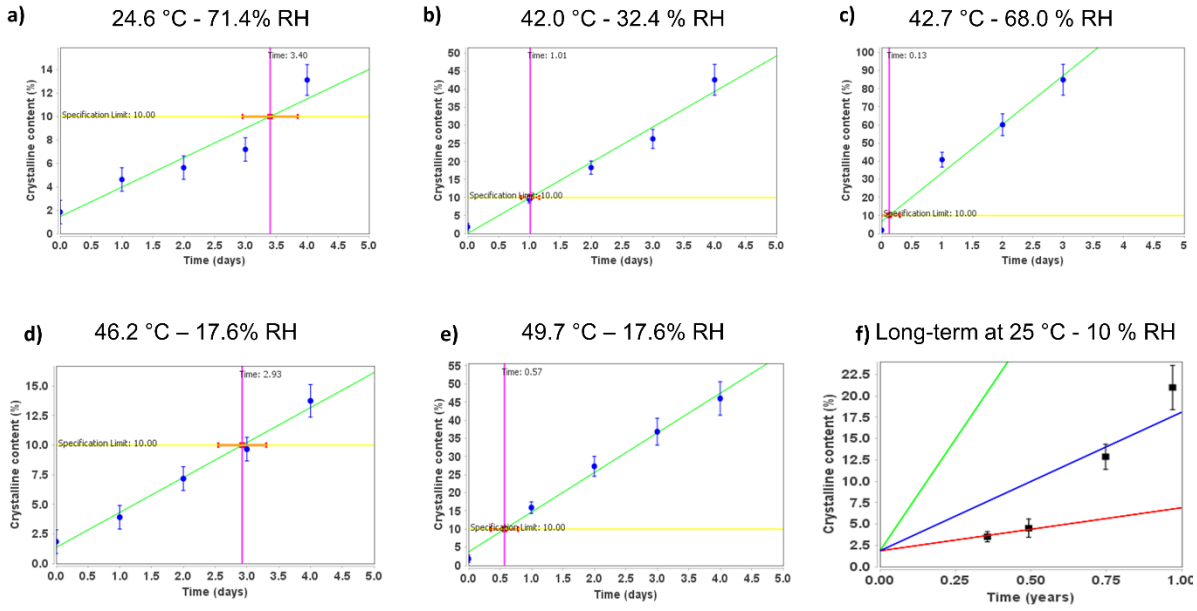

Figure 25: Zero-order modelling of the physical stability of the spray dried budesonide at different condition

a) 24.6°C/71.4% RH, b) 42.0°C/32.4% RH; c) 42.7°C/68.0% RH, d) 46.2°C/17.6% RH, e) 49.7°C/17.6% RH and f) Long-term prediction at 25.0°C/10% RH. Key: the specification limit (10%) is represented in yellow while the isoconversion time (time required for 10% of the drug to recrystallise) is represented in pink color.

Long-term stability was predicted only at 25 °C/10% RH for the spray dried budesonide formulation as drug crystallisation ocurred extremely fast at other conditions. Experimental data were compared with the different crystallisaiton kinetic models up to one year (Fig. 25 & 26). The blue curve represents the mean predicted physical stability at 25°C/10% RH from the modified-Arrhenius equation, the red line refers to one standard deviation above the mean while the green line refers to one standard deviation below the mean. The zero-order kinetic model showed the most accurate prediction of the physical stability of spray dried budesonide (Fig. 25f). Both Avrami and diffusion models overestimated the physical stability of the amorphous system while first and second-order were more conservative and hence, the models understimated its physical stability long term.

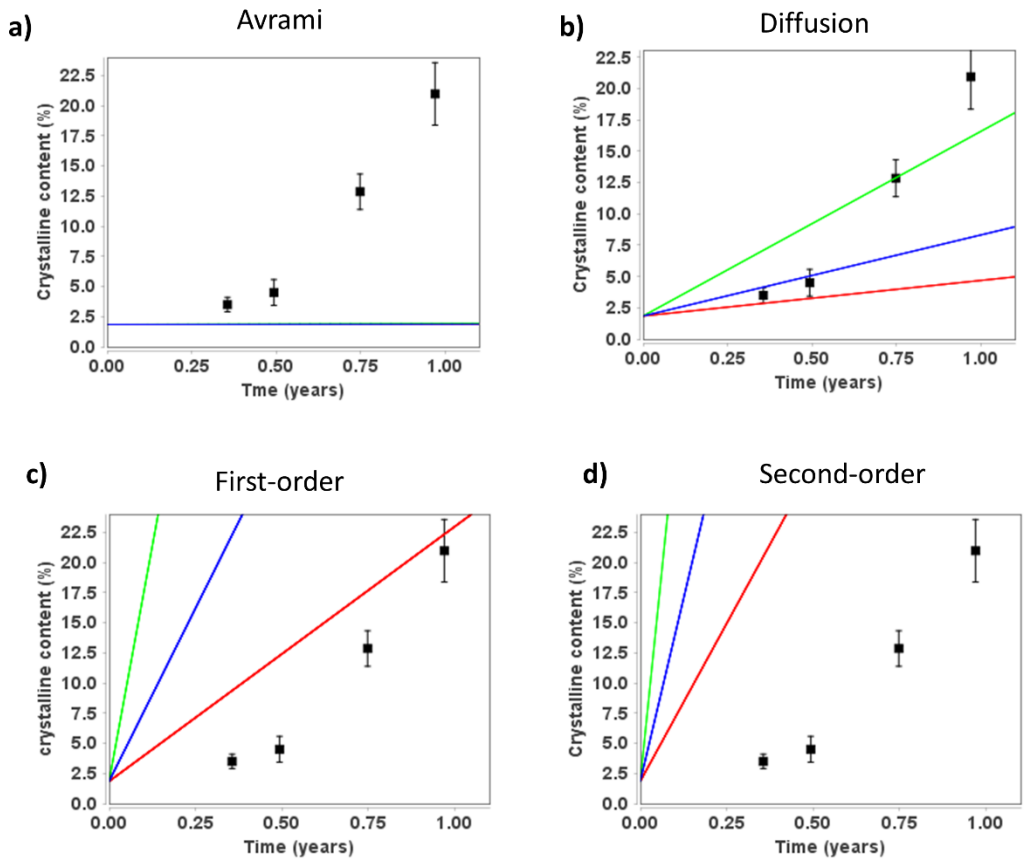

Figure 26: Long-term physical stability prediction of spray dried budesonide formulation using 1st, 2nd, Avrami, and diffusion kinetic models

4.3.2.2 Co-Spray dried budesonide:HMPC AS (1:1, w/w)

The crystalline budesonide content was quantified at several time points at the different ageing conditions (Table S3, Supplementary material). Amongst the assessed kinetic models, all of them exhibited a good correlation coefficient value above 0.9, but the activation energy and the moisture sensitivity factor showed high variability ranging from 20 to 57 Kcal/mol, and 0.025-0.058, respectively (Table S4, Supplementary material). Avrami model was the one that exhibited the best fitting to the experimental data points and the lowest residual levels in all the tested conditions (Fig. 27).

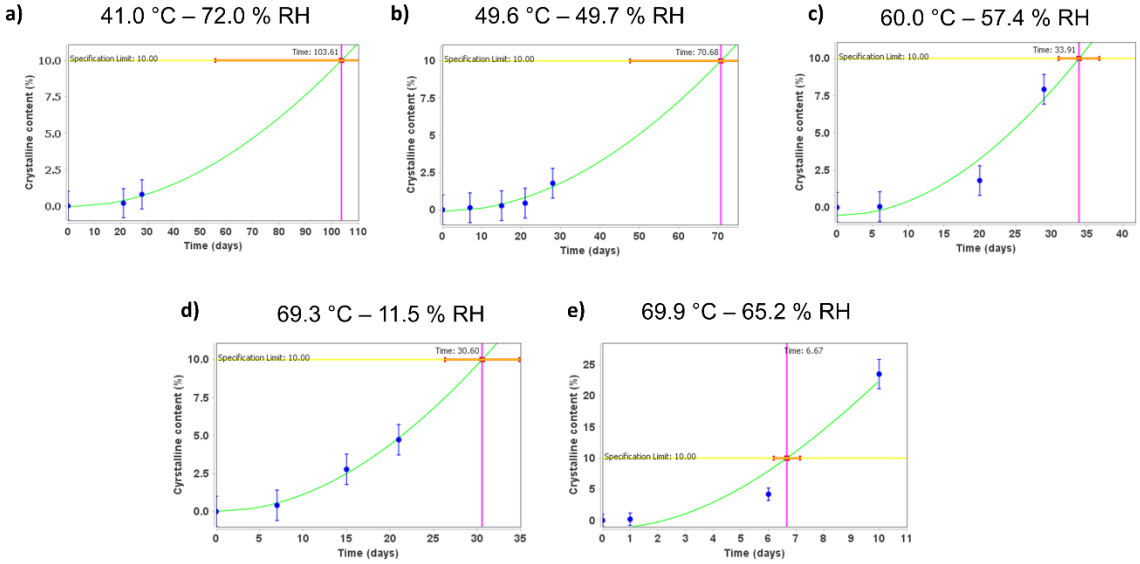

Figure 27: Avrami modelling of the physical stability of the co-spray dried budesonide-HPMC AS formulation at different conditions:

a) 41.0°C/72.0% RH, b) 49.6°C/49.7% RH; c) 60.0°C/57.4% RH, d) 69.3°C/11.5% RH and e) 69.9°C/65.2% RH. Key: the specification limit (10%) is represented in yellow while the isoconversion time (time required for 10% of the drug to recrystallise) is represented in pink color.

Long term stability was predicted at three different conditions of temperature and RH: 25 °C/10% RH, 25 °C/50% RH and 40 °C/75% RH. Experimental data from long-term stability studies was compared with the different prediction models at 4 and 6 and 9 months (Fig. 28 and Fig S3, Supplementary material). Avrami was the most accurate model that correlated better the experimental with the predicted stability data while the rest of the models overestimated the physical stability of this formulation. This kinetic model showed the lowest activation energy and the smaller b term (moisture sensitivity factor), indicating the lower impact of moisture but the

greater impact of temperature on the physical stability of the co-spray dried budesonide-HPMC AS formulation.

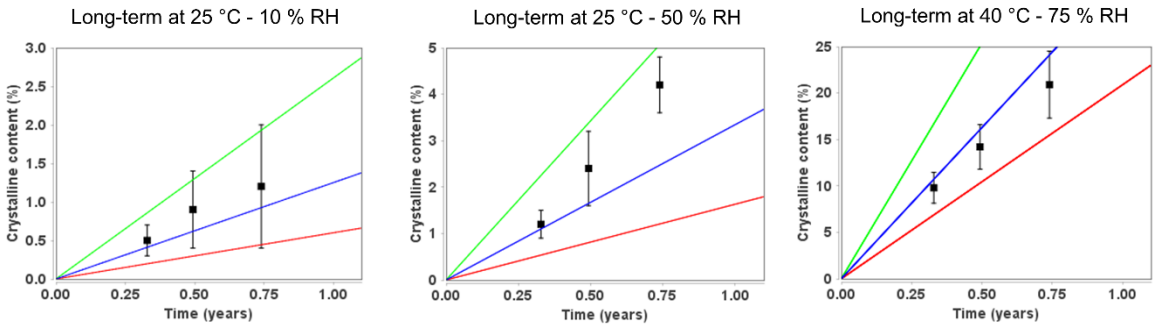

Figure 28: Long-term physical stability prediction of co-spray dried budesonide-HMPC AS formulation using Avrami kinetic model.

4.3.2.3 Co-spray dried budesonide: PVP K90 (1:1, w/w)

After exposition to different relative humidities and temperatures, the crystalline content of the co-spray dried budesonide:PVP K90 formulation was also quantified (Table S5, Supplementary material). Physical stability of the co-spray dried budesonide:PVP K90 formulation was greater than the amorphous budesonide but much poorer than the equivalent formulation manufactured with HPMC AS. All kinetic models showed a high correlation coefficient (R^2> 0.9). However, the diffusion model was the one exhibiting the greatest fitting between the experimental and the prediction data points (Fig. 29). The activation energy was 10.2 Kcal/mol (half of the activation energy for the co-spray dried budesonide:HMPC AS formulation) and the moisture sensitive factor was 0.045 (double than budesonide:HPMC AS) which explains the higher impact of temperature and relative humidity on its physical stability (Table S4, Supplementary material).

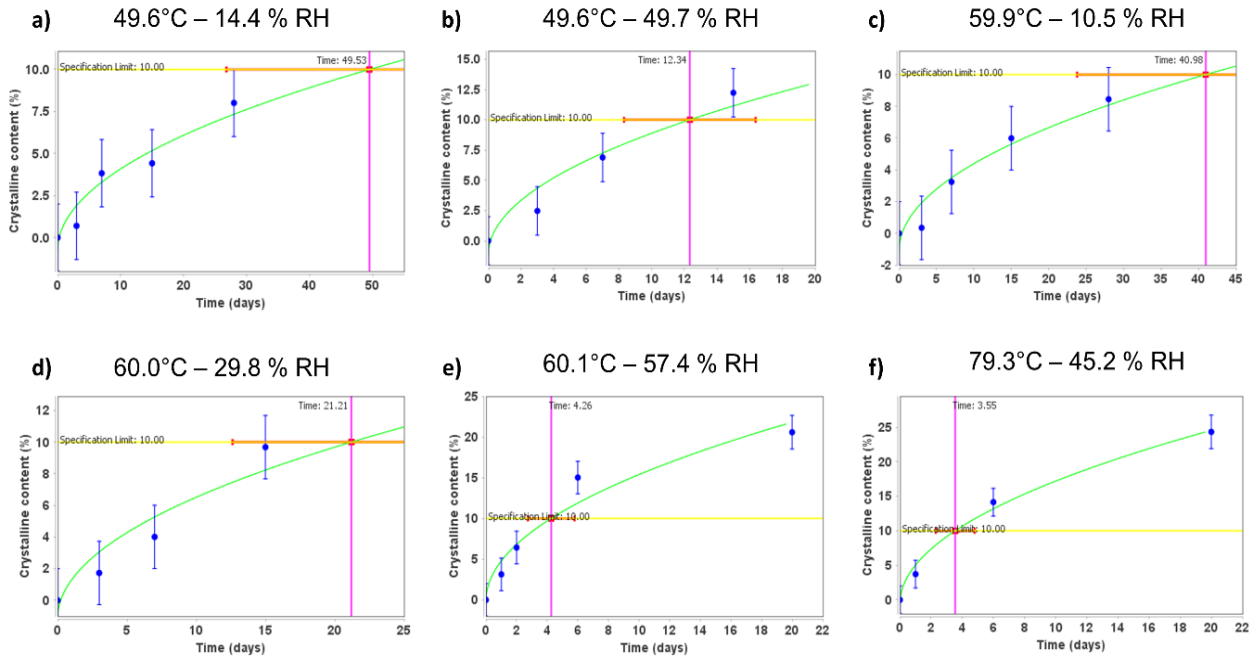

Figure 29: Diffusion modelling of the physical stability of the co-spray dried budesonide-PVP K90 formulation at different conditions:

Key: a) 49.6°C/14.4% RH, b) 49.6°C/49.7% RH; c) 59.9°C/10.5% RH, d) 60.0°C/29.8% RH, e) 60.1°C/57.4% RH and f) 79.3°C/45.2% RH. Key: the specification limit (10%) is represented in yellow while the isoconversion time (time required for 10% of the drug to recrystallise) is represented in pink color.

Long-term stability was calculated and results were compared to those obtained from the prediction models at 25 °C/10% RH, 25 °C/50% RH, and 40 °C/75% RH (Fig. 8). The diffusion kinetic model was the most accurate in those conditions at 25 °C, while the rest of the kinetic models overestimated significantly the crystallisation rate of budesonide in this formulation (Fig. S4, Supplementary material). The overestimation can be the result of the faster crystallisation kinetics compared to the equivalent formulation preparated with HPMC AS which can reduce the accuracy of the models at the specification limit. At 40 °C/75% RH, the crystallisation rate was very fast with a predicted shelf-life (considered as the time required to achieve the specification limit) of ~1 month, indicating the inability of PVP K90 to maintain the amorphous status of budesonide at this condition.

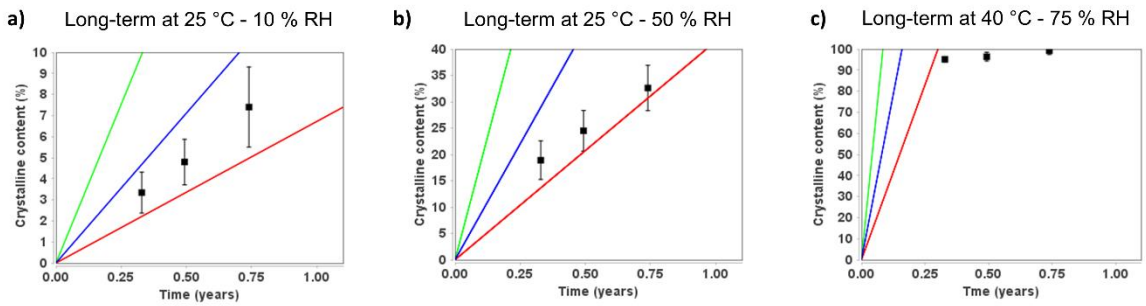

Figure 30: Long term physical stability prediction of co-spray dried budesonide:PVP K90 (1:1 w/w) formulation at 25 °C/10% RH, 25 °C/50% RH and 40 °C/75% RH.

4.3.2.4 Co-spray dried griseofulvin: HMPC AS (1:1, w/w)

The crystalline content of griseofulvin was quantified at several time points at the different ageing conditions (Table S7, Supplementary material). The spray dried griseofulvin: HPMC AS system was the only one tested as the formulation containing PVP K90 was not fully amorphised after spray drying. Among all the fitting models, the diffusion model was the one that best fitted the experimental data, with the greatest correlation coefficient value (R^2>0.9) and acceptable residual values (Figure 31, Table S8, Supplementary material).

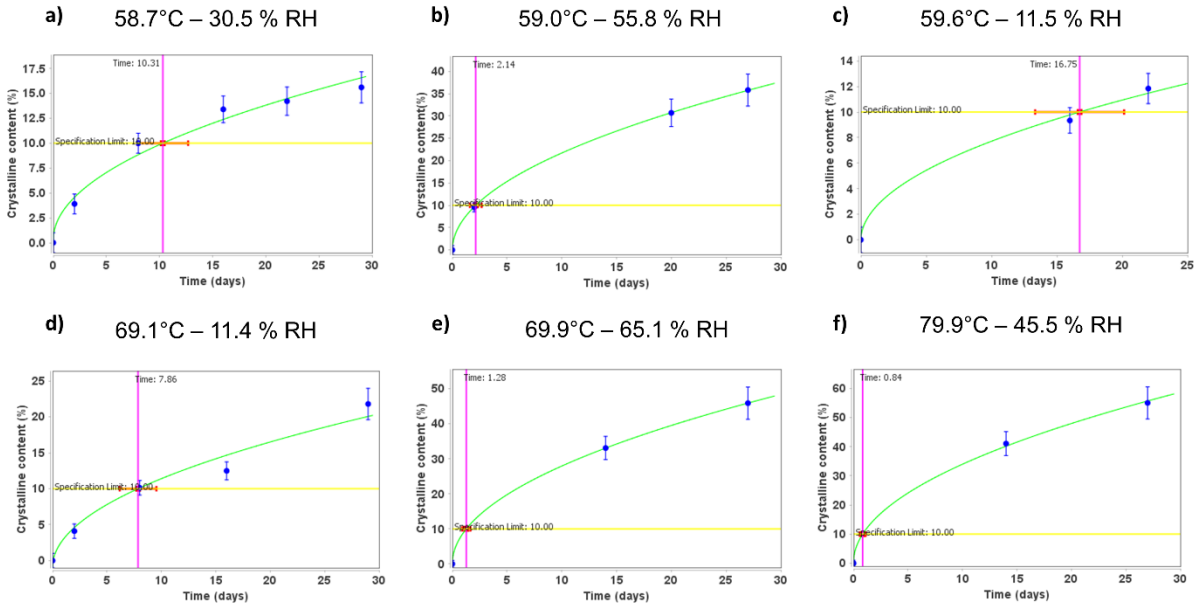

Figure 31: Diffusion modelling of the physical stability of the co-spray dried griseofulvin-HPMC AS formulation at different conditions:

Key: a) 58.7°C/30.5% RH, b) 59.0°C/55.8% RH; c) 59.6°C/11.5% RH, d) 69.1°C/11.4% RH, e) 69.9°C/65.1% RH and f) 79.9°C/45.5% RH. Key: the specification limit (10%) is represented in yellow while the isoconversion time (time required for 10% of the drug to recrystallise) is represented in pink color.

Long term stability experimental data showed the ability of the diffusion model to predict the crystallisation rate of griseofulvin within the HPMC AS amorphous matrix at both 25 °C conditions (Fig. 32). However, the prediction at 45 °C and 75% RH was overestimated, due to the fast crystallisation, well-above the isoconversion limit (10%). The rest of the models underestimated the physical stability of this system, exhibiting predicted cyrstallisation rates much more pronounced than the real kinetics (Fig. S5, Supplementary material).

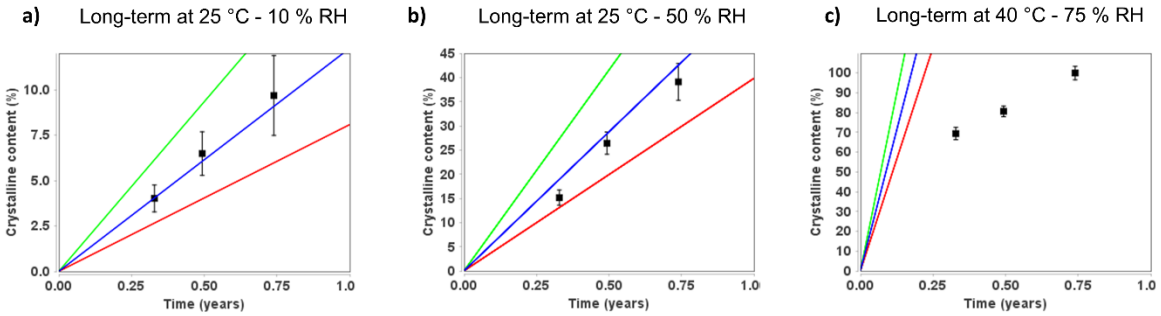

Figure 32: Long term physical stability prediction of co-spray dried griseofulvin-HPMC AS (1:1 w/w) formulation at 25 °C/10% RH, 25 °C/50% RH and 40 °C/75% RH.

4.3.2.5 Co-spray dried ritonavir: HMPC AS (2:1, w/w)

The crystalline content of ritonavir was quantified at several time points at different ageing conditions (Table S9, Supplementary material). Those formulations containing a 1:1 weight ratio between the drug and the excipient did not crystallise in any of the conditions within the timeframe of our study (28 days). For this reason, formulations with a 2:1 drug:excipient weight ratio were prepared and their stability was assessed. The drug crystallised only at the most extreme conditions of temperature and RH. Out of the five tested models, none of them had a very good match between the experimental and the predicted data points, even though the correlation coefficient was high (R^2> 0.9) in some of the cases (Fig. 33, Table S10, Supplementary material). The Avrami model showed a better fit at 60 and 70 °C, while the diffusion model showed a better correlation in the conditions at 80 °C.

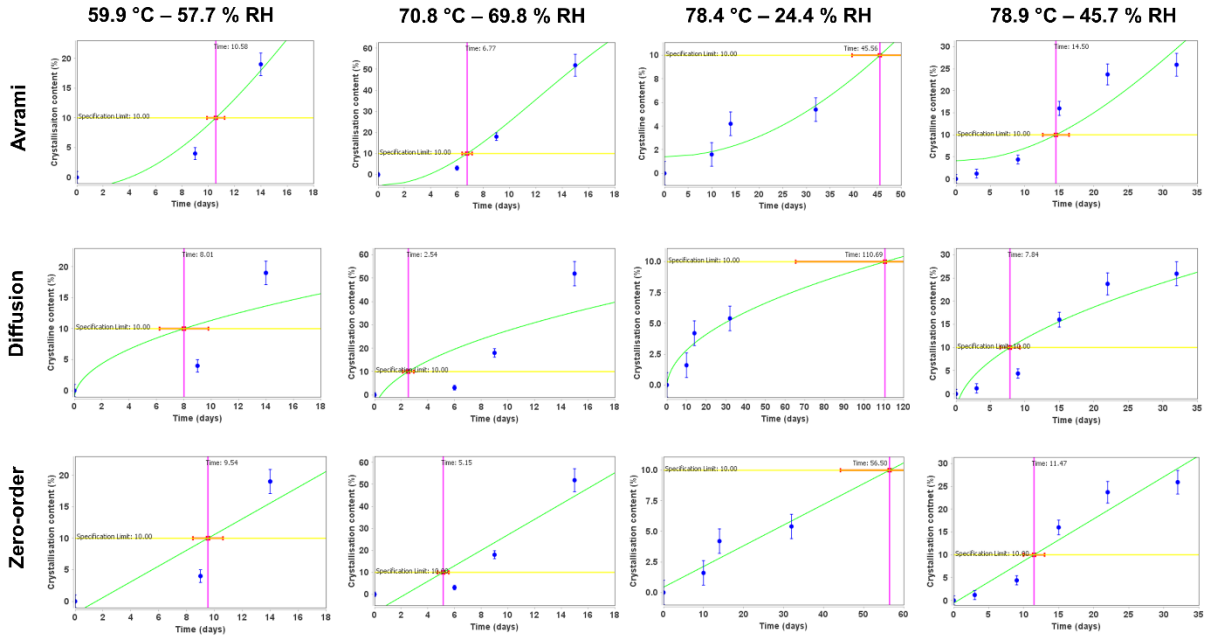

Figure 33: Different models of the physical stability of the co-spray dried ritonavir-HPMC AS formulation (2:1, w:w) at different conditions:

Key: 59.9°C/57.7% RH, 70.8°C/69.8% RH; 78.4°C/24.4% RH and f) 78.9°C/45.7% RH. Key: the specification limit (10%) is represented in yellow while the isoconversion time (time required for 10% of the drug to recrystallise) is represented in pink colour.

Experimental data points showed a sigmodial profile in most conditions (Fig S6, Supplementary material), indicating an Avrami cyrstallisation kinetic at earlier time points followed by diffusion at later stages. The poor fitting between the experimental data and the predicted stability models justifies the lower long-term prediction capacity obtained for this formulation (Fig. 34). The diffusion model was the most accurate out of the five assessed kinetic models at 2, 4 and 6 months; nevertheless, the uncertainty of the model was greater compared to other formulations as observed in the broadening of the predicted region.

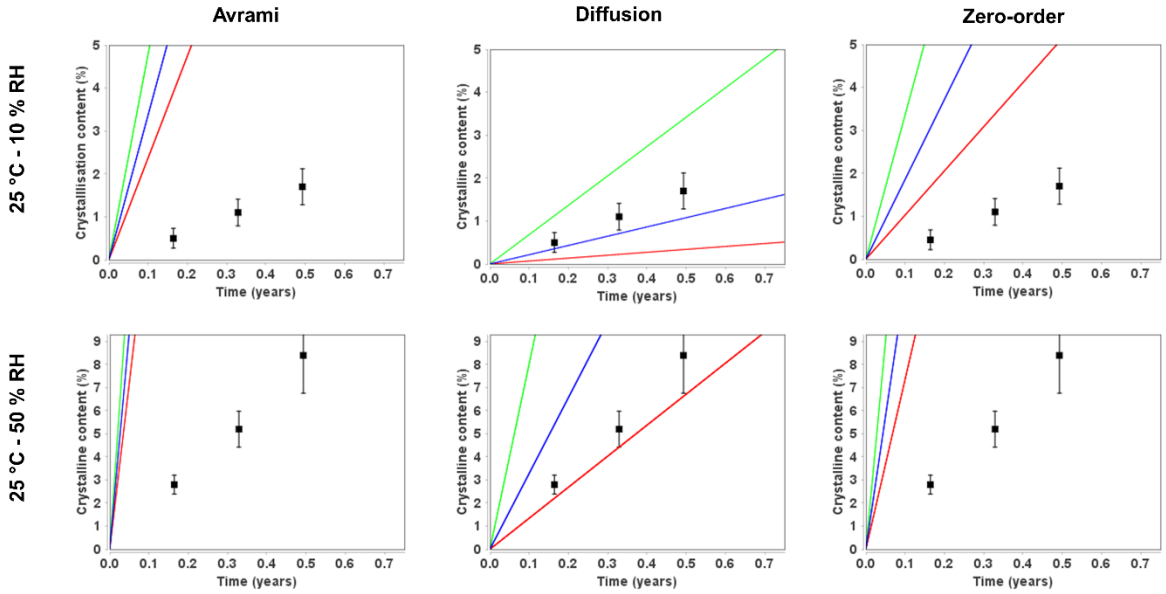

Figure 34: Long term physical stability prediction of co-spray dried ritonavir-HPMC AS (2:1 w/w) formulation at 25 °C/10% RH and 25 °C/50% RH.

4.3.2.6 Co-spray dried ritonavir: PVP K90 (2:1, w:w)

The crystalline content of ritonavir formulated with PVP K90 was also quantified at several time points and different ageing conditions (Table S11, Supplementary material). The models that exhibited the best fitting to the experimental data points were Avrami followed by zero and first-order while the diffusion model showed the worst fitting with the highest residual values and the lowest correlation coefficient (Fig. 35).

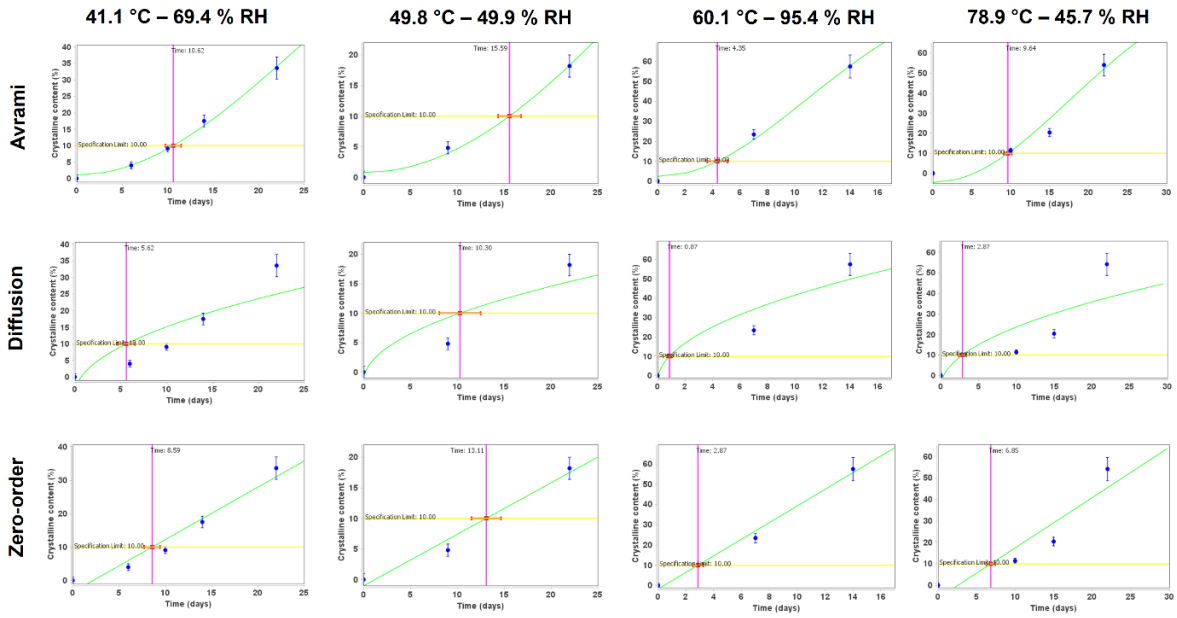

Figure 35: Different models of the physical stability of the co-spray dried ritonavir-PVP K90 formulation (2:1, w:w) at :different conditions

Key 41.1°C/69.4% RH, 49.8°C/49.9% RH; 70.1°C/95.4% RH and f) 78.9°C/45.7% RH. Key: the specification limit (10%) is represented in yellow while the isoconversion time (time required for 10% of the drug to recrystallise) is represented in pink colour.

Similar to the previous system, the experimental data exhibited a sigmoidal profile (Fig S7, Supplementary material). Neither Avrami nor zero-order kinetic profiles had a good prediction capacity of long-term physical stability, while the diffusion model was the most accurate amongst the five assessed crystallisation models (Fig. 36).

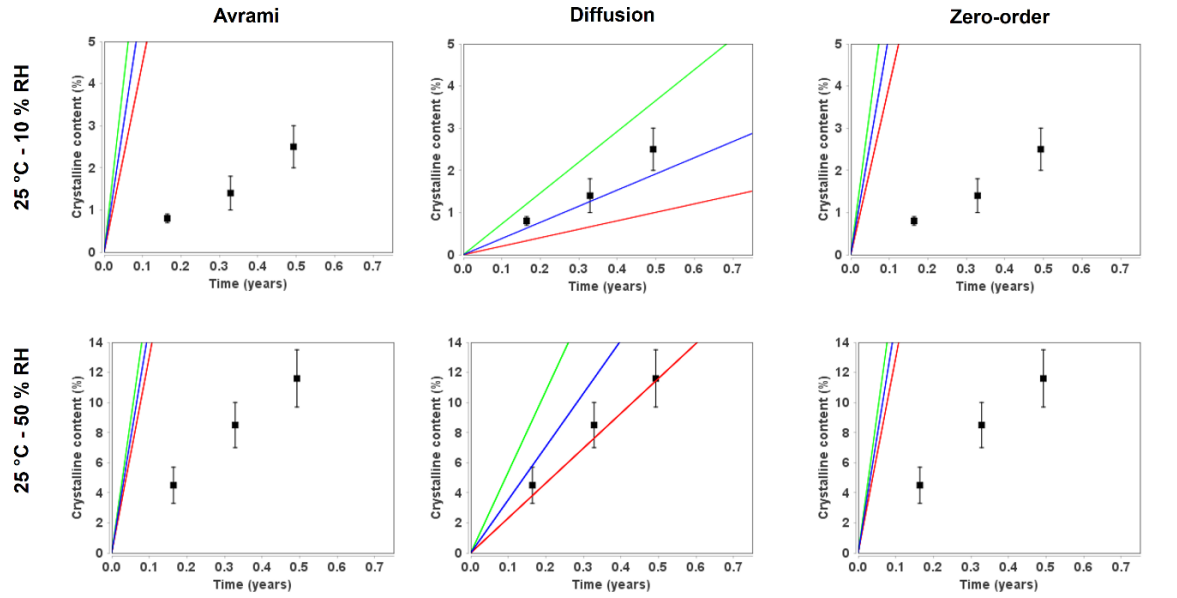

Figure 36: Long term physical stability prediction of co-spray dried ritonavir-PVP K90 (2:1 w/w) formulation at 25 °C/10% RH and 25 °C/50% RH.

The physical stability of the celecoxib amorphous solid dispersions was not modelled as both formulations with HPMC AS and PVP K90 only recrystallised at a single condition (60 ºC/ 90% RH) in the timeframe of the study (30 days), and hence, not enough data points were collected for model development.

4.4 Discussion

Several authors have described multiple parameters involved in the physical stability of amorphous solid dispersions such as drug loading ratio, RH, storage temperature, preparation temperature, molecular weight of the drugs and polymers, physicochemical properties of the drugs such as melting point, solubility, logP and polar surface area [23]. In our work, we are aiming to model accurately the crystallisation kinetics of amorphous solid dispersions under accelerated conditions of temperature and RH only up to the isoconversion time to predict long-term physical stability. This correlation may be challenging, especially in those systems where the testing temperatures are above the T_g composite. Also, during shelf-life storage, amorphous solid dispersions are commonly protected from direct exposure to RH by packageing containers such as HDPE bothers or thermoformed blisters. However, these packing materials are still permeable to water vapour and moisture ingress into the containers results to subsequent sorption of water by the packed prodcuts. A precise prediction of the crystallisation rate constant at ICH conditions is complex, but using this approach shortens the experimentation time significantly. An overestimation of the rate constant is acceptable in this context allowing to make timely decisions in preclinical phases of drug development [24].

To stabilize amorphous solid dispersions, the molecular mobility should be kept as low as possible. The formation of hydrogen bonds between drug and excipient are essential to reduce the molecular mobility of the drug and hence, to find the optimal excipient is crucial to stabilise the amorphous solid dispersion over prolonged periods. HPMCAS has exhibited a greater ability to enhance the physical stability of both budesonide and griseofulvin. HPMCAS has a higher number of donor and acceptor groups in its structure able to form hydrogen bonds compare to PVP (Fig. 37). This effect is clearly remarked for the griseofulvin, as the drug was only amorphised after spray drying with HMPC AS but not when using PVP due to the inability to form hydrogen bonds between drug and excipient. Ritonavir and celecoxib have exhibited a much greater physical stability than both

budesonide and griseofulvin probably related to their chemical structure more likely to form hydrogen bonds with the excipients.

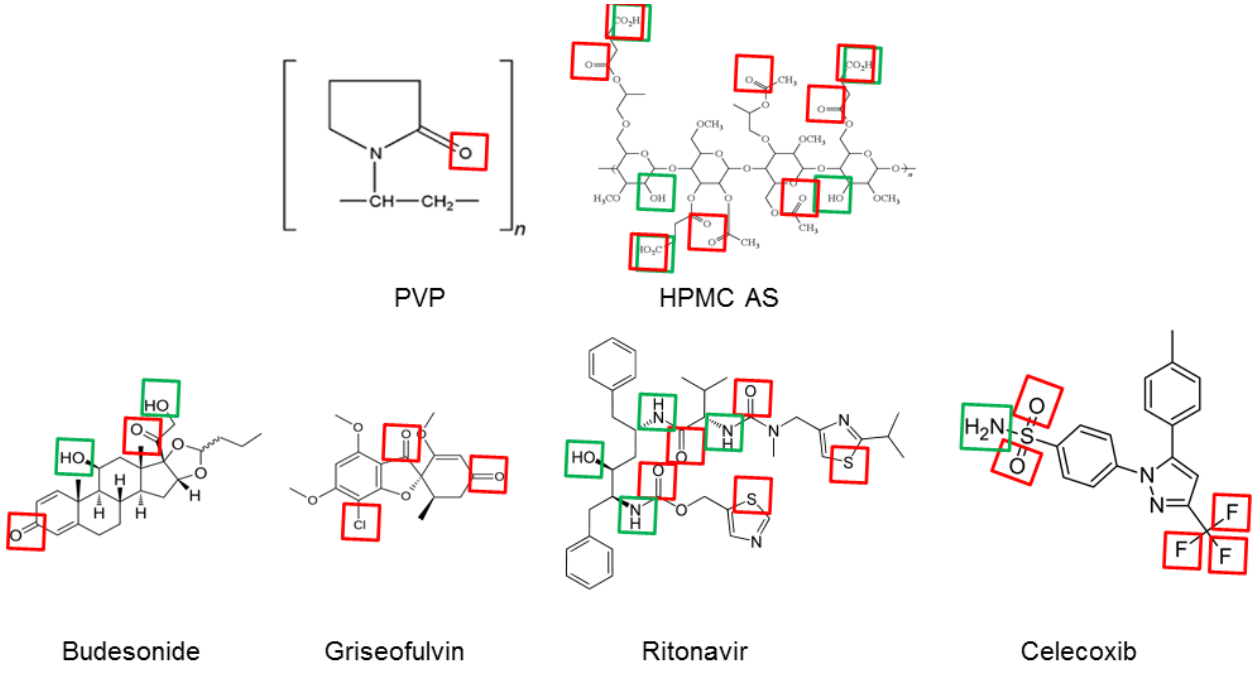

Figure 37: Hydrogen bonding acceptor and donor groups of the different drugs and excipients utilised in the preparation of the amorphous systems.

Key: H-bond donor groups are represented in green while H-bond acceptors are represented in red.

When the molecules are homogeneously dispersed in an amorphous matrix (either PVP or HPMC), two different models are proposed:

(i) nucleation takes place followed by crystal growth or

(ii) the drug molecules diffuse across the amorphous matrix coming together before the nucleation process starts (Fig 38) [25].

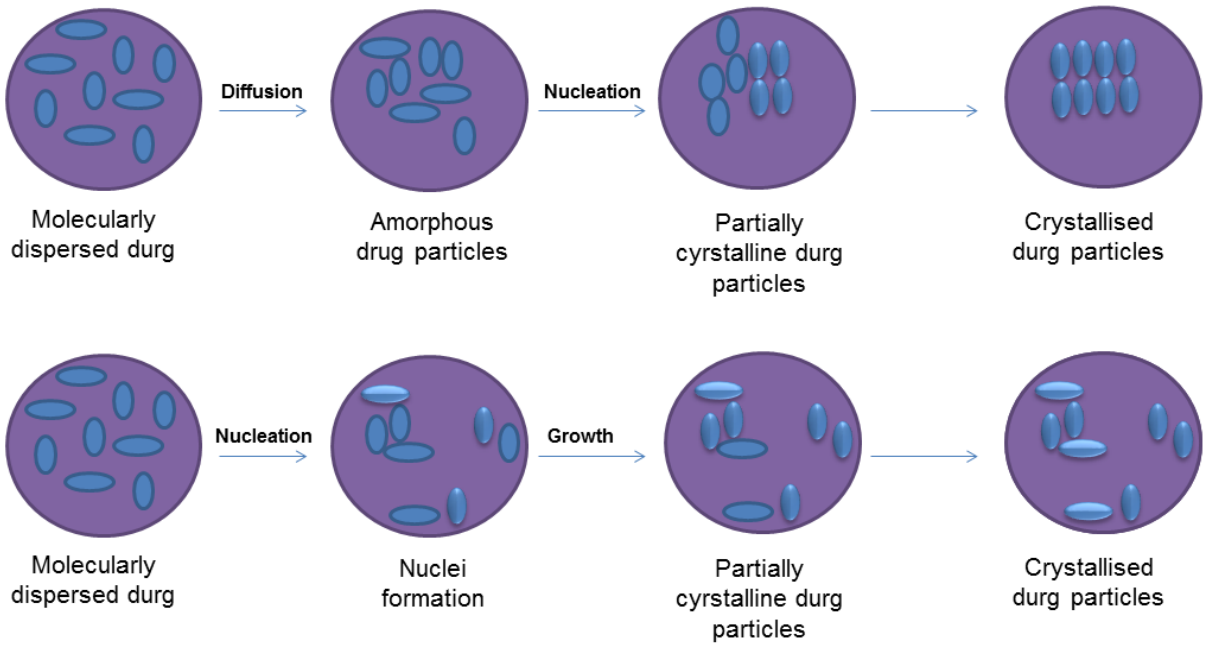

Figure 38: Proposed crystallisation models for amorphous systems.

Solid dispersions, partially or fully amorphous, are thermodynamically unstable. In solid dispersions containing crystalline particles, these particles form nuclei that can be the starting point for further crystallization. The low stability of milled budesonide can be explained by the leftover of nuclei that can trigger the crystallization process much faster. The best fitted crystallisation models for the other formulations are summarized in Table 4-5. In all the systems, a single Tg composite was observed at time zero indicating good miscibility between drug and excipients [26]. However, the physical stability was significantly different over time amongst the different systems. The physical stability of spray dried budesonide was predicted by the Zero-order model. The nucleation can take place without the need of diffusion as all the drug molecules are in contact with each other.

Table 4-5. Summary of the crystallisation models able to predict more accurately the stability of the different spray dried formulations. Specification limit for physical stability was considered as 10% crystallisation.

Formulation	Physical stability	Prediction model	Ea (Kcal/mol)	B value
Budesonide	Poor (< 1 year at 25ºC/10 %RH)	Zero-order	37.72 ± 8.52	0.066 ± 0.020
Budesonide:HMPC AS 1:1 w/w	Good (> 1 year at 25ºC/10 %RH but < 6 months at 40ºC/75 %RH)	Avrami	20.55 ± 3.44	0.025 ± 0.004
Budesonide:PVP K90 1:1 w/w	Medium (> 1 year at 25ºC/10 %RH but < 1 month at 40ºC/75%RH)	Diffusion	10.18 ± 2.45	0.046 ± 0.007
Griseofulvin:HMPC AS 1:1 w/w	Poor (< 1 year at 25ºC/10 %RH)	Diffusion	16.40 ± 2.17	0.039 ± 0.004
Ritonavir:HMPC AS 2:1 w/w	Good (> 1 year at 25ºC/10 %RH)	Mixed model Avrami- Diffusion	-	-
Ritonavir:PVP K90 2:1 w/w	Good (> 1 year at 25ºC/10 %RH)	Mixed model Avrami- Diffusion	-	-

In co-spray dried systems, the drug molecules are molecularly dispersed within the excipient, and diffusion can take place before nucleation. This implies that the drug molecules have to migrate through the matrix. This effect was observed in Budesonide-PVP and Griseofulvin-HMPC solid dispersions. The diffusion model predicted more accurately the physical stability than the Avrami model (Table 4-5). However, Avrami model was the most accurate in the long-term physical stability prediction for the budesonide-HPMC formulation which exhibited the highest stability. This could be explained for the fact that HMPC is able to establish more hydrogen bonds with the drug reducing further its molecular mobility making the diffusion process extremely slow. In this case, crystallization would be triggered by nuclei formed by amorphous drug particles that are adjacent to each other in the system.

A complex scenario takes place when predicting the physical stability of ritonavir formulations. At extreme conditions of temperature and RH, diffusion plays a key role whereas Avrami governs the crystallisation kinetics at less extreme conditions. Based on this premise, Avrami would be a better model to predict what happen at ICH long-term conditions. However, the diffusion model matched better the experimental long-term results. The key point is to determine which crystallisation kinetic governs the process at earlier stages up to the isoconversion time, in our case set at 10% of crystallised drug. Above this limit, there is no pharmaceutical interest on knowing the cyrstallisation kinetics, as the product will not comply with the Pharmacopeia specifications.

In the Avrami equation, n is the exponent that describes the dimensionality of the crystal growth being equal 2, 3 and 4 for rod, plate and spherical geometry respectively for homogeneous nucleation:

$$\alpha(t) = 1 - \exp(-kt^n) \qquad \text{(Equation 7)}$$

where K represents the crystallisation rate constant, t is the time and α(t) is the relative crystallinity calculated as:

$$\alpha(t) = \frac{x(t)}{x\,(\infty)} \qquad \text{(Equation 8)}$$

where α(t) is the relative crystallinity that normalises the true absolute crystallinity x(t) and varies from 0 to 1. In the case of ritonavir systems, the drug did not fully recrystallize to produce 100% crystallised ritonavir regardless of the experimental accelerated storage conditions. In this system, the final extent of ritonavir recrystallization was dependent of temperature and RH. At 80°C/45% RH, the highest cyrstallisation content of ritonavir was 25.9%, being considered as the x(∞) (Data showed in Appendix I in Supplementary material). Initial values of K=0.5 and n=2 were given to compute the optimised values of the model parameters by minimizing the sum of residual squares. n value was bound between 0-4. The fitting of the data (n, K and R^2 values) is illustrated in Appendix I in Supplementary material.

A n value of 3 exhibited a better fitting to the experimental data than a n value of 2. This can be linked with the poorer prediction of Avrami model in conditions of exposure to high RH and temperature when using ASAPprime that fixes the n value to 2. The Avrami equation defines a constant nucleation rate, resulting in a simplification that overpredicts the relative crystallinity (α(t) and underpredicts the time for complete recrystallization as shown in most of the formulations tested. In theory, only small deviations should occur between the real time data and the Avrami equation during primary crystallisation as crystallisation is approximately constant. However, the nucleation rate decreases sharply during secondary or late-stage crystallisation due to the decline of the number of available nucleation sites [27]. Then, it is critical to know at which moment the late crystallisation occurs (before or after the set specification limit) in order to exclude those experimental points when modelling the data using Avrami kinetics.

4.5 Conclusions

An acceptable prediction of long-term physical stability of amorphous solid dispersions has been successful demonstrated using ASAPprime tool which can facilitate the formulation decision making process making it faster and more accurate. The modelling of drug crystallisation kinetics are challenging but the process can be simplified by focusing in the isoconversion approach methodology.

Acknowledgements

This work was supported by Science Foundation Ireland grants co-funded under the European Regional Development Fund (SFI/12/RC/2275 and SFI/12/RC/2275_P2) provided to Prof. A. M. Healy.

References

(1) Lee, T. W.; Boersen, N. A.; Hui, H. W.; Chow, S. F.; Wan, K. Y.; Chow, A. H. Delivery of poorly soluble compounds by amorphous solid dispersions. Current pharmaceutical design 2014, 20 (3), 303-324.

(2) Al-Obaidi, H.; Buckton, G. Evaluation of griseofulvin binary and ternary solid dispersions with HPMCAS. AAPS PharmSciTech 2009, 10 (4), 1172-1177. DOI: 10.1208/s12249-009-9319-x.

(3) Vilhelmsen, T.; Eliasen, H.; Schaefer, T. Effect of a melt agglomeration process on agglomerates containing solid dispersions. Int J Pharm 2005, 303 (1-2), 132-142. DOI: 10.1016/j.ijpharm.2005.07.012.

(4) Vasconcelos, T.; Sarmento, B.; Costa, P. Solid dispersions as strategy to improve oral bioavailability of poor water soluble drugs. Drug discovery today 2007, 12 (23-24), 1068-1075. DOI: 10.1016/j.drudis.2007.09.005.

(5) Karolewicz, B.; Gorniak, A.; Owczarek, A.; Nartowski, K.; Zurawska-Plaksej, E.; Pluta, J. Solid dispersion in pharmaceutical technology. Part II. The methods of analysis of solid dispersions and examples of their application. Polimery w medycynie 2012, 42 (2), 97-107. Kumar, S.; Gupta, S. K. Pharmaceutical solid dispersion technology: a strategy to improve dissolution of poorly water-soluble drugs. Recent patents on drug delivery & formulation 2013, 7 (2), 111-121.

(6) Leuner, C.; Dressman, J. Improving drug solubility for oral delivery using solid dispersions. European journal of pharmaceutics and biopharmaceutics : official journal of Arbeitsgemeinschaft fur Pharmazeutische Verfahrenstechnik e.V 2000, 50 (1), 47-60. van Drooge, D. J.; Hinrichs, W. L.; Visser, M. R.; Frijlink, H. W. Characterization of the molecular distribution of drugs in glassy solid dispersions at the nano-meter scale, using differential scanning calorimetry and gravimetric water vapour sorption techniques. Int J Pharm 2006, 310 (1-2), 220-229. DOI: 10.1016/j.ijpharm.2005.12.007.

(7) Waterman, K. C. The application of the Accelerated Stability Assessment Program (ASAP) to quality by design (QbD) for drug product stability. AAPS PharmSciTech 2011, 12 (3), 932-937. DOI: 10.1208/s12249-011-9657-3 From NLM Medline.

(8) Curtin, V.; Amharar, Y.; Hu, Y.; Erxleben, A.; McArdle, P.; Caron, V.; Tajber, L.; Corrigan, O. I.; Healy, A. M. Investigation of the capacity of low glass transition temperature excipients to minimize amorphization of sulfadimidine on comilling. Molecular pharmaceutics 2013, 10 (1), 386-396. DOI: 10.1021/mp300529a.

(9) Hancock, B. C.; Shamblin, S. L.; Zografi, G. Molecular mobility of amorphous pharmaceutical solids below their glass transition temperatures. Pharmaceutical research 1995, 12 (6), 799-806.

(10) Tajber, L.; Corrigan, O. I.; Healy, A. M. Physicochemical evaluation of PVP-thiazide diuretic interactions in co-spray-dried composites--analysis of glass transition composition relationships. European journal of pharmaceutical sciences : official journal of the European Federation for Pharmaceutical Sciences 2005, 24 (5), 553-563. DOI: 10.1016/j.ejps.2005.01.007. Ford, J. L. The current status of solid dispersions. Pharmaceutica acta Helvetiae 1986, 61 (3), 69-88.

(11) Tajber, L.; Corrigan, D. O.; Corrigan, O. I.; Healy, A. M. Spray drying of budesonide, formoterol fumarate and their composites--I. Physicochemical characterisation. Int J Pharm 2009, 367 (1-2), 79-85. DOI: 10.1016/j.ijpharm.2008.09.030.

(12) Grossjohann, C.; Eccles, K. S.; Maguire, A. R.; Lawrence, S. E.; Tajber, L.; Corrigan, O. I.; Healy, A. M. Characterisation, solubility and intrinsic dissolution behaviour of benzamide: dibenzyl sulfoxide cocrystal. Int J Pharm 2012, 422 (1-2), 24-32. DOI: 10.1016/j.ijpharm.2011.10.016.

(13) Curtin, V.; Amharar, Y.; Gallagher, K. H.; Corcoran, S.; Tajber, L.; Corrigan, O. I.; Healy, A. M. Reducing mechanical activation-induced amorphisation of salbutamol sulphate by co-processing with selected carboxylic acids. Int J Pharm 2013, 456 (2), 508-516. DOI: 10.1016/j.ijpharm.2013.08.025.

(14) Gill, P.; Moghadam, T. T.; Ranjbar, B. Differential scanning calorimetry techniques: applications in biology and nanoscience. Journal of biomolecular techniques : JBT 2010, 21 (4), 167-193.

(15) Freethink Technologies, I. ASAPprime® user's guide. 2013.

(16) Cerda, J. R.; Arifi, T.; Ayyoubi, S.; Knief, P.; Ballesteros, M. P.; Keeble, W.; Barbu, E.; Healy, A. M.; Lalatsa, A.; Serrano, D. R. Personalised 3D Printed Medicines: Optimising Material Properties for Successful Passive Diffusion Loading of Filaments for Fused Deposition Modelling of Solid Dosage Forms. Pharmaceutics 2020, 12 (4). DOI: 10.3390/pharmaceutics12040345.

(17) Bauer, J. F.; Saleki-gerhardt, A.; Chemburkar, S. R.; Patel, K.; Spiwek, H. Amorphous Ritonavir. European Patent EP1418174. Abbott laboratories. 1999.

(18) Lopez, F. L.; Shearman, G. C.; Gaisford, S.; Williams, G. R. Amorphous formulations of indomethacin and griseofulvin prepared by electrospinning. Molecular pharmaceutics 2014, 11 (12), 4327-4338. DOI: 10.1021/mp500391y.

(19) Paradkar, A. R.; Chauhan, B.; Yamamura, S.; Pawar, A. P. Preparation and characterization of glassy celecoxib. Drug Dev Ind Pharm 2003, 29 (7), 739-744. DOI: 10.1081/DDC-120021773.

(20) Quirijns, E. J.; van Boxtel, A. J. B.; van Loon, W. K. P.; van Straten, G. Sorption isotherms, GAB parameters and isosteric heat of sorption. Journal of the Science of Food and Agriculture 2005, 85, 1805-1814.

(21) Roskar, R.; Kmetec, V. Evaluation of the moisture sorption behavior of several excipients by BET, GAB and microcalorimetric approaches. Chem Pharm Bull 2005, 53 (6), 662-665.

(22) Fasina, O.; Sokhansanj, S.; Tyler, R. Thermodynamics of moisture sorption in alfalfa pellets. Dry Technol 1997, 15, 1553-1570.

(23) Han, R.; Xiong, H.; Ye, Z.; Yang, Y.; Huang, T.; Jing, Q.; Lu, J.; Pan, H.; Ren, F.; Ouyang, D. Predicting physical stability of solid dispersions by machine learning techniques. Journal of controlled release : official journal of the Controlled Release Society 2019, 311-312, 16-25. DOI: 10.1016/j.jconrel.2019.08.030.

(24) Liu, B.; Theil, F.; Lehmkemper, K.; Gessner, D.; Li, Y.; van Lishaut, H. Crystallization Risk Assessment of Amorphous Solid Dispersions by Physical Shelf-Life Modeling: A Practical Approach. Molecular pharmaceutics 2021, 18 (6), 2428-2437. DOI: 10.1021/acs.molpharmaceut.1c00270 From NLM.

(25) Kumavar, S. D.; Chaudhari, Y. S.; Badhe, M.; Borole, P. PHYSICAL STABILITY OF AMORPHOUS SOLID DISPERSION: A REVIEW. International Journal of Pharmaceutical Archive 2013, 2 (5), 129-136.

(26) Karagianni, A.; Kachrimanis, K.; Nikolakakis, I. Co-Amorphous Solid Dispersions for Solubility and Absorption Improvement of Drugs: Composition, Preparation, Characterization and Formulations for Oral Delivery. Pharmaceutics 2018, 10 (3). DOI: 10.3390/pharmaceutics10030098.

(27) Yang, J.; Grey, K.; Doney, J. An improved kinetics approach to describe the physical stability of amorphous solid dispersions. Int J Pharm 2010, 384 (1-2), 24-31. DOI: 10.1016/j.ijpharm.2009.09.035.

Supplementary material

Physical Accelerated Predictive Stability of Amorphous Solid Dispersions

Peter O'Connell[1,2,3], Dolores R. Serrano[2], Nigel T. McSweeney[3], Anne Marie Healy[1]*

[1]Synthesis and Solid State Pharmaceutical Centre (SSPC), School of Pharmacy and Pharmaceutical Sciences, Trinity College Dublin, Dublin 2, Ireland.

[2]Department of Pharmaceutics and Food Technology and Instituto Universitario de Farmacia Industrial (IUFI), School of Pharmacy, Universidad Complutense de Madrid, Plaza Ramon y Cajal s/n, 28040-Madrid, Spain.

[3]Cuspor Limited, Dublin 2, Ireland

*Corresponding author:
Anne Marie Healy
School of Pharmacy and Pharmaceutical Sciences
Trinity College Dublin
Dublin 2, Ireland.
Tel +353 1896 1444
Email healyam@tcd.ie

The sorption kinetic profiles of the respective systems are shown in Figure S1. Milled budesonide took up around 0.25% mass at 60% RH followed by a mass loss at higher RH attributed to crystallisation (Fig. 1A) which was verified by PXRD. Spray dried budesonide adsorbed higher amount of water vapour (4.7% mass at 90% RH); however, no mass loss was observed during the first sorption cycle indicating a more physically stable system at high RH (Fig. 1B). However, crystallisation was noticeable in the second sorption cycle as the amount of water uptake was much reduced (less than 1% at 90 % RH). Both co-processed ritonavir and budesonide formulations with HMPC AS showed a vapour uptake of around 6% mass during the first sorption cycle which was comparable to the vapour uptakes for the second sorption cycle (Fig. 1C & E) whereas the co-processed systems using PVP K90 exhibited a much higher vapour uptake around 25-30% which was similar during the second sorption cycle (Fig 1D & F). Celecoxib was not analysed as no crystallisation was observed in any of the conditions tested.

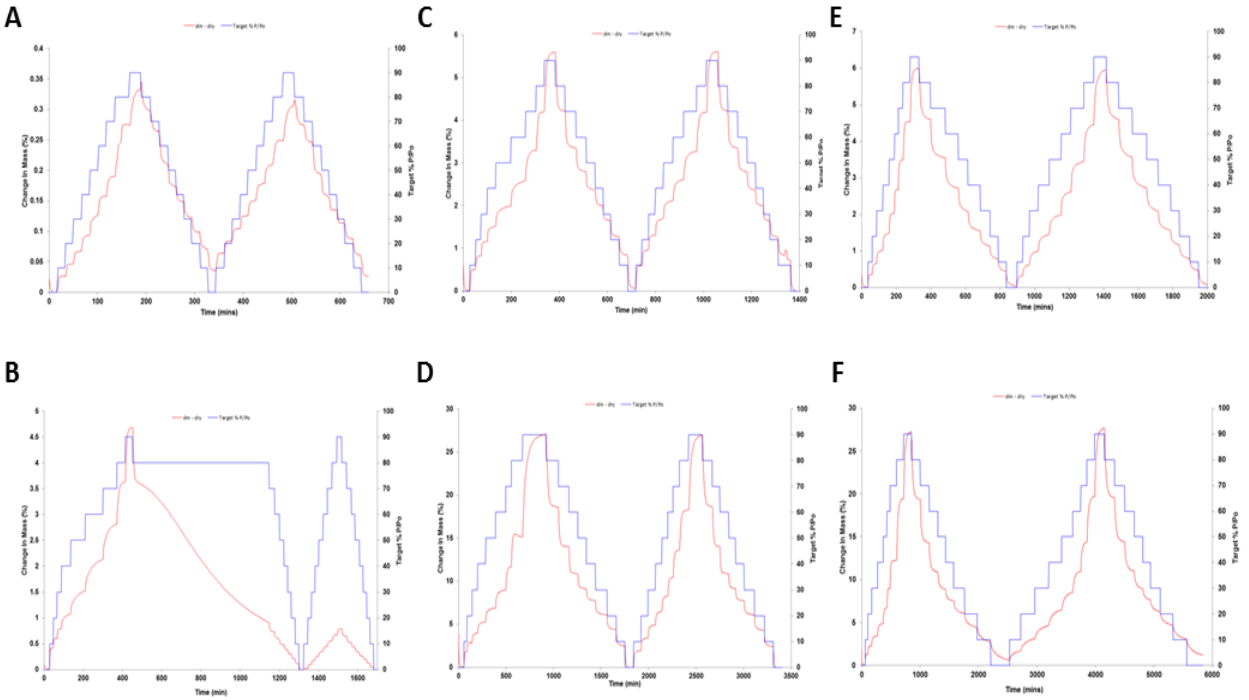

Figure S1. Water sorption kinetics profile for: A) Milled budesonide; B) Spray dried budesonide; C) Co-spray dried budesonide:HMPC AS (1:1, w/w); D) Co-spray dried budesonide:PVP K90 (1:1, w/w); E) Co-spray dried ritonavir:HMPC AS (1:1, w/w); D) Co-spray dried ritonavir:PVP K90 (1:1, w/w).

Table S1. Average content of crystalline drug after aging of spray dried budesonide formulation.

Time (days)	T (°C)	RH (%)	Crystallinity (%)
1	24.6	71.4	4.62
2	24.6	71.4	5.63
3	24.6	71.4	7.19
4	24.6	71.4	13.12
1	46.2	17.6	3.9
2	46.2	17.6	7.17
3	46.2	17.6	9.66
4	46.2	17.6	13.743
1	42	32.4	9.46
2	42	32.4	18.29
3	42	32.4	26.25
4	42	32.4	42.63
1	42.7	68	40.8
2	42.7	68	60.1
3	42.7	68	84.93
1	49.7	17.6	15.93
2	49.7	17.6	27.32
3	49.7	17.6	36.86
4	49.7	17.6	46.01

Table S2. Residual plots and modified-Arrhenius equation parameters of spray dried budesonide formulation.

Fitting method	Ea (kcal/mol)	B	R^2	Residual plot
Avrami	82.377 ± 10.907	0.174 ± 0.023	1	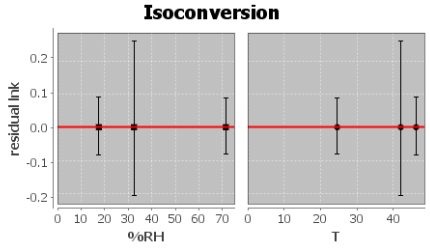
Diffusion	48.684 ± 5.912	0.079 ± 0.013	0.857	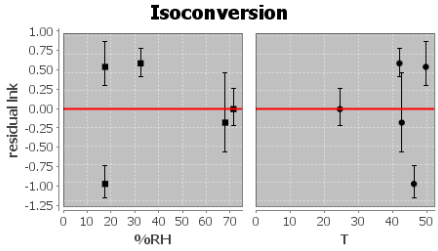
Zero-order	37.723 ± 8.525	0.066 ± 0.02	0.918	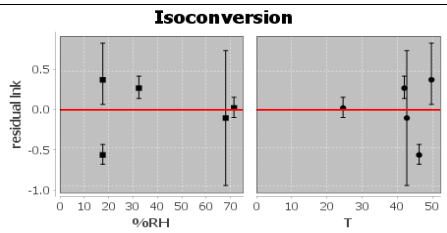
First-order	28.791 ± 6.716	0.045 ± 0.015	0.821	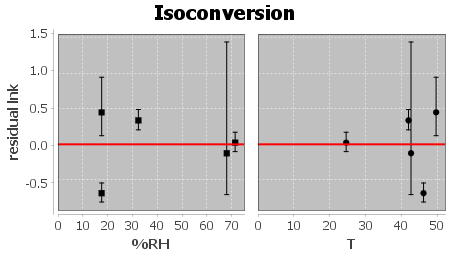
Second-order	23.459 ± 5.949	0.033 ± 0.014	0.727	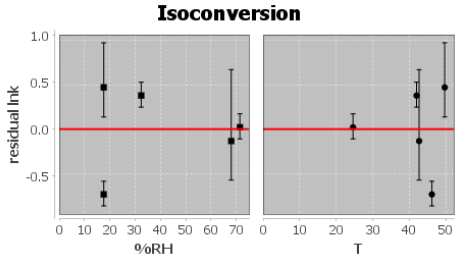

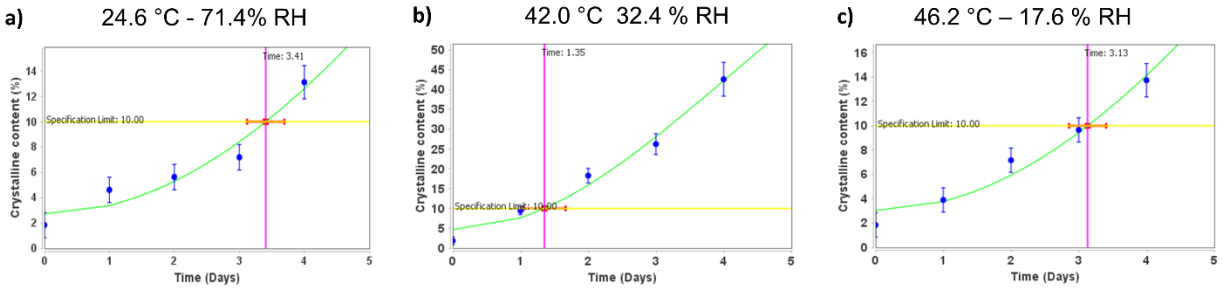

Figure S2. Avrami modelling of the physical stability of the spray dried budesonide formulation at different conditions: a) 24.6°C/71.4% RH, b) 42.0°C/32.4% RH; c) 46.2°C/17.6% RH.

Table S3. Average content of crystalline drug after aging of co-spray dried budesonide- HPMC AS (1:1, w/w) formulation.

Time (days)	T (°C)	RH (%)	Crystallinity (%)
28	41	72	0.794
21	41	72	0.182
7	49.6	49.7	0.135
15	49.6	49.7	0.272
21	49.6	49.7	0.442
28	49.6	49.7	1.783
6	60	57.4	0.049
20	60	57.4	1.8
29	60	57.4	7.929
7	69.3	11.5	0.403
15	69.3	11.5	2.777
21	69.3	11.5	4.723
1	69.9	65.2	0.2
6	69.9	65.2	4.2
10	69.9	65.2	23.5

Table S4. Residual plots and modified-Arrhenius equation parameters of co-spray dried budesonide-HPMC AS formulation.

Fitting method	Ea (kcal/mol)	B	R^2	Residual plot
Avrami	20.559 ± 3.44	0.025 ± 0.004	0.961	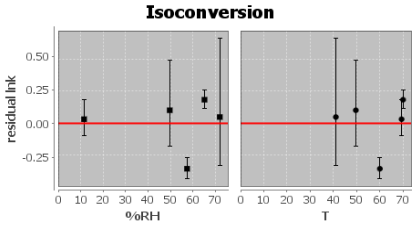
Diffusion	57.265 ± 5.732	0.058 ± 0.013	0.997	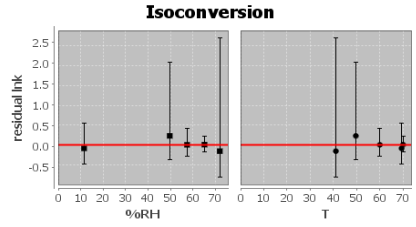
Zero-order	32.533 ± 4.935	0.035 ± 0.07	0.991	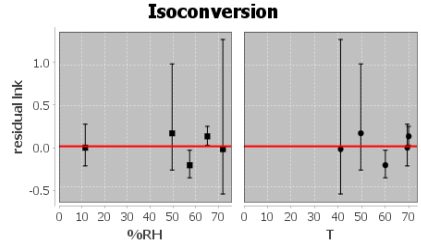
First-order	33.325 ± 5.000	0.036 ± 0.007	0.991	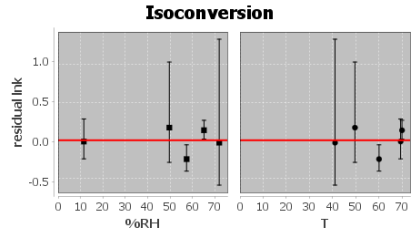
Second-order	34.125 ± 5.060	0.037 ± 0.007	0.990	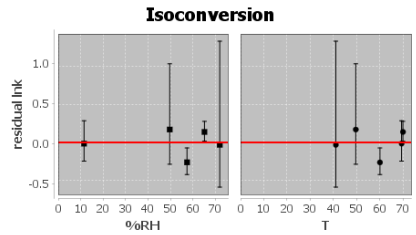

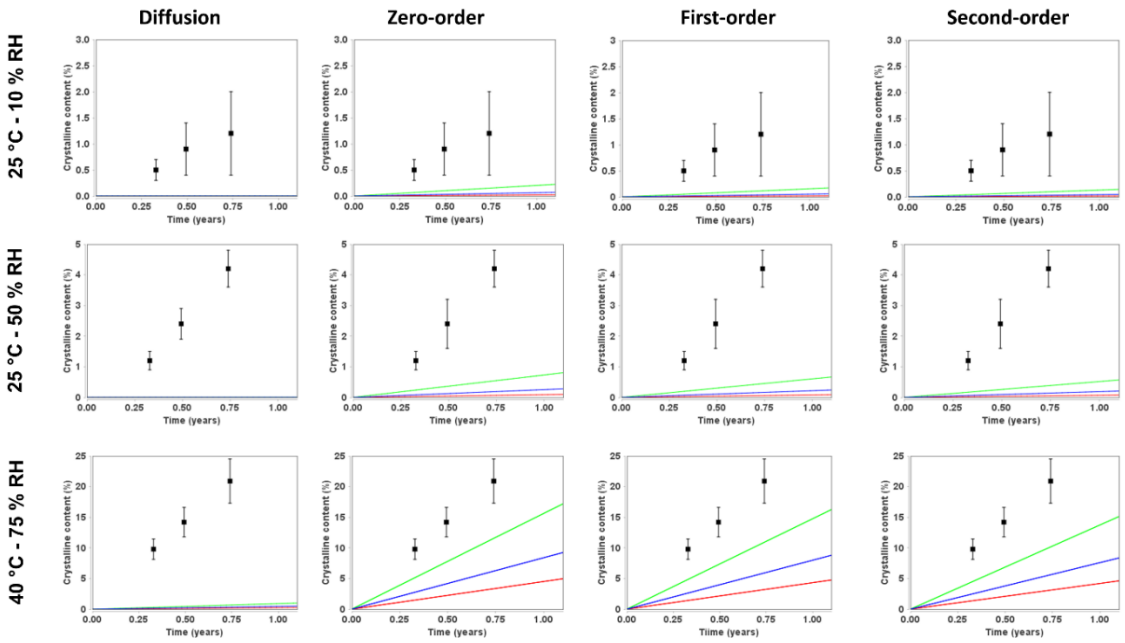

Figure S3. Long-term physical stability prediction of co-spray dried budesonide-HMPC AS formulation using zero, first, second, and diffusion kinetic models.

Table S5. Average content of crystalline budeosnide after aging of co-spray dried budesonide: PVP K90 (1:1, w/w) formulation.

Time (days)	T (°C)	RH (%)	Crystallinity (%)
3	49.6	14.4	0.7
7	49.6	14.4	3.83
15	49.6	14.4	4.42
28	49.6	14.4	8.01
3	49.6	49.7	2.47
7	49.6	49.7	6.89
15	49.6	49.7	12.23
3	59.9	10.5	0.346
7	59.9	10.5	3.24
15	59.9	10.5	5.99
28	59.9	10.5	8.45
3	60	29.8	1.73
7	60	29.8	4.01
15	60	29.8	9.68
1	60.1	57.4	3.13
2	60.1	57.4	6.43
6	60.1	57.4	15.01
20	60.1	57.4	20.58
1	79.3	45.2	3.719
6	79.3	45.2	14.14
20	79.3	45.2	24.32

Table S6. Residual plots and modified-Arrhenius equation parameters of co-spray dried budesonide: PVP K90 formulation.

Fitting method	Ea (kcal/mol)	B	R^2	Residual plot
Avrami	3.442 ± 1.274	0.023 ± 0.003	0.97	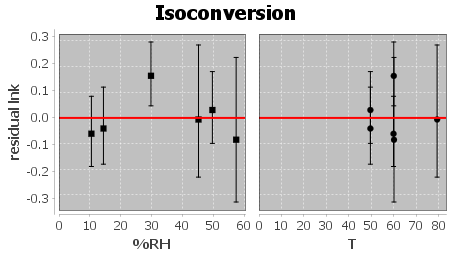
Diffusion	10.18 ± 3.702	0.046 ± 0.011	0.986	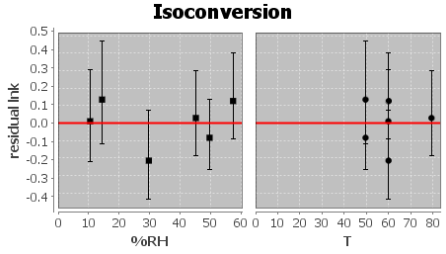
Zero order	5.777 ± 2.705	0.031 ± 0.007	0.999	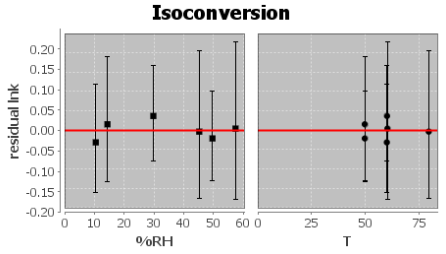
First order	6.224 ± 2.748	0.032 ± 0.007	0.999	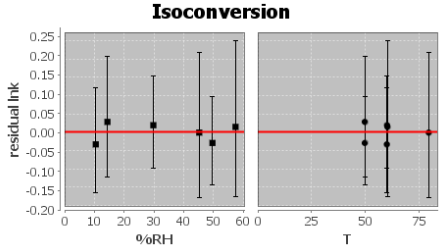
Second order	6.681 ± 3.121	0.034 ± 0.007	0.998	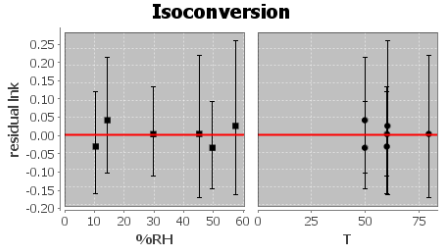

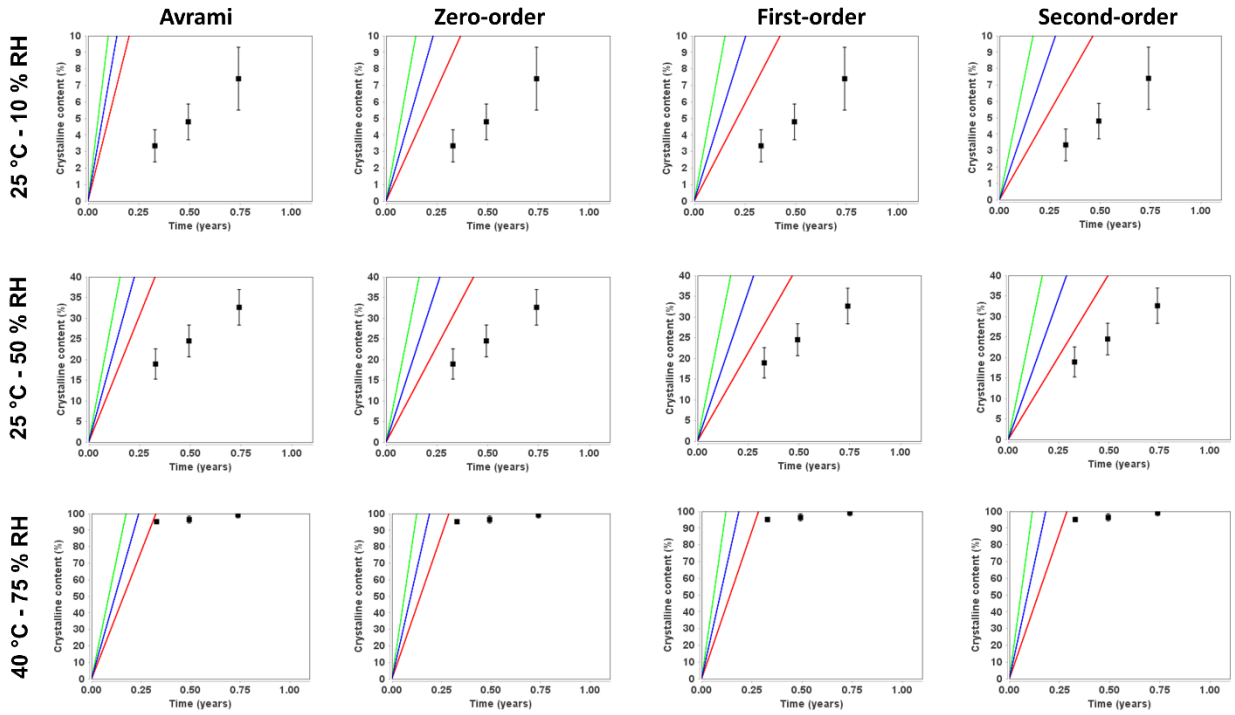

Figure S4. Long-term physical stability prediction of co-spray dried budesonide:PVP K90 formulation using zero, first, second, and Avrami kinetic models.

Table S7. Average content of crystalline drug after aging of co-spray dried griseofulvin: HPMC AS (1:1, w/w) formulation.

Time (days)	T (°C)	RH (%)	Crystallinity (%)
2	41.9	68.9	4.15
8	41.9	68.9	6.28
16	41.9	68.9	18.9
29	41.9	68.9	22.55
2	49.2	14.5	0.19
8	49.2	14.5	1.36
16	49.2	14.5	8.91
22	49.2	14.5	9.28
29	49.2	14.5	9.97
16	59.6	11.5	9.34
22	59.6	11.5	11.84
2	58.7	30.5	3.9
8	58.7	30.5	10
16	58.7	30.5	13.4
22	58.7	30.5	14.22
29	58.7	30.5	15.61
2	59	55.8	9.54
20	59	55.8	30.7
27	59	55.8	35.8
2	69.1	11.4	4.09
8	69.1	11.4	10.13
16	69.1	11.4	12.48
29	69.1	11.4	21.79
14	79.9	45.5	41.04
27	79.9	45.5	55
14	69.9	65.1	33.08
27	69.9	65.1	45.88

Table S8. Residual plots and modified-Arrhenius equation parameters of co-spray dried griseofulvin: HPMC AS formulation.

Fitting method	Ea (kcal/mol)	B	R^2	Residual plot
Avrami	7.352 ± 2.285	0.018 ± 0.005	0.94	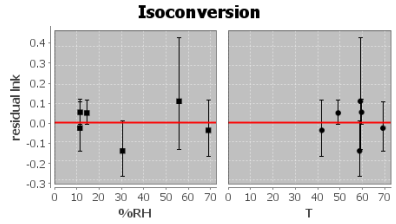
Diffusion	16.406 ± 2.177	0.039 ± 0.004	0.972	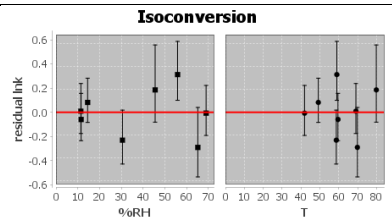
Zero order	9.800 ± 2.477	0.023 ± 0.003	0.959	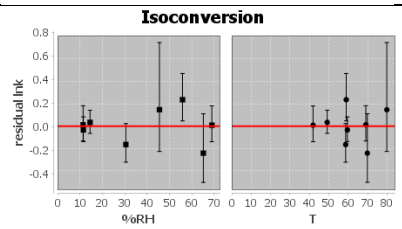
First order	10.960 ± 3.462	0.026 ± 0.005	0.959	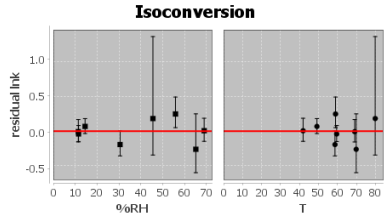
Second order	11.681 ± 4.055	0.028 ± 0.006	0.959	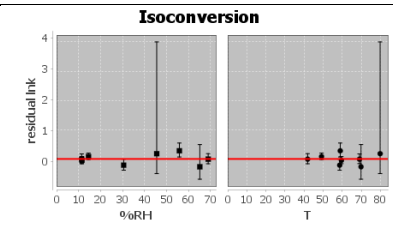

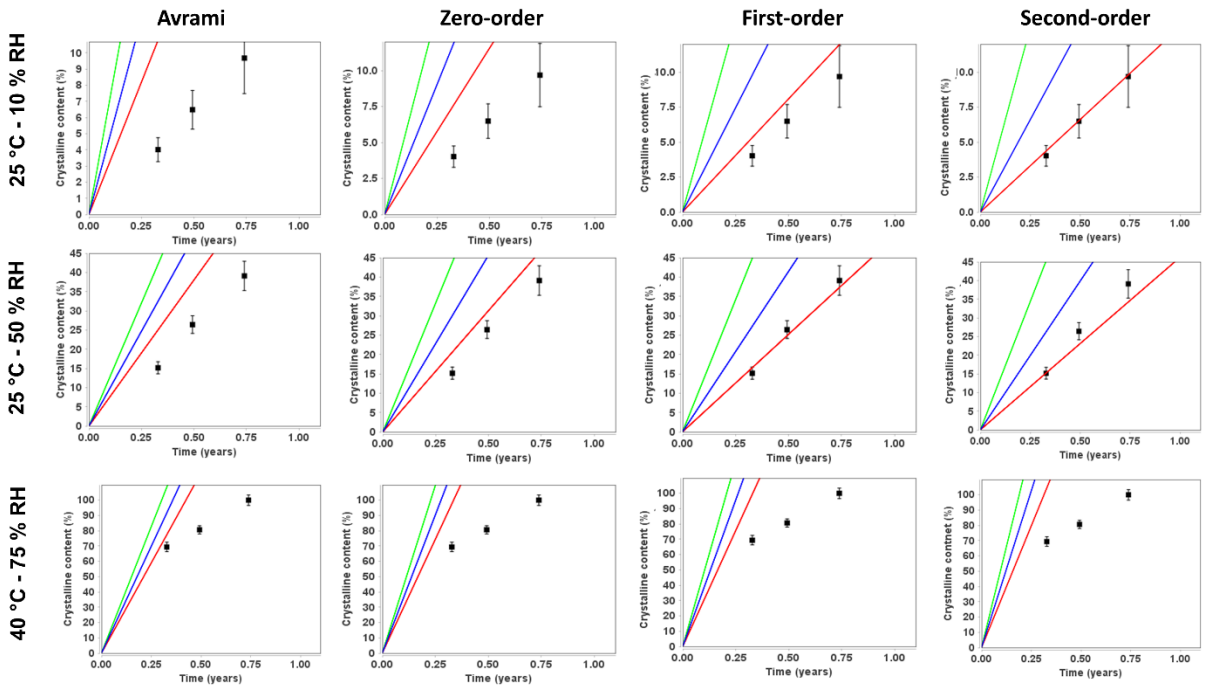

Figure S5. Long-term physical stability prediction of co-spray dried griseofulvin: HPMC AS formulation using zero, first, second, and Avrami kinetic models.

Table S9. Average content of crystalline drug after aging of co-spray dried ritonavir: HPMC AS (2:1, w/w) formulation.

Time (days)	T (°C)	RH (%)	Crystallinity (%)
9	59.9	57.7	4
14	59.9	57.7	19
3	60.1	95.4	3.2
7	60.1	95.4	16.3
9	60.1	95.4	46.7
14	60.1	95.4	63.3
22	60.1	95.4	67.1
6	70.8	69.8	3.1
9	70.8	69.8	18
15	70.8	69.8	51.9
10	78.4	24.4	1.6
14	78.4	24.4	4.2
32	78.4	24.4	5.4
3	78.9	45.7	1.2
9	78.9	45.7	4.4
15	78.9	45.7	16
22	78.9	45.7	23.7
32	78.9	45.7	25.9

Table S10. Residual plots and modified-Arrhenius equation parameters of co-spray dried ritonavir:HPMC AS (2:1, w/w) formulation

Fitting method	Ea (kcal/mol)	B	R^2	Residual plot
Avrami	1.282 ± 1.209	0.043 ± 0.003	0.981	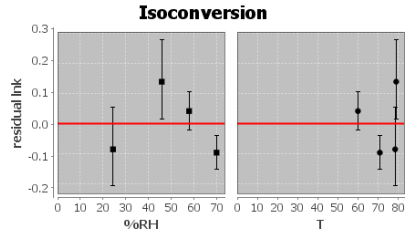
Diffusion	9.471 ± 3.853	0.068 ± 0.008	0.881	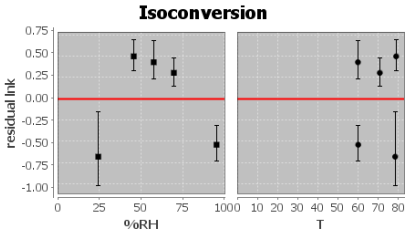
Zero order	3.618 ± 2.014	0.046 ± 0.006	0.941	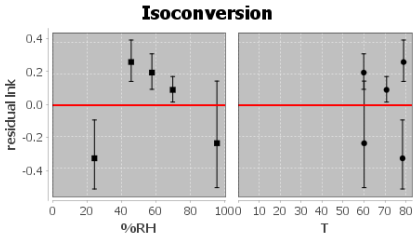
First order	4.180 ± 2.071	0.047 ± 0.009	0.934	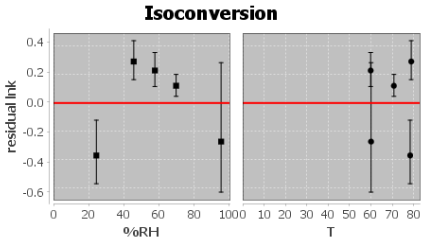
Second order	4.649 ± 2.175	0.048 ± 0.01	0.915	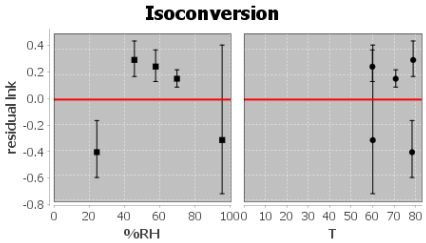

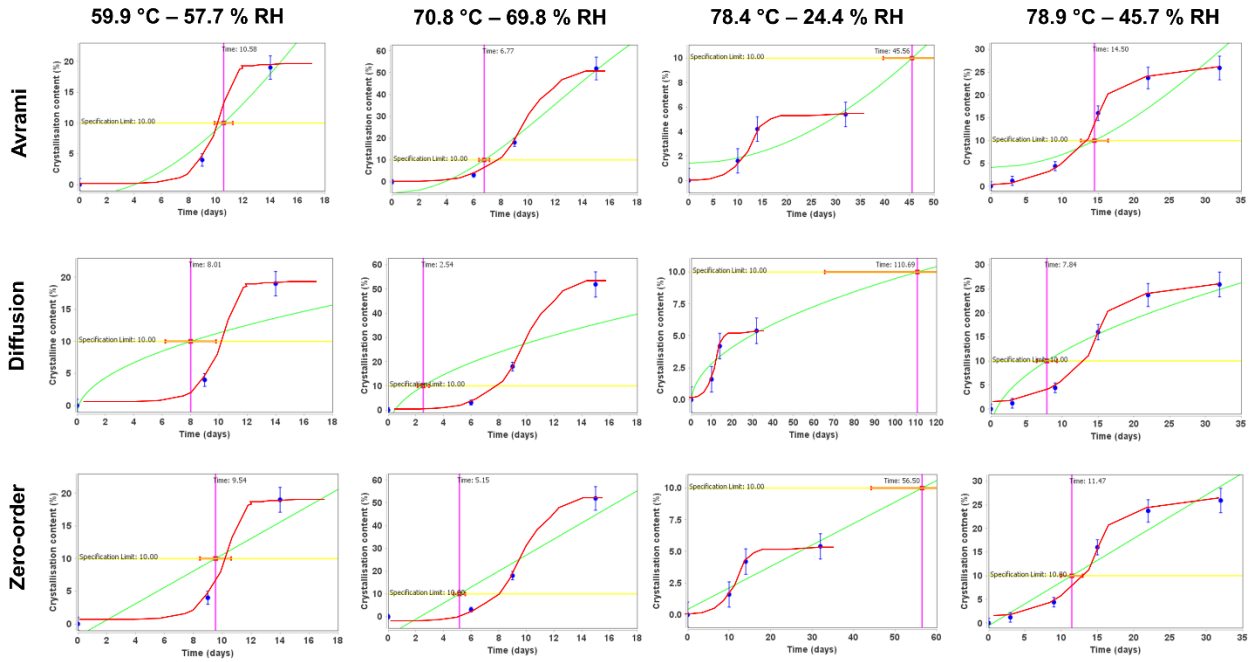

Fig. 6S. A mixed model for the physical stability of the co-spray dried ritonavir-HPMC AS formulation (2:1, w:w) at different conditions: 59.9°C/57.7% RH, 70.8°C/69.8% RH; 78.4°C/24.4% RH and f) 78.9°C/45.7% RH.

Table S11. Average content of crystalline drug after aging of co-spray dried ritonavir: PVP K90 (2:1, w/w) formulation.

Time (days)	T (°C)	RH (%)	Crystallinity (%)
6	41.01	69.4	4
10	41.01	69.4	9.1
14	41.01	69.4	17.5
22	41.01	69.4	33.6
9	49.8	49.4	4.8
22	49.8	49.4	18.2
7	60.1	95.4	23.4
14	60.1	95.4	57.4
3	70.81	69.8	37
9	70.81	69.8	63
22	70.81	69.8	70.3
10	78.9	45.7	11.4
15	78.9	45.7	20.4
22	78.9	45.7	54.1

Table S12 Residual plots and modified-Arrhenius equation parameters of co-spray dried ritonavir:PVP K90 (2:1, w:w) formulation.

Fitting method	Ea (kcal/mol)	B	R^2	Residual plot
Avrami	3.856 ± 0.676	0.023 ± 0.004	0.994	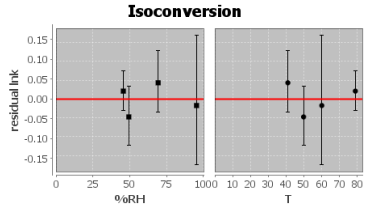
Diffusion	18.996 ± 2.866	0.056 ± 0.07	0.583	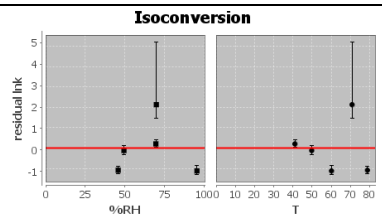
Zero order	5.156 ± 0.817	0.027 ± 0.003	0.994	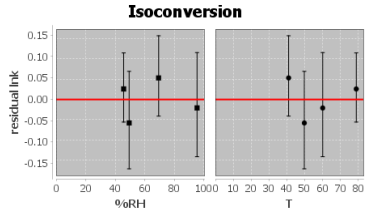
First order	5.403 ± 0.751	0.0028 ± 0.003	0.994	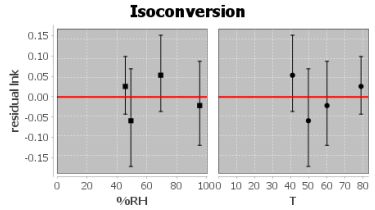
Second order	5.525 ± 0.755	0.0029 ± 0.003	0.993	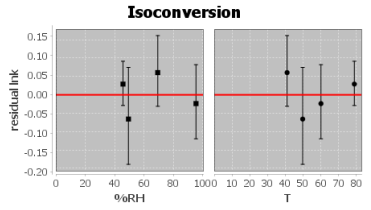

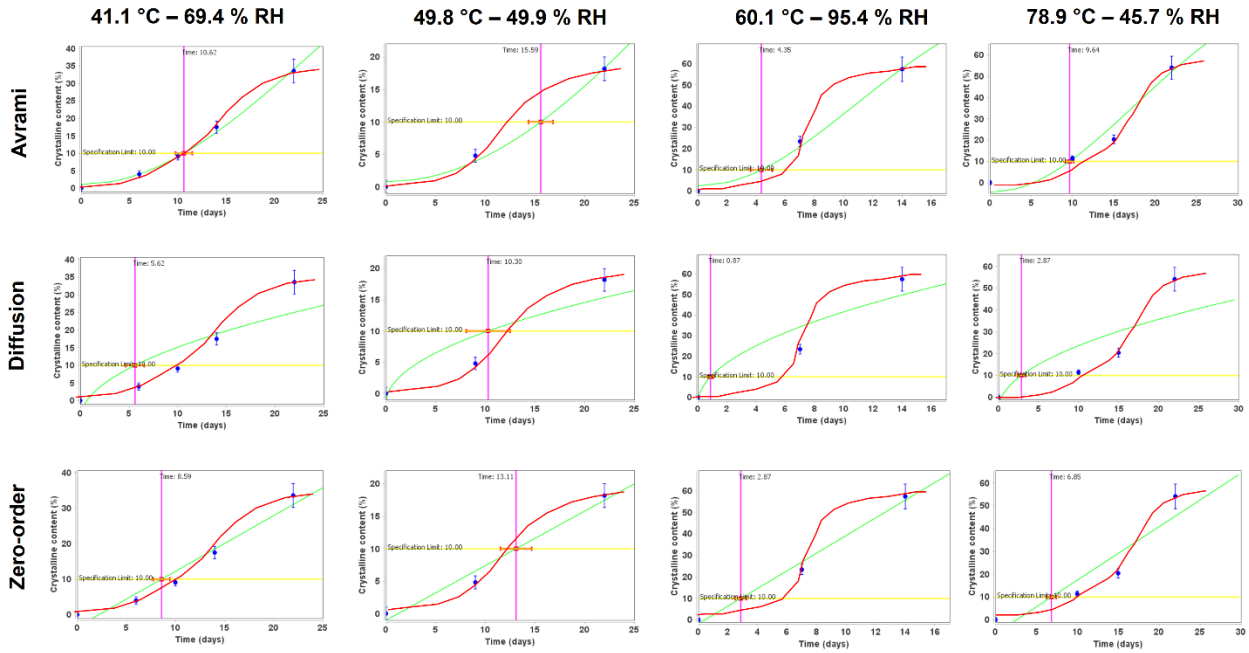

Fig. 7S. A mixed model for the physical stability of the co-spray dried ritonavir-PVP K90 formulation (2:1, w:w) at different conditions: 41.1°C/69.4% RH, 49.8°C/49.9% RH; 60.1°C/95.4% RH and f) 78.9°C/45.7% RH.

Appendix I. Fitting of Avrami curve with a different n Avrami exponent.

Formulation Ritonavir:HPMC (2:1, w/w)

Equation:

$$\alpha(t) = 1 - \exp(-kt^n)$$

Where K represents the crystallisation rate constant, n is the Avrami exponent (that describes the dimensionality of the crystal growth being equal 2,3 and 4 for rod, plate and spherical geometry respectively for homogeneous nucleation), t is the time and α(t) is the relative crystallinity calculated as:

$$\alpha(t) = \frac{x(t)}{x\,(\infty)}$$

Where α(t) is the relative crystallinity that normalises the true absolute crystallinity x(t) and varies from 0 to 1. The formulation will never fully recrystallize to produce 100% crystallised ritonavir regardless of the storage conditions. In this formulation, the final extent of recrystallization of the ritonavir was dependent of temperature and RH. At 80°C/45% RH, the highest crystallisation content of ritonavir was 25.9%, then this values was considered as the x(∞). Also, crystallisation was expressed not in percentage but as a fraction to fit the general Avrami equation.

Time (days)	T (°C)	RH (%)	Crystallinity (%)	Crystallinity (fraction)	Relative crystallinity
3	78.9	45.7	1.2	0.012	0.046332
9	78.9	45.7	4.4	0.044	0.169884
15	78.9	45.7	16	0.16	0.617761
22	78.9	45.7	23.7	0.237	0.915058
32	78.9	45.7	25.9	0.259	1

Initial values of K=0.5 and n=2 were given to compute the optimised values of model parameters by minimizing the sum of residual squares. n value was bound between 0-4. The fitting of the data showed the following n, K and R^2 values:

Fitting	n	k	R^2	Fitting curve
Experimental data	2.856 ± 0.299	3.995E-4 ± 3.23E-4	0.995	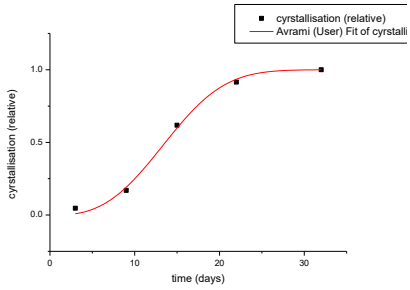
Fixed n=3	3	2.722E-4 ±1.671E-5	0.996	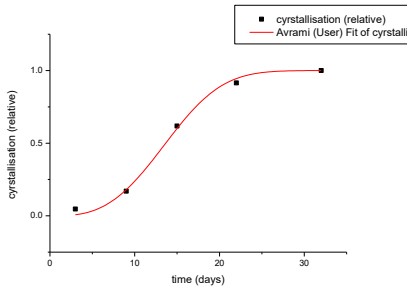
Fixed n=2	2	4.03E-3 ± 4.88E-4	0.978	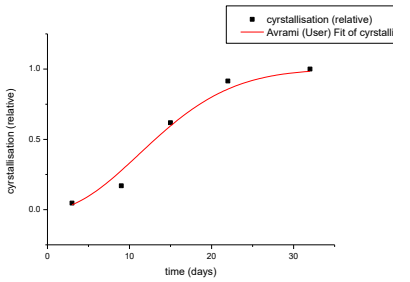

Therefore, for this data a n value of 3 exhibits a better fitting that a n value of 2 which probably would result in a better prediction model also. However, n value seems to be fixed to 2 in the Avrami fitting model of the ASAPprime software.

Avrami: $[deg] = [deg]_\infty - \exp(-kt^2)$ (Eq. 6)

Other parameter to bear in mind is that only one fitting model can be selected for all the conditions tested in the ASAPprime software and then only one x(∞) value can be fixed for all the conditions which reduces the accuracy of the prediction model specially in those amorphous systems where the final extent of recrystallization depends on the T and RH.

The Avrami equation implicity defines a constant nucleation rate, resulting in a simplification that overpredicts the relative crystallinity (α(t) and underpredicts the time for complete recrystallization as shown in most of the formulations tested (ie. Figures 12, 15, 19 and 22). In theory, only small deviations should occur between the real time data and the Avrami equation during primary crystallisation as crystallisation is approximately constant. However, the nucleation rate decreases

sharply during secondary or late-stage crystallisation due to the decline of the number of available nucleation sites. Then, it is critical at which moment the late crystallisation occurs (before or after the specification limit). If the late crystallisation occurs before the specification limit is reached then, it would be more convenient either to exclude this condition from the Avrami model as the prediction will be less accurate or to include a modified-Avrami equation[27] in the software as:

$$\alpha(t) = 1 - \frac{1}{1 + kt^n}$$

Discussion & Future Perspectives

5.0. Discussion

An acceptable prediction of long-term physical stability of amorphous solid dispersions has been successful demonstrated using ASAPprime tool which can facilitate the formulation decision making process making it faster and more accurate.

Four different nifedipine amorphous solid dispersions were manufactured using scalable pharmaceutical techniques by HME and spray drying. All four ASDs demonstrated similar improved drug dissolution rates compared to the crystalline drug alone. However, using APS, significant differences were found in the stability of the formulations. The spray dried powders exhibited greater physical stability than the extrudates, which showed two glass transition (Tg) temperatures, indicating phase separation. In contrast, formulations manufactured by HME were found to have superior chemical stability than spray dried powders, which demonstrated greater moisture sensitivity. The chemical degradation kinetics for both spray dried formulations were more complex than for the equivalent extruded materials. At less extreme conditions of temperature and relative humidity, spray dried systems followed Avrami-type kinetics, but under more extreme conditions, a shift from Avrami to diffusion kinetics was observed, which may be attributed to the miscibility of the degradation products and polymer chains. In conclusion, of all the formulations tested, the spray dried formulation with PVPVA64 exhibited the best balance between physical and chemical stability and would be the recommended candidate for further evaluation. Accelerated predictive stability combined with chemometrics has been demonstrated to be a good methodology to aid in the decision-making process for pharmaceutical amorphous formulations.

The modelling of drug crystallisation kinetics are challenging but the process can be simplified by focusing in the isoconversion approach methodology. A humidity-corrected Arrhenius equation was used to determine the crystalisation kinetic profile and estimate the effect of temperature and relative humidity on the crystallisation rates of several amorphous solid dispersions containing budesonide, griseofulvin, ritonavir or celecoxib formulated with HMPC AS or PVP K90. In budesonide-PVP K90 and griseofulvin-HMPC AS solid dispersions, the diffusion model predicted more accurately the physical stability than the Avrami model implying that drug molecules have to migrate through the matrix before nucleation takes place.

However, an Avrami kinetic model was the most accurate in the long-term physical stability prediction for the budesonide-HPMC AS formulation which exhibited the highest stability which may be linked to the higher capacity to form hydrogen bonds with the drug, reducing further its molecular mobility making the diffusion process extremely slow. An acceptable prediction of long-term physical stability of amorphous solid dispersions was successful demonstrated using this methodology which can assist in the formulation decision making process making it faster and more accurate.

APS approaches can be successfully employed to understand a product's stability, thereby aiding in development strategy decisions and potentially minimizing regulatory stability testing commitments throughout its lifecycle. Acceptance of lean stability strategies, not only during clinical trials but throughout the developmental lifecycle, will require further collaboration between industry and the regulators.

5.1 Future Perspectives

This project continued upon the existing body of work that investigates the use of Accelerated Predictive Stability (APS) strategies. There exists ample research opportunities that would complement the current.

- Investigation of other statistical approaches to model crystallisation kinetics.

All of the predictive models used in this project were made using ASAPprime software which as previously mentioned is a commercial software package which is only available via an annual license. There are limits to the type and format of kinetic models that can be used with ASAPprime and in the interest of making these tools open to a larger user base, the potential of creating open source models / plugins and statisitical tools for more readily accessible and affordable software programs.

- Expand research with further processes / API's and excipients.

This project only covers a select number of processes, API's and excipients. In order to increase the dataset, additional experiments could be conducted with a wider range of API's and excipients, incorporating different manufacturing processes and containing varying ratios of excipients.

This may be a challenging task, given the vast number of different excipients and materials which are used across the pharmaceutical industry.

- Investigation into predictive models for the determination of dissolution stability.

Dissolution analysis is a key component of any stability study. Current approaches for the assessment of dissolution modelling are based on empirical models often with no real mechanistic basis. There is a knowledge gap in the literature around the underlying mechanisms of change and which models best predict future behaviour. Additional research could allow for improved protocols to evaluate impact of temperature and humidity on the dissolution characteristics of formulations during development and manufacturing.

Conclusions
Conclusiones

6.0 Conclusions

- The modelling of drug crystallisation kinetics are challenging but the process can be simplified by focusing in the isoconversion approach methodology.
- An acceptable prediction of long-term physical stability of amorphous solid dispersions was successful demonstrated using Accelerated Predictive Stability Studies which can assist in the formulation decision making process making it faster and more accurate.
- Accelerated predictive stability combined with chemometrics has been demonstrated to be a good methodology to aid in the decision-making process for pharmaceutical amorphous formulations.

6.1 Conclusiones

- El modelado de la cinética de cristalización de fármacos es un reto, pero el proceso se puede simplificar centrándose en la metodología de la isoconversión.
- Los estudios de estabilidad predictiva acelerados son útiles para predecir la estabilidad física a largo plazo de dispersiones sólidas amorfas ayudando en el proceso de toma de decisiones de formulación haciéndolo más rápido y preciso.
- Se ha demostrado que la estabilidad predictiva acelerada combinada con la quimiometría es una buena estrategia para el desarrollo de formulaciones farmacéuticas amorfas físicamente estables.